

**DYNAMIC MODELING AND CONTROL OF HYBRID  
GROUND SOURCE HEAT PUMP SYSTEMS**

**CHANG CHEN**

**A Thesis**

**In**

**Department of Building, Civil & Environmental Engineering**

**Presented in Partial Fulfillment of the Requirements**

**For the Degree of Master of Applied Science at**

**Concordia University**

**Montreal, Quebec, Canada**

**May 2008**

**© CHANG CHEN, 2008**



Library and  
Archives Canada

Bibliothèque et  
Archives Canada

Published Heritage  
Branch

Direction du  
Patrimoine de l'édition

395 Wellington Street  
Ottawa ON K1A 0N4  
Canada

395, rue Wellington  
Ottawa ON K1A 0N4  
Canada

*Your file    Votre référence*  
*ISBN: 978-0-494-42487-2*  
*Our file    Notre référence*  
*ISBN: 978-0-494-42487-2*

**NOTICE:**

The author has granted a non-exclusive license allowing Library and Archives Canada to reproduce, publish, archive, preserve, conserve, communicate to the public by telecommunication or on the Internet, loan, distribute and sell theses worldwide, for commercial or non-commercial purposes, in microform, paper, electronic and/or any other formats.

The author retains copyright ownership and moral rights in this thesis. Neither the thesis nor substantial extracts from it may be printed or otherwise reproduced without the author's permission.

**AVIS:**

L'auteur a accordé une licence non exclusive permettant à la Bibliothèque et Archives Canada de reproduire, publier, archiver, sauvegarder, conserver, transmettre au public par télécommunication ou par l'Internet, prêter, distribuer et vendre des thèses partout dans le monde, à des fins commerciales ou autres, sur support microforme, papier, électronique et/ou autres formats.

L'auteur conserve la propriété du droit d'auteur et des droits moraux qui protègent cette thèse. Ni la thèse ni des extraits substantiels de celle-ci ne doivent être imprimés ou autrement reproduits sans son autorisation.

---

In compliance with the Canadian Privacy Act some supporting forms may have been removed from this thesis.

Conformément à la loi canadienne sur la protection de la vie privée, quelques formulaires secondaires ont été enlevés de cette thèse.

While these forms may be included in the document page count, their removal does not represent any loss of content from the thesis.

Bien que ces formulaires aient inclus dans la pagination, il n'y aura aucun contenu manquant.

  
**Canada**

# **ABSTRACT**

## **DYNAMIC MODELING AND CONTROL OF HYBRID GROUND SOURCE HEAT PUMP SYSTEMS**

**CHANG CHEN**

Ground source heat pump (GSHP) systems are one of the fastest growing applications of renewable energy in the world with annual increases of 10% over the past decade. GSHPs are potentially more efficient than conventional air-to-air heat pumps as they use the relatively constant temperature of the geothermal energy to provide heating or cooling to conditioned rooms at desired temperature and relative humidity. More importantly, GSHP systems can in fact achieve significant energy savings year round, compared to conventional HVAC systems.

A hybrid ground source heat pump (HGSHP) system is designed in this study to heat and cool an office building all the year round. Dynamic models of each component of the heat pump system are developed for simulations of heat transfer between each component of the HGSHP system and for control strategy design and analysis. A detailed multiple-load aggregation algorithm (MLAA) is adapted from the literature to precisely account for and calculate the transient heat conduction in vertical ground heat exchangers with different yearly, monthly, and daily pulses of heat. Feedback PI controllers for heat pump units and

On/Off controllers for boiler and cooling tower are designed and utilized to match anticipated building loads and to analyze transient response characteristics of such outputs as water flow rate and air flow rate of heat pumps, return water temperature and supply air temperature of heat pumps, water temperatures of ground loops and heat exchangers, water temperature of boiler or cooling tower, and fuel flow rate of boiler. Control strategies for the HGSHP system in both heating and cooling modes of operation are also introduced to study the system responses. With the usage of On/Off controllers and well-tuned PI controllers, as well as optimal control strategies for heating and cooling operations, the HGSHP system is expected to give better operating performance and efficiency. As a result, noticeable energy savings can be achieved in both heating and cooling modes of operation.

## ACKNOWLEDGEMENTS

I have to admit this dissertation would not have been achievable without those who helped me directly or indirectly in completing this work. It is my pleasure to take this opportunity to gratefully acknowledge all of them.

First and foremost, I wish to express my deepest appreciation and gratitude to my supervisor, Dr. M. Zaheeruddin, for giving me the opportunity to do an M.A.Sc thesis under his direction, and for his great help and guidance throughout the project. I think I am actually very fortunate, because he not just let me choose my favorite topic but provided me unconditional moral and financial support.

I would like to sincerely thank my colleagues, Lianzhong Li and Min Ning, for their assistance on either programming or engineering problem-solving during the period of the project, and other member staff such as Arash Ranjbaran and Jian Zhang.

No words are able to express how grateful I am to my parents, Zuhao and Liqing, my elder brothers, Qian and Han, and my wife, Suihong, for their love and care and for their support and encouragement. Without their love and support, I would not be what I am. I would also like to mention my baby son, Michael, with whom this thesis was difficult to accomplish, but without whom there would be no meaning in life.

Last but not least, special thanks should also be given to my friends, namely, York Zhang, Edward Yang, Wendong Wang, and Kevin Zhong. It is they who assisted me to settle down when I first came to Canada a few years ago.

# TABLE OF CONTENTS

LIST OF FIGURES

LIST OF TABLES

NOMENCLATURE

ABBREVIATIONS

CHAPTER 1 INTRODUCTION .....	1
1.1 Background.....	1
1.2 Motivation and Objectives.....	4
1.3 Organization of Thesis.....	5
CHAPTER 2 LITERATURE REVIEW.....	7
2.1 Introduction.....	7
2.2 Heat Pump Models.....	7
2.2.1 Steady State Models.....	7
2.2.2 Dynamic Models.....	10
2.3 Ground Heat Exchanger Models.....	12
2.4 Cooling Tower Models.....	17
2.5 Boiler Models.....	19
CHAPTER 3 PHYSICAL MODEL DESCRIPTION AND SYSTEM DESIGN.....	21
3.1 Introduction.....	21

3.2 Cooling and Heating Loads.....	22
3.3 Sizing Ground Heat Exchanger.....	23
3.4 Borehole and Grouting Design.....	26
3.5 Equipments Selection.....	27
3.6 Pipe Insulation.....	28
3.7 Antifreeze Solution.....	29
 <b>CHAPTER 4 DYNAMIC MODELLING AND SIMULATION</b>	
<b>RESULTS .....</b>	<b>31</b>
4.1 Model Description.....	31
4.1.1 Zone Model.....	31
4.1.2 Heat Pump Model.....	34
4.1.3 Ground Heat Exchanger Model.....	38
4.1.4 Cooling Tower Model.....	47
4.1.5 Boiler Model.....	50
4.2 Open Loop Simulation Results.....	53
4.2.1 Heating Mode.....	53
4.2.2 Cooling Mode.....	55
 <b>CHAPTER 5 CONTROL STRATEGIES AND SIMULATION</b>	
<b>RESULTS.....</b>	<b>57</b>
5.1 Introduction.....	57
5.1.1 Two Position Control.....	57

5.1.2 Modulating Control.....	59
5.2 Control Strategies.....	64
5.2.1 Heating Mode of Operation.....	65
5.2.1.1 On/off Controllers for Heat Pump and Boiler.....	65
5.2.1.2 PI Controllers for Heat Pump and Boiler.....	66
5.2.1.3 PI Controller for Heat Pump and On/off control for Boiler .....	67
5.2.2 Heating Mode Simulation Results.....	67
5.2.3 Heating Mode Cases Energy Comparison.....	81
5.2.4 Cooling Mode of Operation.....	86
5.2.4.1 On/off Controllers for Heat Pump and Cooling Tower.....	87
5.2.4.2 PI Control for HP and On/off control for Cooling Tower.....	87
5.2.5 Cooling Mode Simulation Results.....	88
5.2.6 Cooling Mode Cases Energy Comparison.....	100
5.3 Multiple Heat Pumps.....	104
5.3.1 Two Zone Disaggregated System Model.....	105
5.3.1.1 Heating Mode of Operation.....	106
5.3.1.2 Cooling Mode of Operation.....	111
5.3.2 Four Zone Disaggregated System Model.....	115
5.3.2.1 Heating Mode of Operation.....	116
5.3.2.2 Cooling Mode of Operation.....	121
5.4 Optimization of HGSHP System.....	126

5.4.1 Heating Mode of Operation.....	126
5.4.2 Cooling Mode of Operation.....	130
5.5 Overall Performance of HGSHP System.....	134
5.5.1 Heating Mode of Operation.....	134
5.5.2 Cooling Mode of Operation.....	140
 CHAPTER 6 CONTRIBUTIONS, CONCLUSIONS AND RECOMMENDATIONS.....	
6.1 Summary.....	145
6.2 Contributions.....	145
6.3 Conclusions.....	146
6.4 Recommendations for Future Research.....	147
REFERENCES.....	149

## LIST OF FIGURES

Figure 1.1 Schematic diagram of GSHP Unit Layout.....	2
Figure 3.1 Office Building Floor Layouts.....	21
Figure 3.2 Schematic of Hybrid Ground Source Heat Pump System.....	22
Figure 3.3 Schematic of Vertical Ground Heat Exchangers.....	24
Figure 3.4 Schematic Diagram of Borehole.....	27
Figure 4.1 Simulation result of zone model in heating mode.....	32
Figure 4.2 Simulation result of zone model in cooling mode.....	33
Figure 4.3 Simulation result of heat pump model in heating mode.....	36
Figure 4.4 Simulation result of the heat pump model in cooling mode.....	37
Figure 4.5 Multiple-load aggregation Algorithm Scheme.....	39
Figure 4.6 Schematic of the 4x5 borefield.....	42
Figure 4.7 Simulation result of ground loop model for heating .....	45
Figure 4.8 Simulation result of ground loop model for cooling.....	46
Figure 4.9 Simulation result of the cooling tower model.....	49
Figure 4.10 Simulation results of the boiler model.....	52
Figure 4.11 Open loop air temperature responses for heating.....	54
Figure 4.12 Water temperature responses for heating.....	54
Figure 4.13 Open loop air temperature responses for cooling.....	56
Figure 4.14 Water temperature responses for cooling.....	56

Figure 5.1 Two-Position Control.....	58
Figure 5.2 Block Diagram of Closed Loop Control.....	60
Figure 5.3 Proportional plus Integral (PI) Control.....	62
Figure 5.4 Schematic of Control of Hybrid GSHP.....	65
Figure 5.5 Hourly Heating Load Profile on a Specific Day (Tsp=21 °C).....	68
Figure 5.6 Air Temperatures of One Day Simulations (Tsp=21 °C).....	69
Figure 5.7 Outlet Water Temperatures of HP, GL and HX (Tsp=21 °C).....	70
Figure 5.8 Outlet Water Temperatures of Boiler (Tsp=21 °C).....	70
Figure 5.9 Control Variables of 3-way Valve and Pump 2 (Tsp=21 °C).....	71
Figure 5.10 Control Variable of Boiler Burner (Tsp=21 °C).....	71
Figure 5.11 Control Variable of Heat Pump (Tsp=21 °C).....	72
Figure 5.12 Hourly Heating Load Profile on a Specific Day (Tsp=15/21 °C).....	72
Figure 5.13 Air Temperatures of One Day Simulations (Tsp=15/21 °C).....	74
Figure 5.14 Outlet Water Temperatures of HP, GL and HX (Tsp=15/21).....	74
Figure 5.15 Outlet Water Temperatures of Boiler (Tsp=15/21 °C).....	75
Figure 5.16 Control Variables of 3-way Valve and Pump2 (Tsp=15/21 °C).....	75
Figure 5.17 Control Variable of Boiler Burner (Tsp=15/21 °C).....	76
Figure 5.18 Control Variable of Heat Pump (Tsp=15/21 °C).....	76
Figure 5.19 Air Temperatures of One Day Simulations .....	78
Figure 5.20 Outlet Water Temperatures of HP, GL and HX .....	78
Figure 5.21 Outlet Water Temperatures of Boiler .....	79

Figure 5.22 Control Variables of HP and Pump 2 .....	79
Figure 5.23 Control Variable of Boiler Burner .....	80
Figure 5.24 COP of Heat Pump System .....	80
Figure 5.25 Hourly Heating Load Profile (Tsp=15/21 °C) .....	82
Figure 5.26 Air Temperatures of One Day Simulations (Tsp=15/21 °C) .....	83
Figure 5.27 Outlet Water Temperatures of HP, GL and HX (Tsp=15/21 °C) .....	83
Figure 5.28 Outlet Water Temperature of Boiler (Tsp=15/21 °C) .....	84
Figure 5.29 Control Variables of HP and Pump2 (Tsp=15/21 °C) .....	84
Figure 5.30 Control Variable of Boiler Burner (Tsp=15/21 °C) .....	85
Figure 5.31 COP of Heat Pump System (Tsp=15/21 °C) .....	85
Figure 5.32 Hourly Cooling Load Profile on a Specific Day .....	89
Figure 5.33 Zone air and HP outlet air temperatures (Case 1) .....	90
Figure 5.34 Outlet water temperatures of HP, GL and HX .....	90
Figure 5.35 Outlet water temperature of cooling tower .....	91
Figure 5.36 Control variable of HP .....	91
Figure 5.37 Control variable of cooling tower .....	92
Figure 5.38 Control variable of circulating pump 2 .....	92
Figure 5.39 Zone air and HP outlet air temperatures (Case 2).....	94
Figure 5.40 Outlet water temperatures of HP, GL and HX .....	94
Figure 5.41 Outlet water temperature of cooling tower .....	95
Figure 5.42 Control variables of HP and pump 2 .....	95

Figure 5.43 Control variable of cooling tower.....	96
Figure 5.44 Zone air and HP outlet air temperatures (Case 3) .....	97
Figure 5.45 Outlet water temperatures of HP and GL .....	98
Figure 5.46 Outlet water temperature of cooling tower .....	98
Figure 5.47 Control variable of HP .....	99
Figure 5.48 Control variable of cooling tower .....	99
Figure 5.49 Hourly cooling Load Profile ( $T_{sp}=23/26^{\circ}\text{C}$ ) .....	101
Figure 5.50 Zone air and HP outlet air temperatures (cooling mode) .....	102
Figure 5.51 Outlet water temperatures of HP, GL and HX .....	102
Figure 5.52 Outlet water temperatures of cooling tower .....	103
Figure 5.53 Control variables of HP and pump 2 .....	103
Figure 5.54 Control variable of cooling tower .....	104
Figure 5.55 Control Schematic of 2-heat-pump HGSHP.....	106
Figure 5.56 Air temperature responses of zone 1 (2-zone heating mode).....	107
Figure 5.57 Air temperature responses of zone 2.....	107
Figure 5.58 Water temperature responses of heat pumps.....	108
Figure 5.59 Water temperature responses of GL and HX.....	108
Figure 5.60 Water temperature response of boiler.....	109
Figure 5.61 Control variables of heat pumps.....	109
Figure 5.62 Control variable of boiler.....	110
Figure 5.63 Control variable of circulating pump 2.....	110

Figure 5.64 Air temperature responses of zone 1 (2-zone cooling mode) .....	111
Figure 5.65 Air temperature responses of zone 2.....	112
Figure 5.66 Water temperature responses of HPs.....	112
Figure 5.67 Water temperature responses of GL and HX.....	113
Figure 5.68 Water temperature response of cooling tower.....	113
Figure 5.69 Control variables of HPs.....	114
Figure 5.70 Control variable of boiler.....	114
Figure 5.71 Control variable of circulating pump 2.....	115
Figure 5.72 Schematic of 4-zone HGSHP system model.....	116
Figure 5.73 Air temperature responses of zone 1 (4-zone heating mode).....	117
Figure 5.74 Air temperature responses of zone 2.....	117
Figure 5.75 Air temperature responses of zone 3.....	118
Figure 5.76 Air temperature responses of zone 4.....	118
Figure 5.77 Outlet water temperature responses of HPs.....	119
Figure 5.78 Outlet water temperature responses of GL and HX.....	119
Figure 5.79 Outlet water temperature response of boiler.....	120
Figure 5.80 Control variable of HPs.....	120
Figure 5.81 Control variables of Boiler and Pump 2.....	121
Figure 5.82 Air temperature responses of zone 1 (4-zone cooling mode).....	122
Figure 5.83 Air temperature responses of zone 2.....	122
Figure 5.84 Air temperature responses of zone 3.....	123

Figure 5.85 Air temperature responses of zone 4.....	123
Figure 5.86 Outlet water temperature responses of HPs.....	124
Figure 5.87 Outlet water temperature responses of GL and HX.....	124
Figure 5.88 Outlet water temperature response of boiler.....	125
Figure 5.89 Control variable of HPs.....	125
Figure 5.90 Control variables of Boiler and Pump 2.....	126
Figure 5.91 Optimal entering water temperatures in heating mode .....	130
Figure 5.92 Optimal entering water temperatures in cooling mode .....	133
Figure 5.93 Zone air and HP outlet air temperatures (1-week heating).....	137
Figure 5.94 Outlet water temperatures of HP, GL and HX .....	137
Figure 5.95 Outlet water temperature of boiler .....	138
Figure 5.96 Control variables of HP and pump 2 .....	138
Figure 5.97 Control variable of boiler .....	139
Figure 5.98 Zone air and HP outlet air temperatures (1-week cooling).....	142
Figure 5.99 Outlet water temperatures of HP, GL and HX .....	142
Figure 5.100 Outlet water temperature of cooling tower .....	143
Figure 5.101 Control variables of HP and pump 2 .....	143
Figure 5.102 Control variable of cooling tower .....	144

## LIST OF TABLES

Table 4.1 Zone model design parameters.....	33
Table 4.2 Coefficients for 6-ton heat pumps.....	34
Table 4.3 Design parameters of the heat pump model.....	37
Table 4.4 Design parameters of ground loop model.....	47
Table 4.5 Design parameters of the cooling tower model.....	50
Table 4.6 Design parameters of the boiler model.....	53
Table 5.1 Hourly Outdoor Air Temperatures of a specific day in winter .....	68
Table 5.2 Design parameters of PI controllers .....	86
Table 5.3 Hourly Outdoor Air Temperatures of a specific day in summer.....	88
Table 5.4 Lower and upper bounds of variables in heating mode.....	127
Table 5.5 Optimal results at design load in heating mode .....	129
Table 5.6 Lower and upper bounds of variables in cooling mode.....	131
Table 5.7 Optimal results at design load in cooling mode .....	133
Table 5.8 Hourly outdoor temperatures of a specific week in winter.....	134
Table 5.9 Hourly building heating loads of a specific week in winter.....	135
Table 5.10 Hourly outdoor temperatures of a specific week in summer.....	140
Table 5.11 Hourly building cooling loads of a specific week in summer.....	141

## NOMENCLATURE

$a_E$	Heat conductance and thermal capacitance of East node (w/m°C)
$a_N$	Heat conductance and thermal capacitance of North node (w/m°C)
$a_P$	Heat conductance and thermal capacitance of central node (w/m°C)
$a_S$	Heat conductance and thermal capacitance of South node (w/m°C)
$a_W$	Heat conductance and thermal capacitance of West node (w/m°C)
$A$	Area of floor/walls/windows ( $m^2$ , $ft^2$ )
$b$	Source term of borehole (w/m)
$c_p$	Specific heat at constant pressure (J/kg-°C)
$c_{p_a}$	Specific heat of air (J/kg-°C)
$c_{p_w}$	Specific heat of water (J/kg-°C)
$c_{p_{gd}}$	Specific heat of ground (J/kg-°C)
$c_{p_{gt}}$	Specific heat of grout (J/kg-°C)
$C_{a_{con}}$	Thermal capacity of condenser air (J/°C)
$C_{a_{ct}}$	Thermal capacity of air in cooling tower (J/°C)
$C_{a_{eva}}$	Thermal capacity of evaporator air (J/°C)
$C_i$	Thermal capacity of the $i^{th}$ cylindrical node of borefield (J/°C)
$C_i$	Equation fit coefficients of heat pump model
$C_{is}$	Thermal capacity of inner shell of boiler (J/°C)
$C_{ins}$	Thermal capacity of insulation layer (J/°C)

$C_{is}$	Thermal capacity of outer shell (J/°C)
$C_{w\_con}$	Thermal capacity of condenser water (J/°C)
$C_{w\_ct}$	Thermal capacity of water in cooling tower (J/°C)
$C_{w\_eva}$	Thermal capacity of evaporator water (J/°C)
$C_z$	Thermal capacity of zone air (J/°C)
$d_p$	Diameter of U-pipe in borehole (m, ft)
$D_b$	Diameter of borehole (m, ft)
$D_i$	Diameter of the $i^{th}$ equivalent cylinder node of borefield (m, ft)
$e$	Error used for PI control
$f_{bo}$	Factor of boiler efficiency
$F_{bo}$	Safety factor of boiler design
$F_{ct}$	Safety factor of cooling tower design
$F_{gl}$	Safety factor of ground loop heat exchanger design
$F_{hp}$	Safety factor of heat pump design
$F_{sc}$	Short circuit heat loss factor between U-tube legs
$F_o$	Fourier number
$g$	Acceleration due to gravity, $m/s^2$
$G$	G-function
$G_{a\_hp}$	Air flow rate of heat pump units (kg/s)
$G_{a\_con}$	Air flow rate of the condenser (kg/s)
$G_{a\_ct}$	Air flow rate of the cooling tower (kg/s)

$G_{a\_eva}$	Air flow rate of the evaporator (kg/s)
$G_{bo}$	Water flow rate of boiler (kg/s)
$G_{ct}$	Water flow rate of cooling tower (kg/s)
$G_f$	Flow rate of fuel for burner (kg/s)
$G_{fmax}$	Maximum flow rate of fuel for burner (kg/s)
$G_{gl}$	Water flow rate of ground loop (kg/s)
$G_{hp}$	Water flow rate of heat pump (kg/s)
$G_{hx}$	Water flow rate of plate heat exchanger (kg/s)
$G_{w\_con}$	Water flow rate of the condenser (kg/s)
$G_{w\_ct}$	Water flow rate of the cooling tower (kg/s)
$G_{w\_eva}$	Water flow rate of the evaporator (kg/s)
$h$	Head of circulating pumps (m, ft)
$h_v$	Heating value of fuel (J/kg)
$HP_{cap}$	Heat pump capacity (W)
$HP_{pwr}$	Power input of heat pump (W)
$k_g$	Thermal conductivity of grout (w/m°C)
$k_s$	Thermal conductivity of soil (w/m°C)
$K_p$	Proportional gain of PI control
$K_i$	Integral gain of PI control
$L$	Borehole length (m)
$L_c$	Design borehole length for cooling mode (m)

$L_h$	Design borehole length for heating mode (m)
MLAA	All the terms of the multiple-load aggregation algorithm, W
$N_d$	Daily time period of past thermal history in MLAA scheme (hr)
$N_h$	Immediate thermal history (hr)
$N_m$	Monthly time period of past thermal history (hr)
$N_w$	Weekly time period of past thermal history (hr)
$N_y$	Yearly time period of past thermal history (hr)
$PLF_m$	Part load factor during design month
$q$	Non-aggregation ground load (W, Btu/h)
$\bar{q}$	Aggregation ground load (W, Btu/h)
$q_a$	Net annual average heat transfer to the ground (W, Btu/h)
$Q_b$	Building load (W, Btu/h)
$Q_{burner}$	Heat transfer from burner to the inner shell (W)
$Q_{dc}$	Design cooling load of zone (W, Btu/h)
$Q_{dh}$	Design heating load of zone (W, Btu/h)
$Q_{gl}$	Ground load through ground loop (W, Btu/h)
$Q_{inf}$	Heat gain of the zone from infiltration (W, Btu/h)
$Q_{int}$	Internal heat gain of the zone (W, Btu/h)
$Q_{sol}$	Heat gain of the zone from transmitted solar radiation (W, Btu/h)
$R$	Effective thermal resistance of the ground (m-k/kW)
$R_b$	Effective thermal resistance of the borehole (m-k/kW)

$R_{ga}$	Effective thermal resistance of ground for annual pulse (m-k/W)
$R_{gm}$	Effective thermal resistance of ground for monthly pulse (m-k/W)
$R_{gd}$	Effective thermal resistance of ground for daily pulse (m-k/W)
$t$	Time (s)
$t_p$	Temperature penalty for interference of adjacent bores ( $^{\circ}\text{C}$ )
$T_a$	Temperature of air ( $^{\circ}\text{C}$ )
$T_{a\_con}$	Air temperature of the condenser ( $^{\circ}\text{C}$ )
$T_{a\_con\_i}$	Inlet air temperature of the condenser ( $^{\circ}\text{C}$ )
$T_{a\_ct}$	Air temperature of the cooling tower ( $^{\circ}\text{C}$ )
$T_{a\_ct\_i}$	Inlet air temperature of the cooling tower ( $^{\circ}\text{C}$ )
$T_{a\_eva}$	Air temperature of the evaporator ( $^{\circ}\text{C}$ )
$T_{a\_con\_i}$	Inlet air temperature of the evaporator ( $^{\circ}\text{C}$ )
$T_{am}$	Temperature of ambient air for boiler ( $^{\circ}\text{C}$ )
$T_E$	Temperature of East node ( $^{\circ}\text{C}$ )
$T_g$	Undisturbed far-field ground temperature ( $^{\circ}\text{C}$ )
$T_i$	Temperature of the $i^{\text{th}}$ cylindrical node ( $^{\circ}\text{C}$ )
$T_{is}$	Temperature of inner shell of boiler ( $^{\circ}\text{C}$ )
$T_{ins}$	Temperature of inner insulation layer ( $^{\circ}\text{C}$ )
$T_{os}$	Temperature of outer shell of boiler ( $^{\circ}\text{C}$ )
$T_N$	Temperature of North node ( $^{\circ}\text{C}$ )
$T_{od}$	Outdoor air temperature ( $^{\circ}\text{C}$ )

$T_p$	Temperature of central node ( $^{\circ}\text{C}$ )
$T_{sp}$	Setpoint temperature of zone air( $^{\circ}\text{C}$ )
$T_s$	Temperature of South node ( $^{\circ}\text{C}$ )
$T_{wall}$	Borehole wall temperature ( $^{\circ}\text{C}$ )
$T_{w\_con}$	Water temperature of the condenser ( $^{\circ}\text{C}$ )
$T_{w\_con\_i}$	Inlet water temperature of the condenser ( $^{\circ}\text{C}$ )
$T_{w\_ct}$	Water temperature of the cooling tower ( $^{\circ}\text{C}$ )
$T_{w\_ct\_i}$	Inlet water temperature of the cooling tower ( $^{\circ}\text{C}$ )
$T_{w\_eva}$	Water temperature of the evaporator ( $^{\circ}\text{C}$ )
$T_{w\_con\_i}$	Inlet water temperature of the evaporator ( $^{\circ}\text{C}$ )
$T_w$	Temperature of West node ( $^{\circ}\text{C}$ )
$T_{wi}$	Inlet water temperature ( $^{\circ}\text{C}$ )
$T_{wo}$	Outlet water temperature ( $^{\circ}\text{C}$ )
$T_z$	Temperature of zone air ( $^{\circ}\text{C}$ )
$U_{ct}$	Conductance of the cooling tower ( $\text{W}/^{\circ}\text{C}$ )
$U_{i,j}$	Conductance of the $i^{\text{th}}$ cylindrical node to the $j^{\text{th}}$ one ( $\text{W}/^{\circ}\text{C}$ )
$U_{is}$	Conductance of inner shell of boiler ( $\text{W}/^{\circ}\text{C}$ )
$U_{ins}$	Conductance of insulation layer ( $\text{W}/^{\circ}\text{C}$ )
$U_{os}$	Conductance of outer shell ( $\text{W}/^{\circ}\text{C}$ )
$U_z$	Conductance of overall zone air ( $\text{W}/^{\circ}\text{C}$ )
$V$	Volume ( $\text{m}^3, \text{ft}^3$ )

$W_c$	Power input at design cooling load (W)
$W_h$	Power input at design heating load (W)
$X$	Time period length of MLAA scheme (hr)

**Greek Letters:**

$\alpha$	Ground thermal diffusivity ( $m^2/day$ )
$\rho$	Density of air/water/ground/grout ( $kg/m^3$ )
$\lambda$	Integration variable for ground heat exchanger
$\delta$	Differentiation
$\Delta$	Delta
$\theta$	Displacement (m, ft)
$\eta$	Burner efficiency
$\eta_{1,2}$	Circulating pumps efficiency

**Subscripts:**

a	Air
bo	Boiler

con	Condenser
ct	Cooling tower
d	Daily time period in MLAA scheme
eva	Evaporator
gl	Ground loop
h	Hourly time period
hp	Heat pump units
hx	Heat exchanger
in	In(let) /Inside
i	The $i^{\text{th}}$
ins	Insulation layer of boiler
is	Inner shell of boiler
j	The $j^{\text{th}}$
m	Monthly time period
o	Out(let) /Outside
os	Outer shell of boiler
w	Water
w	Weekly time period
y	Yearly time period
z	Zone

## ABBREVIATIONS

ACH	Air change per hour
ASHRAE	American society of heating, refrigerating, and air-conditioning engineers
CHS	Cylindrical heat source
COP	Coefficient of performance
EAT	Entering air temperature
EWT	Entering water temperature
GCHP	Ground-coupled heat pump
GSHP	Ground source heat pump systems
GLHX	Ground loop heat exchanger
HDPE	High-density polyethylene
HGSHP	Hybrid ground source heat pump systems
HVAC	Heating, ventilating, and air-conditioning
IAQ	Indoor air quality
MLAA	Multiple-load aggregation algorithm
P	Proportional control
PI	Proportional plus integral control
PID	Proportional plus integral plus derivative control
PLF	Part load factor
TDMA	Tri-diagonal matrix algorithm

# CHAPTER 1 INTRODUCTION

## 1.1 Background

Heat pumps, like conventional air-conditioners for cooling, are essentially air-conditioners that can also run in reverse mode in the winter for heating. They extract thermal energy from a variety of renewable sources, including the air, earth or water, and upgrade it to a more useful temperature. When the heat source for the system is the earth (or water), it is known as a ground source heat pump (GSHP) system. GSHP systems, also called geothermal heat pumps, come in a wide variety of configurations that use the earth or ground water or surface water as a source of heat to conditioned rooms in winter and as a sink for heat removed from the rooms in summer, while conventional air-to-air systems use ambient air as a heat source or sink (Lund et al. 2004). A simplified GSHP unit layout is shown in Figure 1.1, in which additional domestic hot water heater is not considered in this study.

GSHP systems can be classified as ground-coupled heat pumps, ground water heat pumps, and surface water heat pumps, according to the different heat sources or sinks. Ground-coupled heat pumps are often referred to closed-loop ground source heat pumps, and they consist of a reversible vapor compression cycle that links to closed ground heat exchangers buried in the ground. They can also be subdivided into conventional horizontal ground-coupled heat pumps, vertical ground-coupled heat pumps, and slinky coil ground-coupled heat pumps by the type of ground heat exchanger design (Kavanaugh and

Rafferty 1997).

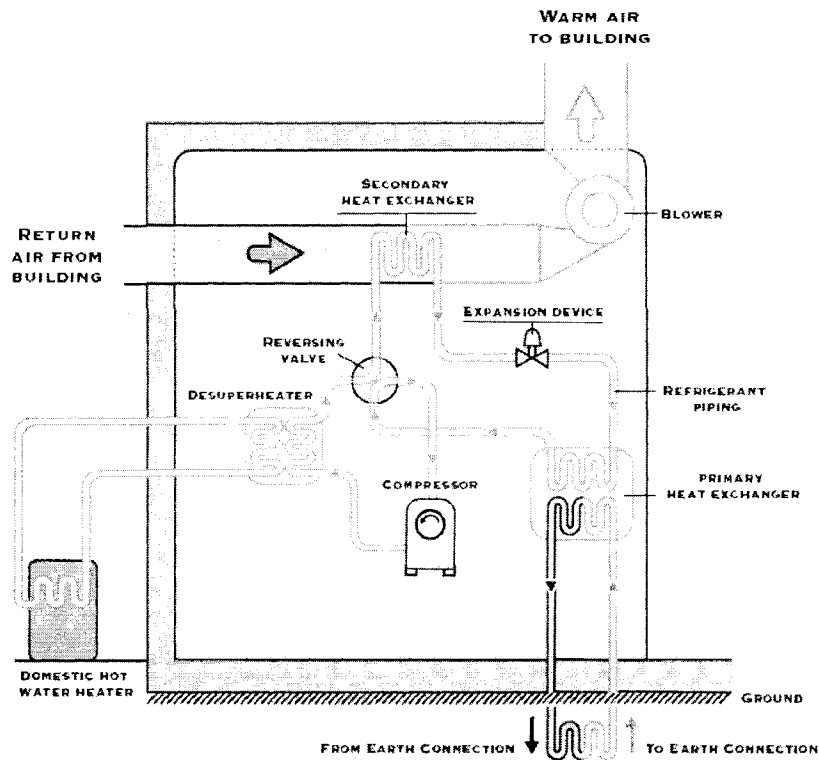


**Figure 1.1 Schematic Diagram of GSHP Unit Layout**

(Natural Sources Canada 2003)

Taking advantage of the earth or ground water as a heat source or sink is pretty attractive from a thermodynamic point of view since its temperature over the whole year is much closer to room conditions than the ambient temperature is. For this reason, GSHP systems are potentially more efficient than conventional air-to-air ones (Spitler et al. 2000). Compared to conventional HVAC systems, GSHP systems can in fact achieve significant energy savings; e.g. typical reductions in energy consumption of 30% to 70% in the heating mode and 20% to 50% in the cooling mode can be obtained (Clean Energy

Project Analysis). A secondary advantage is that GSHP systems improve the performance with water as the working fluid and have lower maintenance costs. Although tapping the underground thermal source can have a higher first cost, GSHP systems will offer better thermal comfort and have lower operating and maintaining costs; that is, the high first cost is offset by the reduced running costs and the system therefore has a lower life cycle cost (Bose et al. 2002). Moreover, GSHP systems with properly designed ventilation system can offer a good solution for indoor air quality (IAQ). As a result, GSHP systems are one of the fastest growing applications of renewable energy in the world with annual increases of 10% in about 30 countries over the past 10 years (Lund et al. 2004).

GSHP systems were originally utilized in residential buildings, while more recently the non-residential applications are beginning to dominate in terms of installed capacity (Bose et al. 2002). The present worldwide installed capacity is estimated at more than 12,000 MW and the annual energy use is at least 72,000 TJ (20,000 GW-h). The actual number of installed units can be as many as 1,100,000 even though the data are incomplete. These numbers are forecast to grow more rapidly in the years ahead (Lund et al. 2004).

Hybrid ground source heat pump (HGSHP) systems are GSHP systems that extract heat from (or reject heat to) not only ground heat exchangers but also supplemental boilers (or supplemental fluid coolers). Because ground heat exchanger for GSHP is costly and more imbalanced loads require more ground heat exchanger length, the cost of installation of a GSHP system can be very expensive in heavy cooling- or

heating-dominated applications. With a hybrid system, the size of the ground heat exchanger can be reduced as the supplemental fluid cooler provides additional heat rejection capacity or/and the supplemental boiler provides additional heat extraction capacity. As a consequence, the overall HGSHP system cost is reduced whereas total energy use may be about the same.

## **1.2 Motivation and Objectives**

The emphases of this thesis are to develop a dynamic model for each component of a HGSHP system, to design PI or On/Off controllers for each component in both heating and cooling modes, to introduce control strategies for the whole system, to determine user-defined optimal set points of control variables in both heating and cooling modes, and to conduct energy simulations of the HGSHP system under realistic cooling and heating modes of operation.

The main objectives of the study are as follows:

(1) To design a hybrid GSHP system for an office building located in Montreal by using practical guidelines and steady state methods.

(2) To examine the influence of design parameters on the system's operation in both heating and cooling modes.

(3) To study the influences of building loads, zone air temperature, ambient temperature, circulating water flow rate, and supply and return water temperatures by carrying out simulation runs. They can also be used to analyze and simulate the responses

of the HGSHP system.

(4) To conduct energy simulations of the system in different operating conditions and to qualitatively evaluate the potential energy savings.

(5) To design PI and On/Off controllers for the HGSHP system in order to improve system efficiency and thermal comfort.

(6) To introduce control strategies and search optimal control variables for hybrid ground source heat pump system in order to improve the overall performance and to achieve energy savings.

### **1.3 Organization of Thesis**

The introduction of the thesis is presented in this Chapter. In Chapter 2, a literature survey of previous studies on steady and dynamic state models of heat pumps, cooling towers, boilers, as well as vertical ground heat exchangers will be reviewed. Then, an overall HGSHP system description, system design, and equipments selection are given in Chapter 3. Next, in Chapter 4, the dynamic models of each component of HGSHP system are presented. A detailed multiple-load aggregation algorithm (MLAA) will be described to account for the transient heat conduction in the vertical ground heat exchanger model. Simulations of each component and overall HGSHP system will be carried out and the simulation results will be shown. After that, On/Off control, PI control, and optimal control strategies for heating and cooling modes of operation are described and simulation results will be presented in Chapter 5. Finally, a summary, contributions, and

conclusions of this study, as well as recommendations for future research will be included in Chapter 6.

## **CHAPTER 2 LITERATURE REVIEW**

### **2.1 Introduction**

Hybrid ground source heat pump systems consist of such components as heat pump units, ground heat exchangers, cooling towers, or/and boilers. Each component has a variety of mathematical models. When considering heat pump system simulations, it was observed that the different models can be broadly classified as steady state and dynamic models. In this study, in addition to steady state and dynamic heat pump models, various vertical ground heat exchanger models – the key component of the system in the thesis – will be surveyed. Not only heat pump and ground loop models, but also a variety of models of other components of the system, like cooling tower and boiler, will also be reviewed in the following sections.

### **2.2 Heat Pump Models**

#### **2.2.1 Steady State Models**

Fischer and Rice (1983) developed a heat pump model at Oak Ridge National Laboratory (ORNL). The model, with a FORTRAN-IV computer program, can predict the steady state performance of conventional vapor compression heat pumps in heating or cooling mode of operation. Given a set of model inputs, such as operating mode, compressor characteristics, refrigerant flow control device, fin and tube heat exchanger parameters, etc., it will calculate system capacity and COP, compressor and fan motors'

energy consumption, coil outlet air temperature, air- and refrigerant-side pressure drops, overall compressor and heat exchanger's efficiencies, and a summary of the refrigerant states throughout the cycle. Despite these, the model cannot predict the refrigerant charge inventory in each component at a specific moment.

Krakow and Lin (1983) presented a model for the simulation of multiple source heat pump systems. The model consists of sub-models such as reciprocating compressor model, evaporator model, condenser model, expansion valve model, and liquid suction sub-cooling heat exchanger model. The heat pump model can determine steady state performance characteristics of a heat pump based on experimental investigations of a multiple source heat pump for cold climates. Krakow and Lin (1987) improved such model. The new model considers additional refrigerant mass flow rate and capacity controls by means of expansion valves responding to the superheat degree of the refrigerant downstream of the evaporator and capillary tubes, and to the evaporator pressure and limiting refrigerant charge. The new model can predict the transition between refrigerant dominant operation modes of capillary-tube-controlled heat pumps. The model omitted variable speed drive efficiency considerations from the analysis and considered only the thermodynamic performance.

Cecchini and Marchal (1991) developed a simulation model based on thermodynamic cycles and experimental data from equipment testing. The model characterizes the performance of chillers using five parameters, namely polytropic exponent, swept volume, built-in volume ratio, evaporator and condenser heat transfer

area, which are identified from two testing points in steady state conditions. The model includes such submodels as evaporator, condenser, thermostatic expansion valve, and compressor models. The refrigeration cycle is described by 11 equations with 11 unknowns: the saturation pressures and temperatures in the evaporator and condenser, the enthalpies before and after each component, the refrigerant mass flow rate and the thermal conductances of the evaporator and condenser. The model can predict the performance of equipments from test data.

Jin and Spitler (2002) developed a parameter-estimation-based simulation model for a water-to-water reciprocating vapor compression heat pump. The model developed from basic thermodynamic principles and heat transfer relations of the refrigeration cycle is intended for using in heat pump system energy calculation and building simulation programs. The model includes several unspecified parameters that are estimated from manufacturers' catalog data by using a multi-variable optimization algorithm. It was developed with the objective of only requiring input data that are readily available from the manufacturers' catalogs. A thermostat signal is used as an input parameter to indicate which set of parameters of operating modes will be used. The objective function evaluation takes advantage of the fact that the heat transfer rates are known. Using the catalog data as an initial guess, the model minimizes the difference between the measured and predicated heat transfer rates. Once the optimal values of the performance parameters have been determined, the model will output temperatures of fluid flows, total capacities, and COP of the model over its full operating range. Compared to curve fit models, a

better match to the catalog data is obtained by using multi-variable optimization

### **2.2.2 Dynamic Models**

MacArthur (1984) presented a detailed model of vapor compression heat pump, which is among the earliest forms of a fully distributed representation of the refrigerant dynamics in the system. The model, based on energy conservation principle, has a submodel of accumulator, in addition to evaporator, condenser, compressor, and expansion valve models. The heat pump model can dynamically predict the spatial values of temperature and enthalpy of the heat exchangers and they are all expressed as a function of time. The space-time dependent conservation equations are simplified by assuming one-dimensional flow in both heat exchangers. The two-phase region in the condenser is regarded as homogenous, while the liquid and vapor phases in the evaporator are treated separately. The temperature and enthalpy in other components can be obtained from the simulations using lumped-parameter approach. The model needs to optimize the component and system design in order to increase energy efficiency of heat pump system.

Murphy and Goldschmidt (1984) experimentally developed simplified system models to study start-up and shut-down transients for an air-to-air heat pump system. In the start-up model, the dynamic treating are those of the capillary tube and the phenomenon of liquid backing up into the condenser during start-up. The compressor is modeled from steady state measurements and actual measurements of evaporator

performance are utilized replacing evaporator model. The condenser dynamics are those of the refrigerant pressure response and the tube material. In the shut-down study, both heat exchangers are modeled as tanks containing two-phase refrigerant at different pressures to begin with air as the secondary fluid cooling or heating the coils by natural convection. The refrigerant is allowed to flow only through the capillary tube initially and then through a valve, which opens shortly after shutdown. In order to ensure an accurate entry condition to the capillary tube, the liquid line is modeled in detailed to obtain the variation in refrigerant quality between entry and exit.

Rossi and Braun (1999) developed a fast mechanistic model of a roof-top air conditioning unit. The study uses real time simulation and automatic integration step sizing algorithm. The algorithm is presented to robustly simulate start-up and On/Off cycling. The system model is constructed with a fully finite volume formulation of the mass and energy balances in the heat exchangers. The model is validated with start up measurements from a 3-ton roof top unit. A good match to smaller capacity units observed, but bigger errors will likely occur with higher capacity units.

Browne and Bansal (2000) presented and compared a simple dynamic model with a dynamic neural network model of a screw chiller system. The screw compressor is modeled as steady state device using a steady flow displacement equation and an energy balance, and assuming isentropic compression. The dynamics of the system are expressed in terms of lumped elements for the heat exchangers material and the water. The refrigerant in the heat exchangers is treated quasi-statically assuming a uniform

refrigerant flow rate through the system.

## 2.3 Ground Heat Exchanger Models

As mentioned in the preceding chapter, geothermal heat pumps are categorized ground-coupled heat pumps (GCHP), ground water heat pumps, and surface water heat pumps according to the different type of heat source or sink. This chapter will concentrate on the vertical ground-coupled heat pumps and ground heat exchanger models for such heat pumps.

There are a number of models developed for the analysis and sizing the vertical ground heat exchangers. Most of these models are mainly based on the Kelvin's line source theory, cylindrical source theory, or numerical methods. The main ideas of them are briefly introduced as follows.

Kelvin (1882) developed the line source theory assuming the ground is infinite medium, and heat conduction process is simplified as one-dimensional due to the fact that the length of the vertical ground heat exchanger is much greater than its diameter. Ingersoll (1954) assumed that heat transfers from an infinite long line source or sink in an infinite medium. The line source model uses a simply steady-state heat transfer equation.

$$q = \frac{L(T_g - T_w)}{R} \quad (2-1)$$

where

q = heat transfer rate, kW

L = required bore length, m

$T_g$  = ground temperature, °C

$T_w$  = liquid temperature, °C

$R$  = effective thermal resistance of the ground, m-k/kW

The equation is used to handle hourly heat transfer rate variations. It can also be rearranged to solve for the required borehole length  $L$ . These models are only for a true infinite line source and the heat flow must be radial. That is, they are not accurate for finite length of boreholes in the real applications, and they neglect the axial heat flow. In addition, such models do not take heat transfer between the ground and the top and bottom of boreholes into account. Furthermore, they cannot account for the leg-to-leg thermal short-circuiting effects for the most popularly used U-tube boreholes, which is significant in transient heat transfer.

Carslaw and Jaeger (1947) used the cylindrical heat source (CHS) analytical solution,  $G$  functions, to account for cylindrical heat transfer in soil. The CHS analytical solution,  $G(Fo)$ , is a function of Fourier number,  $Fo$ , which is defined as:

$$Fo = 4\alpha t / d_b^2 \quad (2-2)$$

where

$\alpha$  = ground thermal diffusivity,  $m^2/day$

$t$  = time, day

$d_b$  = cylindrical diameter, m

For the cylindrical heat source models, the boreholes are subjected to varying ground loads,  $q$ . The boreholes wall temperatures at time  $t$ ,  $T_{w,t}$ , can be obtained using the CHS

analytical solution.

$$T_{w,t} = T_g - \frac{q}{L} \frac{G(Fo)}{k_s} \quad (2-3)$$

where

q = heat transfer rate, W (a positive value for heating, negative for cooling)

L = borehole length, m

Fo = dimensionless Fourier number

G(Fo) = CHS analytical solution

k<sub>s</sub> = ground thermal conductivity, W/m-k

Hart and Couvillion (1986) developed Kelvin's line source theory by employing its continuous time dependent heat transfer between the line source and the ground to derive a time dependent temperature distribution around the line source heat exchanger.

$$T(r,t) - T_g = \frac{Q(t)}{4\pi k} \int_{\frac{r^2}{4\alpha t}}^{\infty} \frac{e^{-\lambda}}{\lambda} d\lambda \quad (2-4)$$

where

T<sub>g</sub> = far-field undisturbed ground temperature, °C

Q(t) = heat transfer rate at time t, W

k = ground thermal conductivity, W/m-k

r = radius from the line source, m

α = ground thermal diffusivity, m<sup>2</sup>/day

t = time, day

λ = integration variable

The far field radius,  $r_{\infty}$ , and the undisturbed temperature,  $T_g$ , are introduced to this model. The radius  $r_{\infty}$  can be computed by  $r_{\infty}=4(\alpha t)^{0.5}$ , and the temperature  $T_g$  mainly depends on the diffusivity of the ground and the period of time the line source heat exchanger operates. Then the superposition principle is applied to account for the model thermal interference effects. This model is quite similar to the simple line source model except interference effects.

Eskilson (1987) studied the problem of determining the temperature response of a multiple borehole ground heat exchanger. It is a hybrid model combining analytical and numerical solution techniques. The mathematical formulations of this model are based on dimensionless temperature response factors, called g-functions, which are different from the g functions used in the cylinder source solution. The g-functions are essentially the temperature responses of the borehole field to unit step function heat pulses and can be pre-calculated for individual configurations using a finite difference program and spatial superposition. Once the response factors are determined, the response of the ground loop heat exchanger to any heat transfer versus time profile can be determined by decomposing the heat transfer versus time profile into a set of unit step functions. Then, the response of the ground heat exchanger to each unit step function can be superimposed to determine the overall response. This model is intended to provide the response of the ground to the heat exchanger over a long period of time, like up to 20 years. However, it cannot accurately provide the shorter term response as the g-functions do not account for the local borehole geometry.

Yavuzturk et al. (1999) developed a numerical model to describe the transient heat transfer process in and around the vertical ground heat exchanger based on finite volume method. Heat conduction in the ground loop heat exchanger presented is in two dimensions. The horizontal transient conduction equation in polar coordinates was expressed as follows:

$$\frac{1}{\alpha} \frac{\partial T}{\partial t} = \frac{\partial^2 T}{\partial r^2} + \frac{1}{r} \frac{\partial T}{\partial r} + \frac{1}{r^2} \frac{\partial^2 T}{\partial \theta^2} \quad (2-5)$$

This equation has been discretized with a fully implicit finite volume approach of Patankar (1980, 1991). First order backwards differencing in time and second order central differencing in space have been used, and the resulting discrete equation turns out to be:

$$a_P T_P = a_N T_N + a_S T_S + a_E T_E + a_W T_W + b \quad (2-6)$$

where

$$a_P = a_N + a_S + a_E + a_W + a_P^0$$

$$a_P^0 = \frac{(\rho c)_P \Delta V}{\Delta t}$$

$$a_N = \frac{k_n r_n \Delta \theta_n}{(\delta r)_n}$$

$$a_S = \frac{k_s r_s \Delta \theta_s}{(\delta r)_s}$$

$$a_E = \frac{k_e \Delta r_e}{r_e (\delta \theta)_e}$$

$$a_W = \frac{k_w \Delta r_w}{r_w (\delta \theta)_w}$$

$$b = S_C \Delta V + a_p^0 T_p^0$$

$T_N$ ,  $T_S$ ,  $T_E$ , and  $T_W$  refer to temperatures at neighboring points of the central node.

Applying this equation to each point of the calculation domain, a linear set of algebraic equations were obtained. The resulting algebraic equations are linear and were solved using a line-by-line tri-diagonal matrix algorithm (TDMA). The calculation results of the model were found to be accurate. However, the numerical model using polar or cylindrical grids cannot model multiple borehole configurations. Furthermore, the computational resources to obtain the time-varying average borehole field temperature on the more complex grids would be considerably high.

## 2.4 Cooling Tower Models

Cattan and Fabre (1989) studied wind effects on the water temperature in natural draft cooling towers. They found that cooling water temperature would increase 3 degrees Celsius at a wind speed of around 10 m/s measured 11 meters above ground rather than ground level. Probability of wind occurrence was used in the study, and a conclusion that the towers should be designed for a wind conditions of 4 m/s rather than the conventional zero wind velocity was drawn. Accordingly, the study reached a conclusion that suppliers of cooling towers should take the wind effect into account and provide the variation of the heat exchanger coefficient and the pressure drop coefficient for the tower as a function of wind velocity as part of the supplied documentation to users to evaluate the cooling tower performance.

Rennie and Hay (1990) presented a simple one-dimensional numerical cooling tower model. The model, ignoring non-uniformity effects, derives an approximate expression to estimate the wind induced resistance. The results of the adopted simple model are not accurate enough as the model underestimates the wind effects at low speed. Also, the model has limitations for assessing major changes in tower packing and for modeling the devices for reducing wind induced performance losses. Rennie (1992) developed a two-dimensional cooling tower model after studying one-dimensional and two-dimensional numerical modes, in which some marked discrepancies in temperature or velocity distributions between those predicted by the two dimensional model and full scale measurements were observed. The model was validated by employing full scale experimental tests results. The predicted data from the model at the eliminators were adequate, but some errors in the effective flow resistance at the tower inlet and exit still exist. A three-dimensional model may be needed to enable the effects of wind on tower performance.

Du Preez (1992) employed an isothermal physical model, a numerical one and full scale tests to study the effect of cross wind flow on the performance of dry cooling towers. The study pointed out that parameters, e.g. wind speed, the approaching wind profile shape, the inlet diameter to the inlet height ratio of the tower, tower height, shape of the tower shell, the pressure loss coefficient of the heat exchanger, and amount of heat rejected by the tower, would impact on the action of the wind on such towers. Due to the assumption that the form of the approaching wind profile have little effect on the pressure

loss coefficient, the test results of the model are generally in quantitative agreement with those from other full scale cooling towers. However, when an increase in the wind effect on the performance of the tower was obtained at higher heat rejection rates, the opposite results were also observed on the full scale tower. Some flow conditioning devices were also developed and applied to the models, and significant reductions in the wind effect on the tower performance were found. Though he observed that the approaching wind profile had a very small effect on the pressure coefficient, the coefficient cannot be neglected.

## **2.5 Boiler Models**

The most important process influencing boilers' performance is the heat transfer process, so the key effort in boiler modeling is the development of more reliable method for boiler heat transfer predictions. A wide range of mathematical boiler models developed will be briefly reviewed as follows.

Huang et al. (1988) presented a nonlinear steady state thermal performance model of a fire-tube boiler. The model consists of two semi-empirical equations for the heat fluxes: one for radiative heat flux from the combustion gas to the boiling water and the other for the heat loss flux from the body surface to the ambient. Six unknown parameters in the model were assumed to be constant for any given boiler and were determined by the experimental data. The model was utilized to simulate boiler performance under nominal operating conditions.

Claus (1985) developed a computer simulation model for boilers. The model is used to calculate the thermal state of a boiler with the method of indirect determination of the boiler efficiency. The model is a semi-analytic model and it is applied to investigate the effects of different parameters on the behavior of the boiler and energy consumption.

Steward (1974) presented a mathematical model for the heat transfer in a large modern boiler. The model shows that the simulation of the heat transfer can be performed by using the data available in an operating plant. The model uses mathematical technique for evaluating the radiative heat transfer in a furnace enclosure.

Richter et al. (1984) presented an advanced computer model for 3-dimension furnaces. The model can provide combustion analysis for furnace design and performance study. The 3-D furnace model allows the predictions of parameters, such as local and overall heat transfer rates, temperature profile, and burnout of solid fuel particles in boiler combustion chambers that are dependent on actual furnace geometry and operating conditions, and fuel characteristics.

Fiveland and Wessel (1986) developed a model to simulate steady-state 3-dimension combustion for practical furnace geometries. The model is based on a fundamental description of various interacting processes occurring during combustion, such as turbulent flow, homogeneous and heterogeneous chemical reactions, and heat transfer. The model, with detailed analysis, was used to evaluate furnace performance and to interpret laboratory and utility test data.

# CHAPTER 3 PHYSICAL MODEL DESCRIPTION AND SYSTEM DESIGN

## 3.1 Introduction

The physical model of a HGSHP system for an office building located in downtown Montreal is considered in this thesis. It is actually one floor of a high-rise office building. The layout of the floor is shown in Figure 3.1, and it has a total area of 30,000 ft<sup>2</sup> (2,787 m<sup>2</sup>). The office building consists of eight zones and is designed to be served by eight heat pumps.

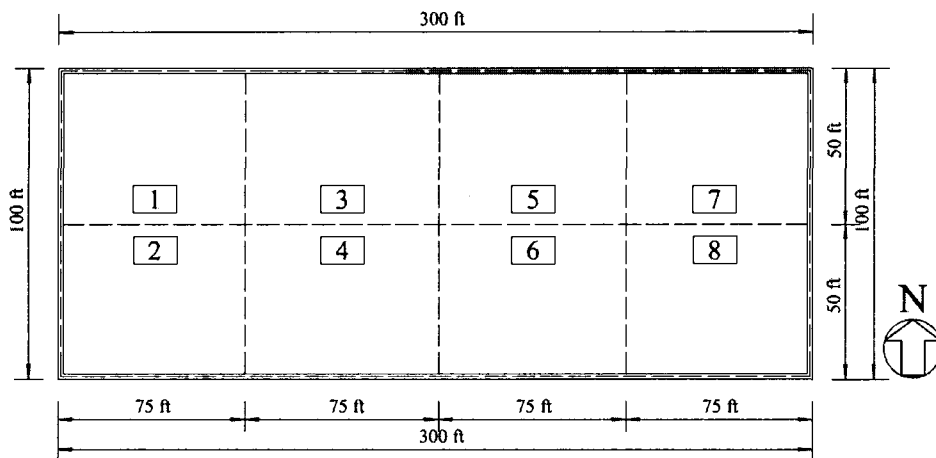
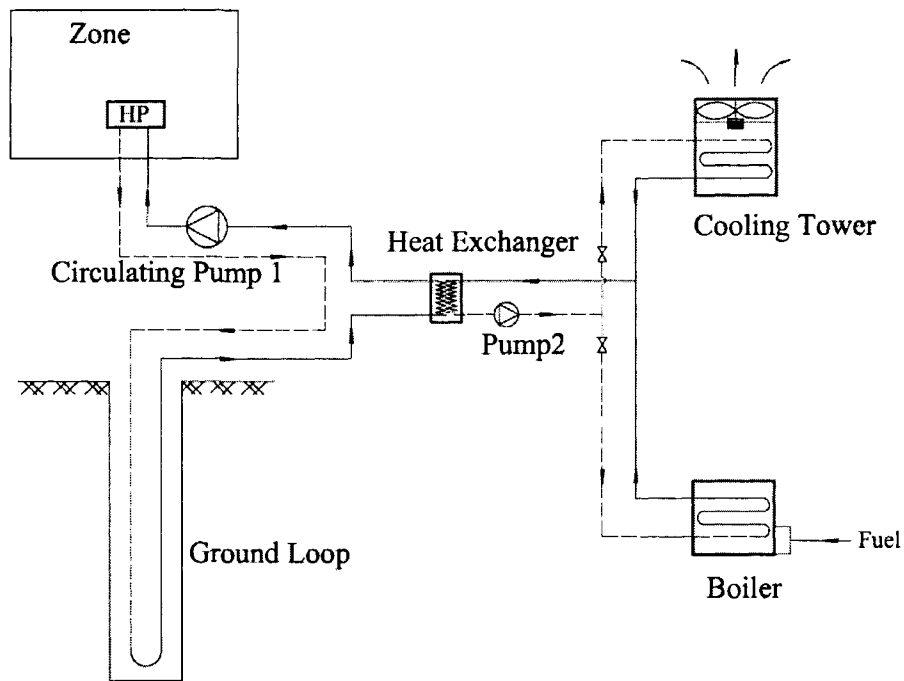


**Figure 3.1 Office Building Floor Layout**

To simplify the analysis, to begin with an aggregate zone and a heat pump system in considered as shown in Figure 3.2. A hybrid ground source heat pump system will be

designed to heat and cool this office space. The HGSHP system consists of such components as water-to-air heat pumps, vertical ground loop heat exchangers, circulating pumps, a plate heat exchanger, a supplemental cooler, and a supplemental boiler.



**Fig**

**ure 3.2 Schematic of Hybrid Ground Source Heat Pump System**

### **3.2 Heating and Cooling Loads**

Building cooling load calculation can be done with Heat Balance Method or Time Series Method recommended by ASHRAE (2005), or by computer programs, such as DOE-2.1E, EE4-CBIP, BLAST, TRACE600, HVACSIM+, etc.. Building loads can also be approximately determined by rules of thumb. For instance, heating load for office building ranges between 30 to 40 Btu/h-ft<sup>2</sup>, and cooling load ranges from 300 to

350ft<sup>2</sup>/ton (ASHRAE 2005). Generally, calculations from rules of thumb are less accurate and mostly used in preliminary design stage.

Hourly heating and cooling loads on each design day for the building in this case are calculated with the computer program of EE4-CBIP from Natural Resources Canada's Office of Energy Efficiency. The peak heating load is 435,000 Btu/h (127,455 W) occurring in January, and the design cooling load is 565,000 Btu/h (165,545 W) occurring in July.

### **3.3 Sizing Ground Heat Exchangers**

Assuming the building is located in downtown and lacks the available land requirement around the building for vertical ground heat exchangers, a ground heat exchanger is designed to satisfy only 50% of heating and cooling capacities of the building. The excess loads will resort with a supplemental boiler in heating mode of operation and with a supplemental cooling tower in cooling mode of operation.

This study focuses on HGSHP systems that mainly use vertical ground heat exchangers to heat and cool the building. As shown in Figure 3.3, the ground heat exchanger used in the project is made up of a number of boreholes, in which U-tube is inserted, in a plot of borefield. The diameter of boreholes is 4 inches, while that of U-tube is 1.5 inches. The boreholes are filled with a thermally enhanced grout in order to make a better connection between U-tubes and the ground and consequently have a better thermal conduction.

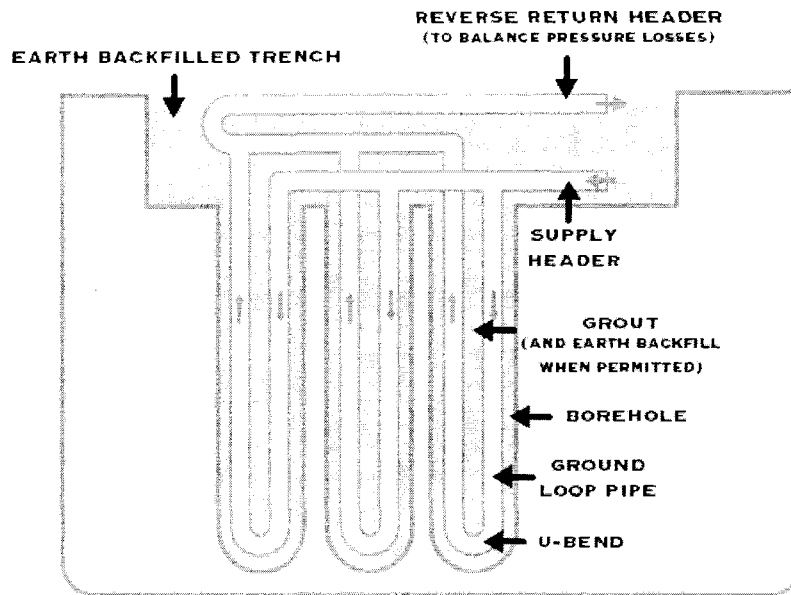


**Figure 3.3 Schematic of Vertical Ground Heat Exchangers**  
(Clean Energy Project Analysis 2005)

According to ASHRAE (2003), the borehole length for cooling is calculated using the equation,

$$L_c = \frac{q_a R_{ga} + (q_c - W_c)(R_b + PLF_m R_{gm} + R_{gd} F_{sc})}{t_g - \frac{t_{wi} + t_{wo}}{2} - t_p} \quad (3-1)$$

while the required borehole length for heating is,

$$L_h = \frac{q_a R_{ga} + (q_h - W_h)(R_b + PLF_m R_{gm} + R_{gd} F_{sc})}{t_g - \frac{t_{wi} + t_{wo}}{2} - t_p} \quad (3-2)$$

where

$L_c$  = required borehole length for cooling, m

$L_h$  = required borehole length for heating, m

$q_a$  = net annual average heat transfer to the ground, W

$q_c$  = building design cooling block load, W

$q_h$  = building design heating block load, W

$R_{ga}$  = effective thermal resistance of ground for annual pulse, m-k/W

$R_{gm}$  = effective thermal resistance of ground for monthly pulse, m-k/W

$R_{gd}$  = effective thermal resistance of ground for daily pulse, m-k/W

$PLF_m$  = part load factor during design month

$R_b$  = thermal resistance of borehole, m-k/W

$W_c$  = power input at design cooling load, W

$W_h$  = power input at design heating load, W

$F_{sc}$  = short circuit heat loss factor between U-tube legs

$t_g$  = undisturbed ground temperature, °C

$t_p$  = temperature penalty for interference of adjacent bores, °C

$t_{wi}$  = water temperature at heat pump inlet, °C

$t_{wo}$  = water temperature at heat pump outlet, °C

Note that heat transfer rate, building loads, and temperature penalties are positive for heating operation and negative for cooling. The above equations consider three different pulses of heat to account for long-term heat imbalances, average monthly heat rates during the design month, and maximum heat rates for a short-term period during a design day. This period can be as short as an hour, but a 4-hour block is usually recommended (ASHRAE 2003).

When taking 50 per cent of the known design building heating and cooling loads, we

get total borehole length for heating  $L_h=1,502$  m (4,928 ft) and for cooling  $L_c=1,917$  m (6,289 ft) respectively. Then, the maximum one, 1,917 m (6,289 ft), is used as total design borehole length of the system.

### **3.4 Borehole and Grouting Design**

The most commonly used borehole design is the single high-density polyethylene (HDPE) U-tube grouted with thermally enhanced grout. This design can protect aquifers from contamination and is considered to be very reliable. A schematic diagram of boreholes is given as shown in Figure 3.4. As borehole length cannot be designed as deep as possible due to its huge installation cost, lengths ranging from 40 to 180 m (131 to 591ft) are used (ASHRAE 2003). In this study, a moderate borehole length of 100 m (328 ft) is taken. As a result, the total number of borehole in the borefield is  $n =20$ . That is, 4-by-5 boreholes are contained and installed in the plot. In order to lower mutually thermal interference of any borehole with adjacent boreholes, the distance among boreholes is kept around 20 feet (6.1 meters).

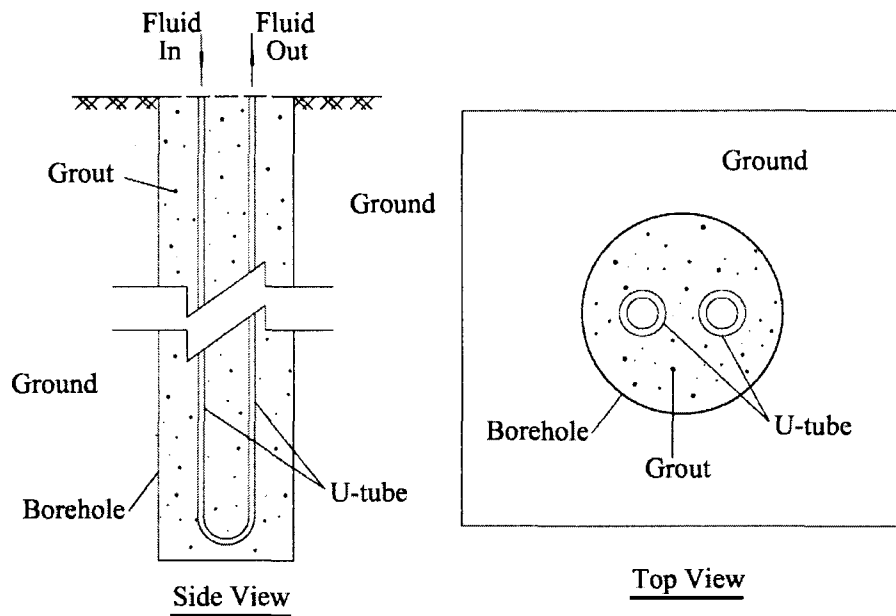


**Figure 3.4 Schematic Diagram of Borehole**

The diameter of a borehole generally ranges from 4 to 6 inches, and that of the HDPE U-tube is from 0.75 to 1.5 inches (ASHRAE 2003). In this study, 6 inches and 1.5 inches are taken for borehole and U-tube diameters, respectively.

For the grout of the borehole, a thermally enhanced cement grout is chosen in order that heat transfer between the working fluid and the ground can be better. The thermal conductivity of typical thermally enhanced cement grout ranges from 0.75 to 1.07 Btu/hr-ft-k (1.29 to 1.85 W/m-k). Of course, the value can be even lower for some other specific grouting materials (ASHRAE 2003).

### **3.5 Equipments Selection**

According to the building design heating and cooling loads of 435,000 Btu/h and

565,000 Btu/h respectively, 8 heat pump units of 6-ton (72,000 Btu/h) capacity each are selected for the building.

Since only 50 per cent of building peak cooling load can be rejected to the ground by means of ground loop heat exchangers, there is still a load of 282,500 Btu/h left to transfer to ambient by a supplemental cooling tower. Also, taking into account the power input of heat pump compressors and circulating pumps, a closed circuit cooling tower with a 32-Ton capacity is selected for the plant.

Due to the fact that 60 per cent of heat at design load can be extracted from the ground with the ground loop in heating mode of operation, a boiler with a capacity of 200,000 Btu/h is installed for the plant, considering a safety factor of 1.15.

As for circulating pump 1, two identical multiple speed pumps are selected; one for main pump and the other standby. Each pump has a maximum flow rate of 10.6 kilograms per second and a total head of 38 meters.

Similarly, two identical multi-speed pumps are selected for circulating pump 2, one for main pump and the other standby. Each pump has a maximum flow rate of 5.6 kilograms per second and a total head of 21 meters.

### **3.6 Pipe Insulation**

All pipes from the top of boreholes and the manifolds in the ground to the main pipe in the building were insulated in order to prevent fluid from freezing in the winter. In addition, all pipes from boiler to the plate heat exchanger were also insulated.

Both the insulation material and the insulation thickness were specified based on specific design conditions. According to ASHRAE (2002), fiberglass piping insulation layer was used in this study: 1 inch thick for pipe sizes up to 1'', 1.5 inches thick for pipe sizes 1.25'' to 4'', and 2 inches for pipe over 5''.

### **3.7 Antifreeze Solution**

When GSHP systems are operating in heating mode, exiting water temperature from heat pump units can drop as low as  $-3^{\circ}\text{C}$ . It is much less than its freezing point and water will therefore be frozen and have ill effects on the performance of GSHP systems. As a result, the systems should have an antifreeze solution in order to prevent water from freezing. Antifreeze mixtures are commonly and widely used as the solution. The closed-loop system in this study uses an antifreeze mixture of 12.9% propylene glycol by weight, which has a  $-3.9$  degrees Celsius freezing point. Actually, different concentrations of antifreeze will affect the sizing results and system performance, but it is always chosen as a reasonably typical value and applied in every case even though different locations might have different optimal concentrations (Deng O'neill et al. 2006). The antifreeze mixture used in the system has also other effects. These include the cost of the antifreeze, the change of the borehole resistance, the change of the system performance, the change of circulation pumping power.

In this study, though the antifreeze mixture used in the system has a low freezing point of  $-3.9^{\circ}\text{C}$ , the system is designed to maintain a safety margin of  $2^{\circ}\text{C}$  between the

minimum exiting fluid temperature from heat pump and the working fluid freezing point at its full load in heating mode of operation.

# CHAPTER 4 DYNAMIC MODELING AND SIMULATION RESULTS

## 4.1 Model Description

In this chapter component models and integrated system models are developed.

### 4.1.1 Zone Model

For a single aggregated zone building, the energy conservation equation on the zone air side is given by:

$$C_{a_z} \frac{dT_{a_z}}{dt} = G_{a_{hp}} c_{p_a} (T_{a_{hp_o}} - T_{a_z}) + U_z (T_{od} - T_{a_z}) + Q_{int} + Q_{sol} + Q_{inf} \quad (4-1)$$

where

$C_{a_z}$  = thermal capacity of zone air, J/°C

$T_{a_z}$  = zone air temperature, °C

$G_{a_{hp}}$  = air flow rate of heat pump units, kg/s

$c_{p_a}$  = specific heat of air, J/kg-°C

$T_{a_{hp}}$  = outlet air temperature of heat pump units, °C

$U_z$  = conductance of zone air, W/°C

$T_{od}$  = outdoor air temperature, °C

$Q_{int}$  = internal heat gain of the zone, W

$Q_{sol}$  = heat gain of the zone from transmitted solar radiation, W

$Q_{inf}$  = heat gain of the zone from infiltration, W

The summation of the latter four terms on the right side of Equation (4-1) is actually the

building load,  $Q_b$ , which is positive when operating in heating mode, and negative in cooling mode.

By solving Equation 4-1, the temperature response can be determined. The simulation results of the zone model at design condition in both heating mode and cooling mode are shown in Figures 4.1 and 4.2, respectively. It is noted that the open loop system reaches near steady state in 10,000 seconds in heating mode and about 8,000 seconds in cooling mode. The response times are affected by the loads acting on the system.

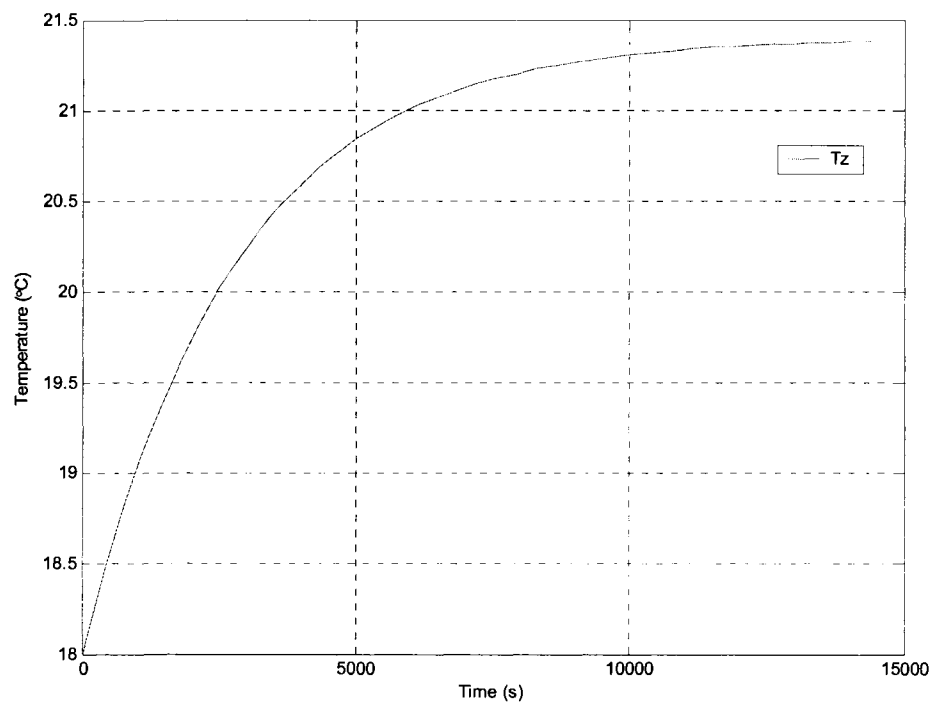


**Figure 4.1 Simulation result of zone model in heating mode**

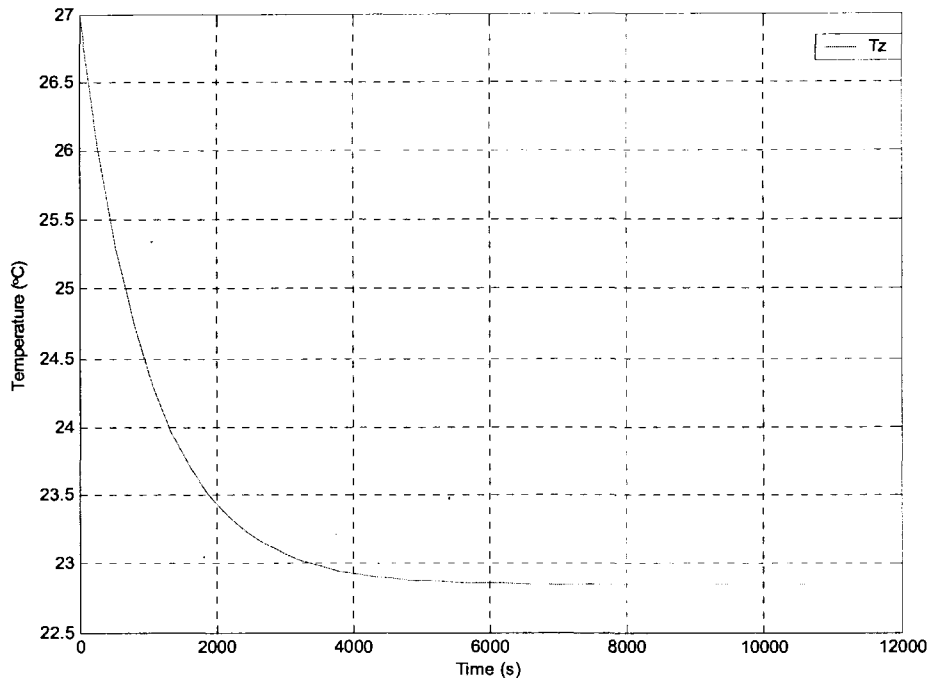


**Figure 4.2 Simulation result of zone model in cooling mode**

The design parameters used in simulations of the model are listed in Table 4.1 as follows.

**Table 4.1 Aggregated single zone model design parameters**

Symbol	Magnitude	Units
$C_{a_z}$	16,362,000	J/°C
$G_{a_{hp}}$ (Heating Mode)	5,900	Kg/s
$T_{a_{hp}}$ (Heating Mode)	39.5	°C
$Q_b$ (Heating Mode)	127,455	W
$G_{a_{hp}}$ (Cooling Mode)	16,000	Kg/s

$T_{a\_hp}$ (Cooling Mode)	12.5	°C
Symbol	Magnitude	Units
$Q_b$ (Cooling Mode)	165,545	W

#### 4.1.2 Heat Pump Model

The water-to-air heat pump model used in this study is modeled based on the approach given in HVACSIM+ using a polynomial equation (Deng O'Neill 2006):

$$HP\_cap = C1 + C2 * EWT + C3 * EWT^2 \quad (4-2)$$

$$HP\_pwr = C4 + C5 * EWT + C6 * EWT^2 \quad (4-3)$$

where

HP\_cap = the heat pump capacity, W

C<sub>i</sub> = equation fit coefficients (i=1,2...6), dimensionless

EWT = entering water temperature, °C

HP\_pwr = power input of the heat pump, W

As heat pump units selected for the HGSHP system are commercially available water-to-air heat pumps with a nominal capacity of 6 tons each, the equation fit coefficients for the 6-ton heat pumps are listed in Table 4.2.

**Table 4.2 Coefficients for 6-ton heat pumps**

	C1	C2	C3	C4	C5	C6
--	----	----	----	----	----	----

Heating Mode	16,186	489.8	-2.88	6,417	8.73	1.07
Cooling Mode	25,993	-180.6	-0.48	4,472	73.10	0.08

When heat pump units are operating in heating mode, the condenser component of the model has following dynamic equation. The energy conservation equation on the air side is given by:

$$C_{a\_con} \frac{dT_{a\_con}}{dt} = G_{a\_con} c_{p\_a} (T_{a\_con\_i} - T_{a\_con}) + HP\_cap \quad (4-4)$$

where

$C_{a\_con}$  = thermal capacity of condenser air, J/°C

$T_{a\_con}$  = outlet air temperature of the condenser, °C

$G_{a\_con}$  = outlet air flow rate of the condenser, kg/s

$c_{p\_a}$  = specific heat of air, J/kg-°C

$T_{a\_con\_i}$  = inlet air temperature of the condenser, °C

For the evaporator component, the energy conservation equation on the water side is given by:

$$C_{w\_eva} \frac{dT_{w\_eva}}{dt} = G_{w\_eva} c_{p\_w} (T_{w\_eva\_i} - T_{w\_eva}) - HP\_cap + HP\_pwr \quad (4-5)$$

where

$C_{w\_eva}$  = thermal capacity of evaporator water, J/°C

$T_{w\_eva}$  = outlet water temperature at the evaporator, °C

$G_{w\_eva}$  = outlet water flow rate of the evaporator, kg/s

$c_{p\_w}$  = specific heat of water, J/kg-°C

$T_{w\_eva\_i}$  = inlet water temperature at the evaporator, °C

While in cooling mode of operation, the evaporator component has following dynamic equation. The energy conservation equation on the air side is given by:

$$C_{a\_eva} \frac{dT_{a\_eva}}{dt} = G_{a\_eva} c_{p\_a} (T_{a\_eva\_i} - T_{a\_eva}) - HP\_cap \quad (4-6)$$

where

$C_{a\_eva}$  = thermal capacity of the evaporator air, J/°C

$T_{a\_eva}$  = outlet air temperature of the evaporator, °C

$G_{a\_eva}$  = outlet air flow rate of the evaporator, kg/s

$c_{p\_a}$  = specific heat of air, J/kg-°C

$T_{a\_eva\_i}$  = inlet air temperature of the evaporator, °C

For the condenser component, the energy conservation equation on the water side is given by:

$$C_{w\_con} \frac{dT_{w\_con}}{dt} = G_{w\_con} c_{p\_w} (T_{w\_con\_i} - T_{w\_con}) + HP\_cap + HP\_pwr \quad (4-7)$$

where

$C_{w\_con}$  = thermal capacity of condenser water, J/°C

$T_{w\_con}$  = outlet water temperature at the condenser, °C

$G_{w\_con}$  = outlet water flow rate of the condenser, kg/s

$c_{p\_w}$  = specific heat of water, J/kg-°C

$T_{w\_con\_i}$  = inlet water temperature at the condenser, °C

The air temperature responses of the heat pump model in cooling mode of operation are

shown in Figure 4.4. From these responses it can be seen that the steady state times of evaporator are of the order of 500 – 1500s. The thermal capacity of heat exchangers has dominant effect on steady state time. In the absence of experimental data, the thermal capacity was assumed by trial and error.

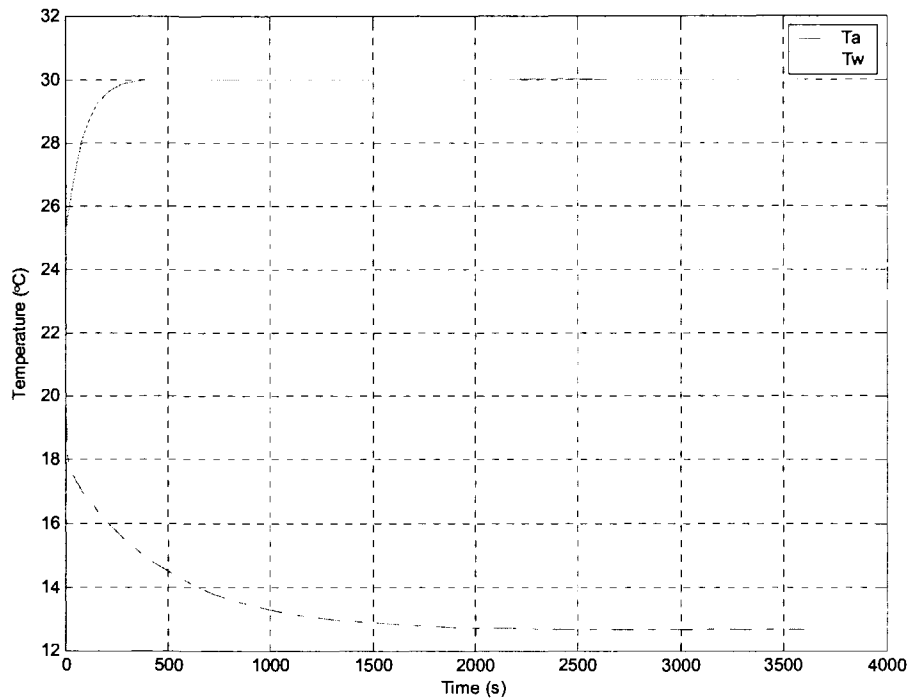


**Figure 4.4 Simulation result of the heat pump model in cooling mode**

The design parameters of the heat pump model are listed in Table 4.3.

**Table 4.3 Design parameters of the heat pump model**

Symbol	Magnitude	Units
$C_{a\_con}$ (Heating Mode)	8,400	J/°C

$G_{a\_con}$ (Heating Mode)	5,900	Kg/s
$T_{a\_con\_i}$ (Heating Mode)	21	°C
HP_cap (Heating Mode)	18,099	W
HP_pwr (Heating Mode)	6,469	W
$G_{w\_eva}$ (Heating Mode)	6.8	Kg/s
$T_{w\_eva\_i}$ (Heating Mode)	4	°C
$C_{a\_eva}$ (Cooling Mode)	8,400	J/°C
$G_{a\_eva}$ (Cooling Mode)	16,000	Kg/s
$T_{a\_eva\_i}$ (Cooling Mode)	23	°C
HP_cap (Cooling Mode)	20,578	W
HP_pwr (Cooling Mode)	7,304	W
$G_{w\_con}$ (Cooling Mode)	10.6	Kg/s
$T_{w\_con\_i}$ (Cooling Mode)	25	°C

### 4.1.3 Ground Loop Model

The vertical ground loop heat exchanger model used in this study is a cylindrical heat source (CHS) model adapted from Bernier et al. (2004). The model aggregates heating or/and cooling loads and takes into consideration the thermal interference among surrounding boreholes in the borefield. This model is referred to as multiple-load aggregation algorithm (MLAA).

As mentioned in Chapter 2, for a constant ground load  $q$ , the borehole wall temperature at time  $t$ ,  $T_{w,t}$ , can be determined from Equation (2-3). In order to obtain temperature of the fluid in the U-tube,  $T_f$ , the thermal capacitance of the borehole is neglected. Under the steady state assumption, the fluid temperature  $T_f$  is given by

$$T_{f,t} = T_g - \frac{q}{L} R_b - \frac{q}{L} \frac{G(Fo)}{k_s} \quad (4-8)$$

where  $R_b$  = the equivalent steady state borehole thermal resistance,  $m^{\circ}C/W$

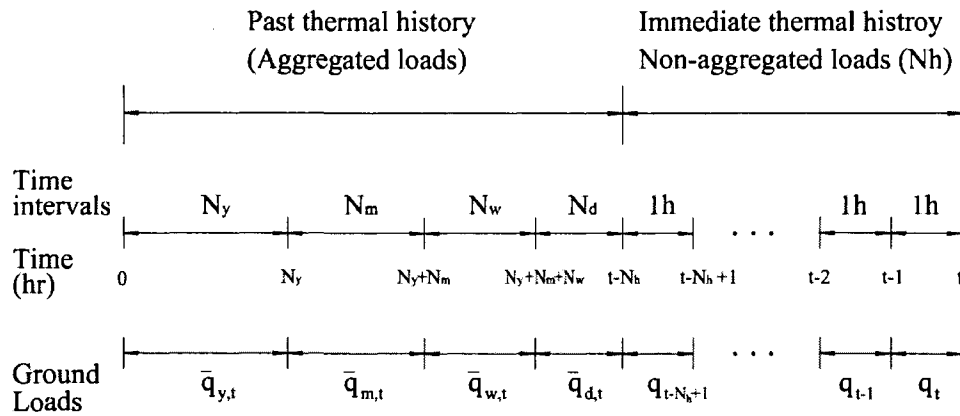


**Figure 4.5 Multiple-load aggregation Algorithm Scheme**

(Bernier et al. 2004)

The MLAA is an extension of Equation (4-8) for cases when ground loads vary with time. A schematic of MLAA shown in Figure 4.5 describes two major thermal history periods, e.g. referred to as *past* and *immediate* ones. The immediate thermal history noted by  $h$  is set to  $N_h$  hours, while the past thermal history is subdivided into four time intervals, denoted by the indices  $d$ ,  $w$ ,  $m$ , and  $y$ , which reflect the fact that the time periods are of the

order of a day (d), a week (w), a month (m), and years (y). In the scheme, constant ground loads are assumed over a given time interval. Meanwhile, ground loads in the past thermal history are aggregated, but loads in the immediate thermal history are not. On the other hand, values of  $q$  in the past history are aggregated loads obtained by taking the average of all ground loads of the time period interval and represented by an over-bar sign. For example,  $\bar{q}_d$  is an aggregated load obtained by taking the average of all ground loads of the last day, i.e. between the start of the  $(N_y + N_m + N_w + 1)^{\text{th}}$  hour and the end of the  $(N_y + N_m + N_w + N_d)^{\text{th}}$  hour (Bernier et al. 2004).

In the MLAA scheme, all of these periods except the yearly one have a fixed length, like  $X_h$ ,  $X_d$ ,  $X_w$  and  $X_m$  respectively. When the current time is smaller than the fixed length of immediate history period ( $t < X_h$ ) in the beginning of the simulation, the non-aggregated period,  $h$ , contains a number of hours equal to the time ( $N_h = t$ ). Then, it contains  $X_h$  hours ( $N_h = X_h$ ). The daily aggregated period,  $d$ , contains 0 hour ( $N_d = 0$ ) until the time reaches  $X_h + X_d$ . After that, it contains  $X_d$  hours ( $N_d = X_d$ ). The same method applies to the weekly and monthly periods ( $N_w = 0$  or  $X_w$ , and  $N_m = 0$  or  $X_m$ ). The yearly period  $N_y$  does not have a fixed length as it contains the rest of the hours ( $N_y = t - N_m - N_w - N_d - N_h$ ) (Bernier et al. 2004). For instance, assuming that  $X_h$ ,  $X_d$ ,  $X_w$ , and  $X_m$  are fixed at 12, 48, 168, and 360 hours, then at  $t = 400$  hours we get  $N_h$ ,  $N_d$ ,  $N_w$ ,  $N_m$  and  $N_y$  of 12, 48, 168, 0, and 172 hours, respectively. With this approach, the mean fluid temperature in the ground heat exchanger at time  $t$  is given by:

$$T_{f,t} = Tg - \frac{q_t}{L} R_b - \frac{1}{k_s L} (\bar{q}_{y,t}[A-B] + \bar{q}_{m,t}[B-C] + \bar{q}_{w,t}[C-D] + \bar{q}_{d,t}[D-E] + q_{t-N_h+1}[E-F_1] + q_{t-N_h+2}[F_1-F_2] + \dots + q_{t-1}[F_{N_h-1}-F_{N_h}] + q_t[F_{N_h}]) \quad (4-9)$$

where

$$A=G(F_{O_{t=t}}), B=G(F_{O_{t=t-N_y}}), C=G(F_{O_{t=t-N_y-N_m}}), D=G(F_{O_{t=t-N_y-N_m-N_w}}), E=G(F_{O_{t=N_h}}),$$

$$F_1=G(F_{O_{t=N_h-1}}), F_2=G(F_{O_{t=N_h-2}}), \dots, F_{N_h}=G(F_{O_{t=1}})$$

$\bar{q}_{i,t}$  = mean ground loads on each aggregation period (i=d, w, m, and y), W

$q_j$  = hourly non-aggregated ground loads (j=t-N<sub>h</sub>+1, ..., t), W

For convenience, Equation (4-9) can be represented as

$$T_{f,t} = Tg - \frac{q}{L} R_b - \frac{1}{k_s L} (MLAA) \quad (4-10)$$

where MLAA= all the terms of the multiple-load aggregation algorithm in Eq.4-9

The fixed length of each of these time periods can be determined with any optimization techniques. According to Bernier et al. (2004), these time period lengths X<sub>h</sub>, X<sub>d</sub>, X<sub>w</sub>, and X<sub>m</sub> are fixed at 12, 48, 168, and 360 hours, respectively, and these values are used for simulations in the study.

The ground loop model adopted in the study consists of 20 bore holes in the field. For each borehole with a 6x6 ft<sup>2</sup> ground area can be divided into three equivalent concentric cylinders. Thus, by applying MLAA approach, the 4x5 borehole field with a 500-metre-wide thermal reservoir has 60 dynamical equations plus 3 more for the three equivalent concentric cylinders for the thermal reservoir. The schematic of the 4x5 borefield is shown in Figure 4.6.

For instance, the dynamic equations for the first borehole and its two surrounding ground cylindrical nodes are shown as follows:

$$C_1 \frac{dT_1}{dt} = MLAA(t) + U_{1,2}(T_2 - T_1) \quad (4-11)$$

$$C_2 \frac{dT_2}{dt} = U_{2,1}(T_1 - T_2) + U_{2,3}(T_3 - T_2) \quad (4-12)$$

$$C_3 \frac{dT_3}{dt} = U_{3,2}(T_2 - T_3) + U_{3,6}(T_6 - T_3)/4 + U_{3,18}(T_{18} - T_3)/4 + U_{3,61}(T_{61} - T_3)/2 \quad (4-13)$$

where

$C_i$  = thermal capacity of the  $i^{\text{th}}$  cylindrical node ( $i=1,2,3$ ),  $J/^\circ\text{C}$

$T_i$  = temperature of the  $i^{\text{th}}$  cylindrical node,  $^\circ\text{C}$

$MLAA(t)$  = all the terms of the multiple-load aggregation algorithm at time  $t$ ,  $W$

$U_{i,j}$  = conductance of the  $i^{\text{th}}$  cylindrical node to the  $j^{\text{th}}$  cylindrical node,  $W/^\circ\text{C}$

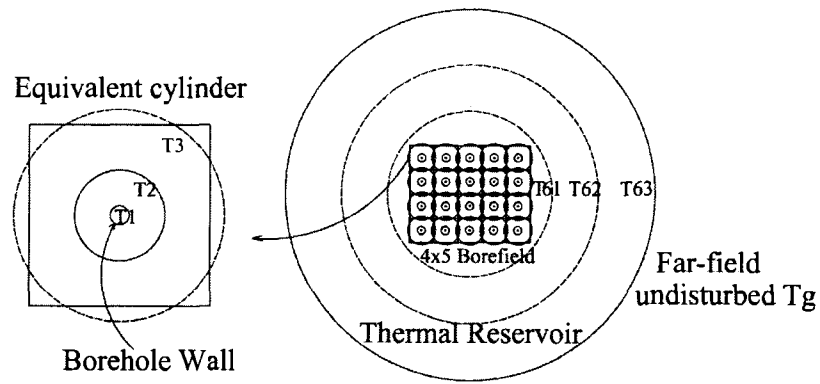


**Figure 4.6 Schematic of 4x5 Borefield**

Similarly, for the other boreholes and their surrounding nodes, dynamic equations are

expressed as follows:

$$C_i \frac{dT_i}{dt} = \text{MLAA}(t) + U_{i,i+1}(T_{i+1} - T_i) \quad (4-14,17,\dots,68)$$

$$C_{i+1} \frac{dT_{i+1}}{dt} = U_{i+1,i}(T_i - T_{i+1}) + U_{i+1,i+2}(T_{i+2} - T_{i+1}) \quad (4-15,18,\dots,69)$$

$$C_{i+2} \frac{dT_{i+2}}{dt} = U_{i+2,i+1}(T_{i+1} - T_{i+2}) + U_{i+2,j}(T_j - T_{i+2}) + U_{i+2,k}(T_k - T_{i+2}) \\ + \dots + U_{i+2,n}(T_n - T_{i+2}) \quad (4-16,19,\dots,70)$$

where

$C_i$  = thermal capacity of the  $i^{\text{th}}$  cylindrical node ( $i=4,7, \dots,58$ ),  $J/^\circ\text{C}$

$T_i$  = temperature of the  $i^{\text{th}}$  cylindrical node ( $i=4,7, \dots,58$ ),  $^\circ\text{C}$

$\text{MLAA}(t)$  = all the terms of the multiple-load aggregation algorithm at time  $t$ ,  $\text{W}$

$U_{i,j}$  = conductance of the  $i^{\text{th}}$  cylindrical node to the  $j^{\text{th}}$  cylindrical node,  $\text{W}/^\circ\text{C}$

$j,k, \dots,n$  = the number of any cylindrical node directly surrounding the  $i+2^{\text{th}}$  one.

Likewise, three equivalent concentric cylindrical nodes are taken for the 500-metre-wide thermal reservoir surrounding the borefield, and the dynamic equations are expressed as follows:

$$C_{61} \frac{dT_{61}}{dt} = U_{61,3}(T_3 - T_{61})/2 + U_{61,15}(T_{15} - T_{61})/2 + U_{61,48}(T_{48} - T_{61})/2 + U_{60,61}(T_{60} - T_{61})/2 \\ + U_{61,6}(T_6 - T_{61})/4 + U_{61,9}(T_9 - T_{61})/4 + U_{61,12}(T_{12} - T_{61})/4 + U_{61,18}(T_{18} - T_{61})/4 + U_{61,30}(T_{30} - T_{61})/4 \\ + U_{61,33}(T_{33} - T_{61})/4 + U_{61,45}(T_{45} - T_{61})/4 + U_{61,51}(T_{51} - T_{61})/4 \\ + U_{61,54}(T_{54} - T_{61})/4 + U_{61,57}(T_{57} - T_{61})/4 \quad (4-71)$$

$$C_{62} \frac{dT_{62}}{dt} = U_{62,61}(T_{61} - T_{62}) + U_{62,63}(T_{63} - T_{62}) \quad (4-72)$$

$$C_{63} \frac{dT_{63}}{dt} = U_{63,62}(T_{62} - T_{63}) + U_{63,g}(T_g - T_{63}) \quad (4-73)$$

where

$C_i$  = thermal capacity of the  $i^{\text{th}}$  cylindrical node ( $i=61,62,63$ ), J/°C

$T_i$  = temperature of the  $i^{\text{th}}$  cylindrical node ( $i=1,2\dots 63$ ), °C

MLAA(t) = all the terms of the multiple-load aggregation algorithm at time t, W

$U_{ij}$  = conductance of the  $i^{\text{th}}$  cylindrical node to the  $j^{\text{th}}$  cylindrical node, W/°C

$T_g$  = undisturbed far-field ground temperature, °C

Once the above 63 equations, Equations 4-11 to 4-73, are solved simultaneously, the temperature of all borehole walls, namely, T1, T4, T7... and T58, can be determined. Then take an average value of the temperatures as the mean borehole wall temperature,  $T_{\text{wall}}$ , of the borefield.

In order to obtain working fluid temperature, the thermal capacitance of the boreholes is neglected. Accordingly, under the steady-state assumption, the fluid temperature,  $T_f$ , can be determined by:

$$T_f = T_{\text{wall}} - QR_b/L \quad (4-74)$$

where

$T_{\text{wall}}$  = mean borehole wall temperature, °C

$Q$  = heat transfer rate (positive for heating and negative for cooling), W

$R_b$  = the equivalent steady-state borehole thermal resistance, °C-m/W

$L$  = borehole length, m

The outlet temperature of fluid,  $T_{f,o}$ , is obtained by applying an energy balance to the borefield.

$$T_{f,o} = T_f + Q/(2GC_p) \quad (4-75)$$

$$T_f = (T_{f,o} + T_{f,i})/2 \quad (4-76)$$

where

$G$  = the fluid mass flow rate, kg/s

$C_p$  = the fluid specific heat, J/kg-°C

$T_{f,i}$  = inlet fluid temperature, °C

The simulation results of the ground loop model in heating and cooling modes are shown in Figures 4.7 and 4.8, respectively.

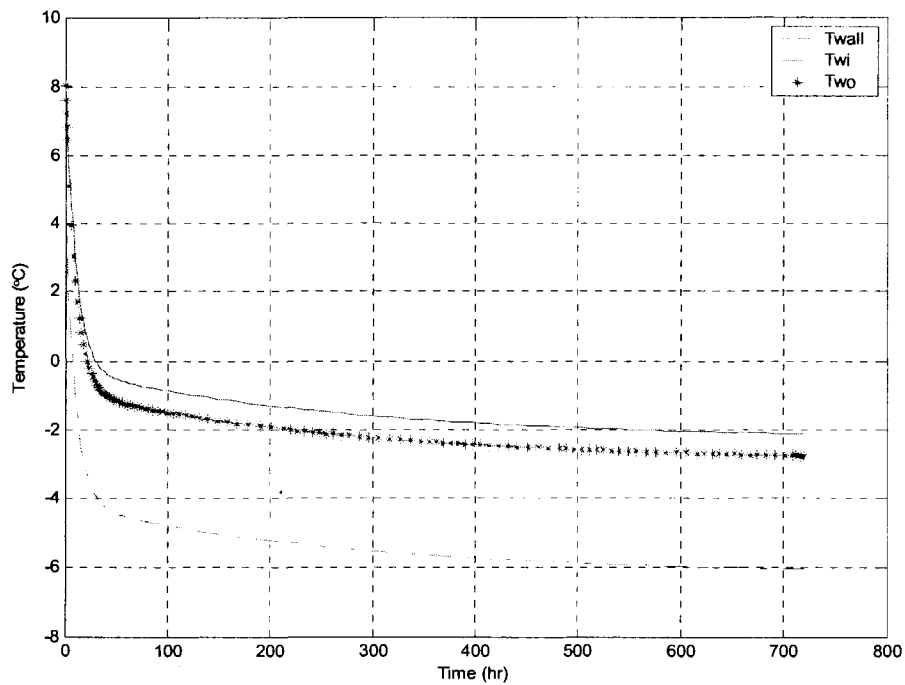


**Figure 4.7 Simulation result of ground loop model for heating**

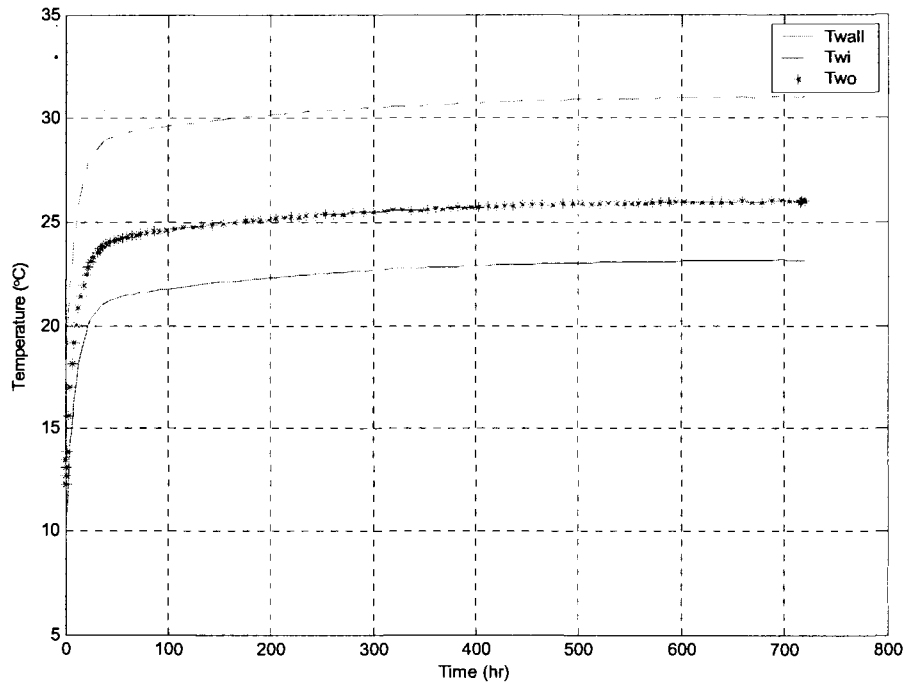


**Figure 4.8 Simulation result of ground loop model for cooling**

From Figures 4.7 and 4.8 the following observations can be made:

- a) The steady state response time of borehole wall and water inlet /outlet temperatures are of the order of 300 – 400 hours.
- b) The outlet water temperature under full load condition could reach  $-2^{\circ}\text{C}$  and therefore need to be reheated before supplying it to the heat pump.
- c) The temperature difference between inlet and outlet water was found to be around  $4^{\circ}\text{C}$  in heating mode and around  $5^{\circ}\text{C}$  in cooling mode.
- d) The outlet water temperature in cooling mode could exceed  $26^{\circ}\text{C}$ , which may have to be cooled before supplying it to condenser.

The design parameters of the ground loop heat exchanger model used in the simulation are listed in Table 4.4.

**Table 4.4 Design parameters of ground loop model**

Symbol	Magnitude	Units	Symbol	Magnitude	Units
C1,C4...C58	4.5434e+4	J/°C	D <sub>b</sub>	0.152	m
C2,C5...C59	5.5789e+6	J/°C	L <sub>b</sub>	100	m
C3,C6...C60	9.8464e+7	J/°C	R <sub>b</sub>	0.1	m-°C/W
C61	8.9305e+9	J/°C	K <sub>ground</sub>	1.3	W/m-°C
C62	1.0609e+11	J/°C	K <sub>grout</sub>	2.6	W/m-°C
C63	2.2194e+12	J/°C	ρ <sub>ground</sub>	2000	Kg/m <sup>3</sup>
T <sub>g</sub>	9	°C	ρ <sub>grout</sub>	1762	Kg/m <sup>3</sup>
Cp <sub>ground</sub>	1400	J/kg-°C	d1,d4...d58	0.152	m
Cp <sub>grout</sub>	1421	J/kg-°C	d2,d5...d59	1.60	m
Q <sub>h</sub>	155,357	Btu/h	d3,d6...d60	6.88	m
G <sub>h</sub>	6.8	Kg/s	d61	70.8	m
Q <sub>c</sub>	-363,214	Btu/h	d62	230.8	m
G <sub>c</sub>	10.16	Kg/s	d63	1030.8	m

#### 4.1.4 Cooling Tower Model

The cooling tower model used in this study is the one called closed-circuit dry cooling tower model. The energy conservation equation on the air side is given by:

$$C_{a\_ct} \frac{dT_{a\_ct}}{dt} = G_{a\_ct} c_{p\_a} (T_{a\_ct\_i} - T_{a\_ct}) - U_{ct} (T_{a\_ct} - T_{w\_ct}) \quad (4-77)$$

where

$C_{a\_ct}$  = thermal capacity of cooling tower air,  $J/^\circ C$

$T_{a\_ct}$  = outlet air temperature of the cooling tower,  $^\circ C$

$G_{a\_ct}$  = outlet air flow rate of the cooling tower,  $kg/s$

$c_{p\_a}$  = specific heat of air,  $J/kg-^\circ C$

$T_{a\_ct\_i}$  = inlet air temperature of the cooler,  $^\circ C$

$U_{ct}$  = conductance of the cooling tower,  $W/^\circ C$

$T_{w\_ct}$  = outlet water temperature of the cooling tower,  $^\circ C$

The energy conservation equation on the water side is given by:

$$C_{w\_ct} \frac{dT_{w\_ct}}{dt} = G_{w\_ct} c_{p\_w} (T_{w\_ct\_i} - T_{w\_ct}) - U_{ct} (T_{w\_ct} - T_{a\_ct}) \quad (4-78)$$

where

$C_{w\_ct}$  = thermal capacity of cooler water,  $J/^\circ C$

$T_{w\_ct}$  = outlet water temperature of the cooler,  $^\circ C$

$G_{w\_ct}$  = outlet water flow rate of the cooler,  $kg/s$

$c_{p\_w}$  = specific heat of water,  $J/kg-^\circ C$

$T_{w\_ct\_i}$  = inlet water temperature of the cooler,  $^\circ C$

$U_{ct}$  = conductance of the cooler,  $W/^\circ C$

$T_{a\_ct}$  = outlet air temperature of the cooler, °C

By solving Equations 4-77 and 4-78 simultaneously with the set of design parameters listed in Table 4.5, the temperature responses were determined. The simulation result is shown in Figure 4.9.

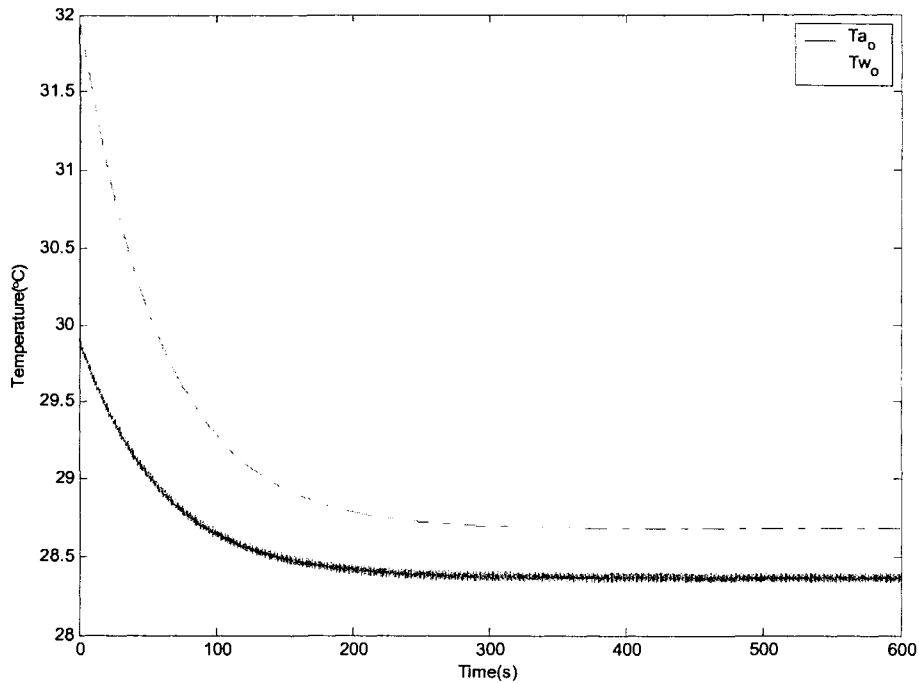


**Figure 4.9 Simulation result of the cooling tower model**

From the above Figure 4.9 it can be seen that the cooling tower model reaches near steady state in 300 seconds under design condition and the response times are affected by the loads acting on the model.

The design parameters of the cooling tower model used in the simulation are listed in the following Table 4.5.

**Table 4.5 Design parameters of the cooling tower model**

Symbol	Magnitude	Units	Symbol	Magnitude	Units
$C_{a\_ct}$	18,180	J/°C	$G_{a\_ct}$	107	Kg/s
$C_{w\_ct}$	4.180e+6	J/°C	$G_{w\_ct}$	5.1	Kg/s
$U_{ct}$	92,000	W/°C	$T_{a\_ct\_i}$	28.1	°C

#### 4.1.5 Boiler Model

The boiler model used in this study is a gas-fired boiler model by Liao and Parand (2002). The model consists of four major components, an inner shell, a water channel, an outer shell, and an insulation layer, among which heat transfer are modeled. The energy conservation equation on the inner shell side is given by:

$$C_{is} \frac{dT_{is}}{dt} = Q_{burner} - U_1(T_{is} - T_w) \quad (4-79)$$

where

$C_{is}$  = thermal capacity of inner shell, J/°C

$T_{is}$  = temperature of the inner shell, °C

$Q_{burner}$  = heat transfer from burner to the inner shell, W

$U_1$  = conductance of the inner shell to water, W/°C

$T_w$  = outlet water temperature of the water channel, °C

The energy conservation equation on the water side is given by:

$$C_w \frac{dT_w}{dt} = G_w c_p (T_{w\_i} - T_w) + U_1(T_{is} - T_w) + U_2(T_{os} - T_w) \quad (4-80)$$

where

$C_w$  = thermal capacity of water channel, J/°C

$T_w$  = outlet water temperature of the water channel, °C

$c_p$  = specific heat of water, J/kg-°C

$T_{w,i}$  = inlet water temperature of the water channel, °C

$U_2$  = conductance of the outer shell with water, W/°C

$T_{os}$  = temperature of the outer shell, °C

The energy conservation equation on the outer shell side is given by:

$$C_{os} \frac{dT_{os}}{dt} = U_2(T_w - T_{os}) - U_3(T_{os} - T_{ins}) \quad (4-81)$$

where

$C_{os}$  = thermal capacity of outer shell, J/°C

$T_{os}$  = temperature of the outer shell, °C

$U_2$  = conductance of the outer shell with water, W/°C

$T_w$  = outlet water temperature of the water channel, °C

$U_3$  = conductance of the outer shell with insulation layer, W/°C

$T_{ins}$  = temperature of the insulation layer, °C

The energy conservation equation on the insulation layer side is given by:

$$C_{ins} \frac{dT_{ins}}{dt} = U_3(T_{os} - T_{ins}) + U_4(T_{am} - T_{ins}) \quad (4-82)$$

where

$C_{ins}$  = thermal capacity of the insulation layer, J/°C

$T_{ins}$  = temperature of the insulation layer, °C

$U_3$ = conductance of the outer shell with insulation layer, W/°C

$U_4$ = conductance of the insulation layer with ambient, W/°C

$T_{am}$ = temperature of ambient air, °C

The boiler temperature responses are depicted in Figure 4.10.

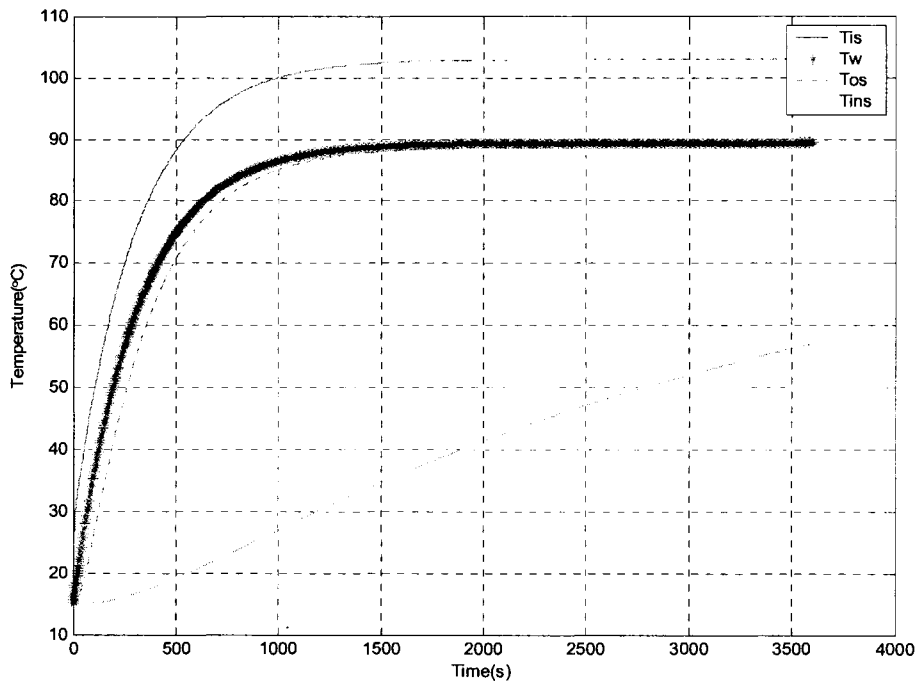


**Figure 4.10 Simulation results of the boiler model**

From Figure 4.10 it is noted that the boiler model reaches near steady state in 2,000 seconds at its design load and the response times are affected by the thermal capacity of components and the loads acting on the model.

The design parameters of the boiler model used in the simulation are listed in Table 4.6.

**Table 4.6 Design parameters of the boiler model**

Symbol	Magnitude	Units	Symbol	Magnitude	Units
$C_{os}$	18,100	J/°C	$U_3$	4	W/°C
$C_w$	627,000	J/°C	$U_4$	0.5	W/°C
$C_{os}$	19,000	J/°C	$Q_{burner,d}$	71,000	W
$C_{ins}$	14,181	J/°C	$\eta$	0.85	--
$U_1$	47,00	W/°C	$G_w$	0.518	Kg/s
$U_2$	310	W/°C	$T_{am}$	15	°C

## 4.2 Open Loop Simulations

### 4.2.1 Heating Mode

After integrating all the component models above, the hybrid ground source heat pump system model was obtained. In order to test the temperature responses of the whole HGSHP system, open loop simulations in both heating and cooling mode of operation are performed. The simulation results of the aggregated HGSHP system in heating mode at the design load are shown in Figures 4.11 and 4.12.

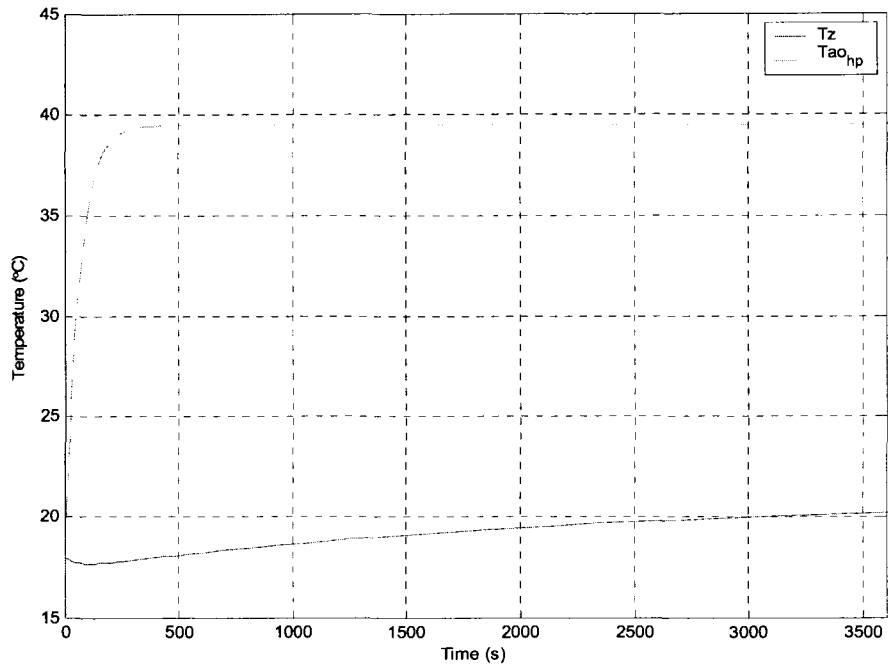


**Figure 4.11 Open loop air temperature responses for heating**

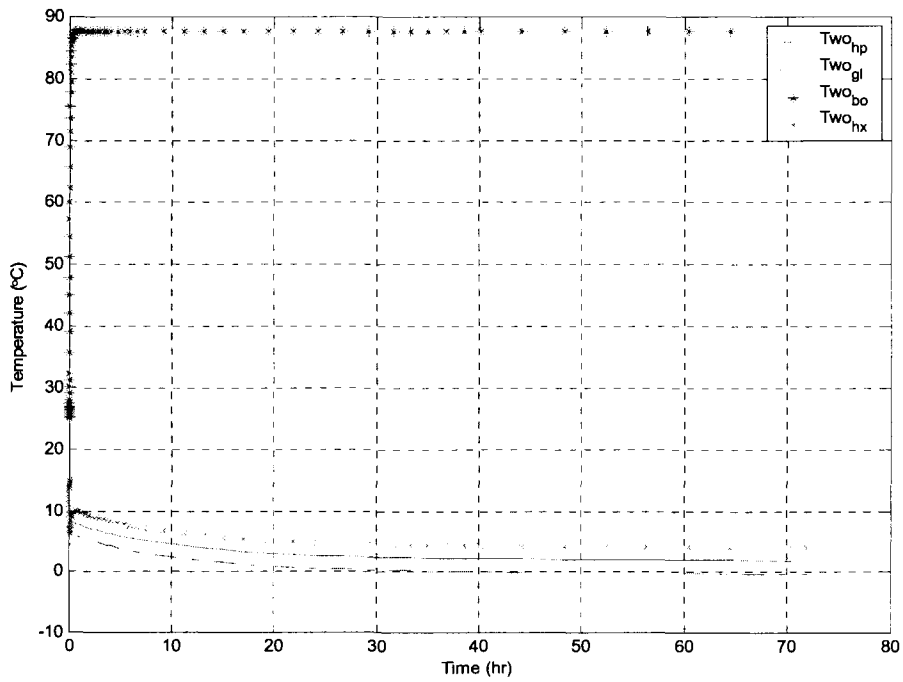


**Figure 4.12 Water temperature responses for heating**

From Figures 4.11 and 4.12 the following observations can be made:

a) The temperature response of outlet air from the heat pump reaches its steady state in 500 seconds, while that of zone air does in 3,500 seconds.

b) The water temperature response of boiler reaches its steady state in few hours, but that of heat pump, ground loop, and heat exchanger do in around 30 hours.

c) The temperature responses highly depend on the thermal capacity of each component. The higher thermal capacity is, the slower temperature response will be.

d) The temperature responses could also depend on the loads acting on the system.

#### **4.2.2 Cooling Mode**

Similarly, open loop simulation results of the HGSHP system in cooling mode at the design load are shown in Figures 4.13 and 4.14.

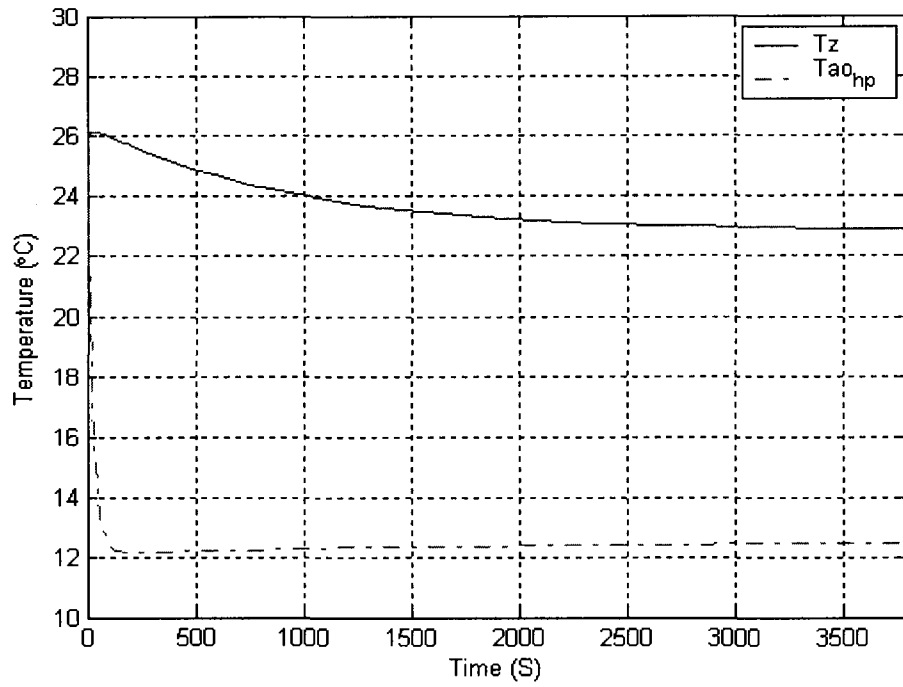


**Figure 4.13 Open loop air temperature responses for cooling**

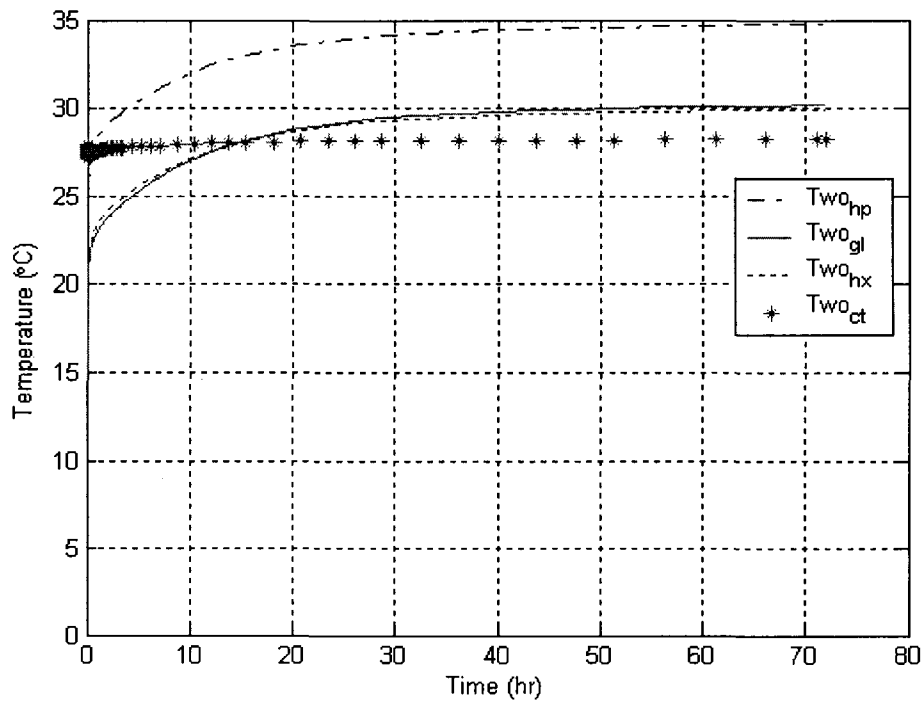


**Figure 4.14 Water temperature responses for cooling**

From Figures 4.13 and 4.14, it can be observed that the maximum temperature of water from the heat pump reached 34°C, the maximum temperature of water from the ground loop and heat exchanger reached around 30°C, and the maximum temperature of water from the cooling tower reached around 28°C.

The open loop simulation results from the aggregated HGSHP model show expected trends during heating and cooling modes of operation. It is of interest to use this model and develop operating strategies for the system. This is described in the following chapter.

# CHAPTER 5 CONTROL STRATEGIES AND SIMULATION RESULTS

## 5.1 Introduction

Automatic HVAC control systems are designed to maintain temperature, humidity, etc. in buildings. Automatic control primarily modulates, stages, or sequences mechanical equipment to satisfy load requirements and safe equipment operation. Control system can use digital, pneumatic, mechanical, electrical, and electric control devices. Control loops can be classified by the adjustability of the controlled device. A two-position controlled device has two operating states (e.g. on and off), whereas a modulating controlled device has a continuous range of operating states (e.g. 0 to 100% open) (ASHRAE 2005). This chapter focuses on simple control strategies for the hybrid ground source heat pump system, and simulation results of the system.

### 5.1.1 Two Position Control

As shown in Figure 5.1, two-position control device can be positioned only to a maximum or minimum state; that's, on or off state. Two-position control is used extensively for both industrial and commercial control because it is simple and inexpensive. A typical home thermostat that starts and stops a furnace is an example. When its controlled variable, air temperature, is less than a lower setting value, it starts the furnace. That's, control variable,  $U$ , is equal to 1 and the furnace is turned on. Once air temperature warms up until

its higher setting value, thermostat stops the furnace; that's, control variable  $U$  is equal to 0 and it is switched off. When air temperature goes down to the lower setting value, control variable  $U$  is equal to 1 and the furnace is turned on again (ASHRAE 2005).

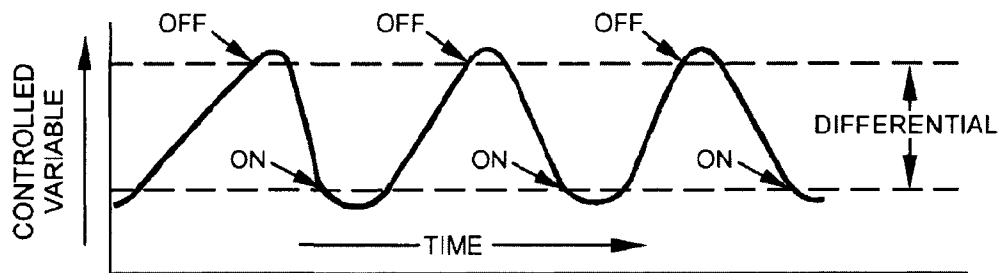


**Figure 5.1 Two-Position Control**

(ASHRAE Handbook 2005)

### 5.1.2 Modulating Control

A modulating control, also referred to closed loop or feedback control, must contain a sensor, a controller, and a controlled device. It typically offers more precise controlled variable and higher efficiency than two-position control. The control measures actual changes in the controlled variable and actuates the controlled device to bring about a change. The corrective action may continue until the variable is brought to a desired value within the design limitations of the controller. This arrangement of having the controller sense the value of the controlled variable is known as feedback (ASHRAE 2005). A typical block diagram of closed loop control is shown in the following Figure 5.2. A modulating control is comprised

of proportional (P) control, proportional plus integral (PI) control, and proportional plus integral plus derivative (PID) control.

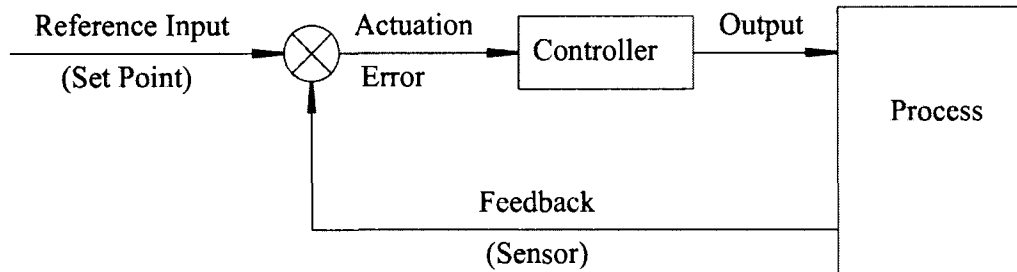


**Figure 5.2 Block Diagram of Closed Loop Control**

(ASHRAE Handbook 2005)

Proportional control is the simplest modulating control that contains only proportional term. Proportional term makes a change to the output that is proportional to the current error value. The proportional response can be adjusted by multiplying the error by a constant  $K_p$ , called the proportional gain. The proportional term is given by:

$$u_p = K_p e(t) \quad (5-1)$$

where

$u_p$  = Proportional output variable

$K_p$  = Proportional gain

$e$  = Error (desired setpoint – measured processing variable)

$t$  = Time or instantaneous time

A high proportional gain results in a large change in the output for a given change in the

error. If the proportional gain is too high, the system might become unstable; that is, oscillation might occur. Conversely, a small gain results in a small output response to a large input error, and a less sensitive P controller will be. If the gain is too low, the control action may be too small when responding to system disturbances. In the absence of disturbances, pure P control will not settle at its target value, but it will retain a steady state error. In spite of the steady state offset, both control theory and industrial practice indicate that the proportional term should contribute the bulk of the output change (ASHRAE 2005).

Proportional plus integral control contains not only proportional term but also integral term. The contribution from the integral term is proportional to both the magnitude of the error and the duration of the error. Integrating the error over time gives the accumulated offset that should have been corrected previously. The accumulated error is then multiplied by the integral gain,  $K_i$ , and added to the controller output. The magnitude of the contribution of the integral term to the overall control action is determined by  $K_i$ . Thus, PI control output is given by:

$$u = K_p e(t) + K_i \int_0^t e(t) dt \quad (5-2)$$

where

$u$  = control output variable

$K_p$  = Proportional gain

$K_i$  = Integral gain

$e$  = Error

$t$  = Time or instantaneous time

The integral term of PI control can accelerate the movement of the process towards set point and eliminates the residual steady state error that occurs with a pure proportional controller. Nevertheless, the integral term can cause the present value to overshoot the set point value since it is responding to accumulated errors from the past (ASHRAE 2005). A typical PI control is shown in Figure 5.3.

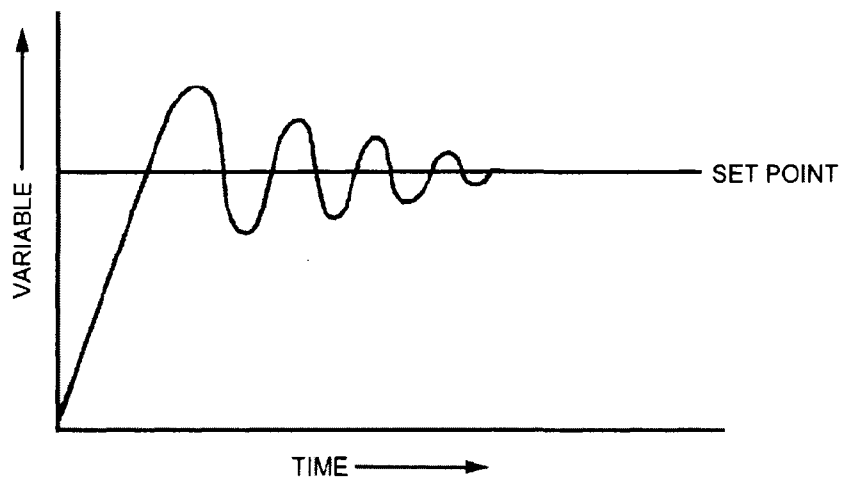


**Figure 5.3 Proportional plus Integral (PI) Control**

(ASHRAE Handbook 2005)

Proportional plus integral plus derivative control contains one more term, derivative term, in addition to proportional and integral terms, compared to PI control. The rate of change of the process error is calculated by determining the slope of the error over time and multiplying this rate of change by the derivative term,  $K_d$ . The magnitude of the contribution of the derivative term to the overall control action is determined the derivative gain. The control output is given by:

$$u = K_p e(t) + K_i \int e(t) dt + K_d \frac{de(t)}{dt} \quad (5-3)$$

where

$u$  = control output variable

$K_p$  = Proportional gain

$K_i$  = Integral gain

$K_d$  = derivative gain

$e$  = Error

$t$  = Time or instantaneous time

The derivative term generally slows the rate of change of the controller output, and this effect is noticeable close to the controller set point. Therefore, derivative control can be utilized to reduce the magnitude of the overshoot produced by the integral component, and derivative term improves the combined controller process stability. Differentiation of a signal, however, can amplify noise in the signal. Hence, this term in the controller is highly sensitive to noise in the error term, and it can cause a process to become unstable if the noise and the derivative gain are sufficiently large (ASHRAE 2005).

In HVAC engineering field, PI control is widely utilized, while P control and PID control are seldom used due to such ill characteristics as offset for P control and sensibility and noise for PID control.

## 5.2 Control Strategies

Both PI and On/Off controllers are designed for the hybrid ground source heat pump

system, shown in Figure 5.4. For instance, a PI or on/off controller for heat pump is to control the performance of heat pump to match various building loads, and the two-way valve for boiler, with an On/Off controller, is to control the flow rate of fuel to the burner. In order to achieve a better performance of the system, optimal control strategies are introduced to the system in heating and cooling modes of operation. Furthermore, two changeover valves are utilized on the boiler pipe and cooling tower pipe. That's, when operating in heating mode, the valve on boiler pipe is open and the other is off, and when operating in cooling mode, the valve on cooling tower pipe is open and the other is closed.

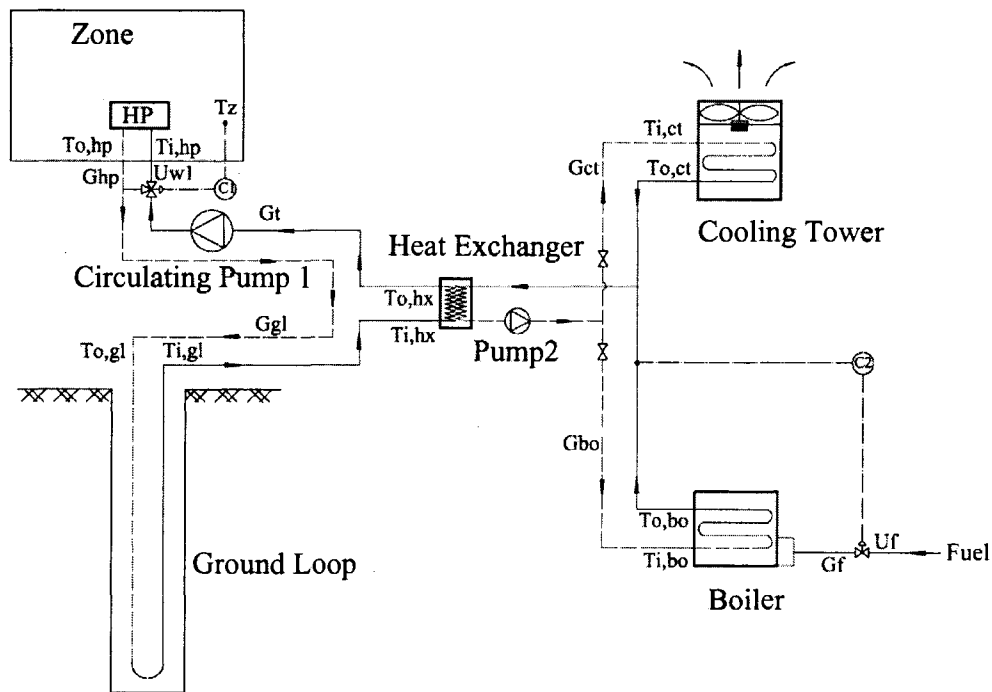


**Figure 5.4 Control Schematic of Hybrid GSHP**

### 5.2.1 Heating Mode of Operation

In the following three different control strategies based on PI /On-Off control in different combinations are proposed.

### 5.2.1.1 On/off controllers for Heat Pump and Boiler

- For heat pump, *if*  $T_z \leq T_{sp} - \Delta T/2$ ,  $U_{hp}=1$ ; *elseif*  $T_z \geq T_{sp} + \Delta T/2$ ,  $U_{hp}=0$ .

Heat pump is turned on when zone air temperature,  $T_z$ , is less than  $T_{sp} - \Delta T/2$ , e.g. 20.5°C, while it is switched off when  $T_z$  is greater than  $T_{sp} + \Delta T/2$ , e.g. 21.5°C.

- For circulating pump 1, *if*  $U_{hp}=1$ ,  $U_{p1}=1$ ; *elseif*  $U_{hp}=0$ ,  $U_{p1}=0$ .

Circulating pump1 is turned on only when heat pump is on. Otherwise, it is off.

- For circulating pump 2, *if*  $(U_{hp}=1 \ \& \ T_z \leq T_{sp} - \Delta T/2)$  OR  $T_w \leq T_{w,sp}$ ,  $U_{p2}=1$ ; *else*

$U_{p2}=0$ . Circulating pump2 is turned on only when heat pump is on and zone air temperature  $T_z$  is still less than 20.5°C, or entering water temperature to heat pump is less than or equal to setpoint temperature. Otherwise, it is turned off.

- For boiler, *if*  $U_{p2}=1 \ \& \ T_w \leq T_{sp1}$ ,  $U_f=1$ ; *elseif*  $T_w \geq T_{sp2}$ ,  $U_f=0$ .

Boiler is turned on when circulating pump2 is on and its outlet water temperature is less than  $T_{sp1}$ , e.g. 40°C, whereas it is switched off when water temperature is greater than  $T_{sp2}$ , e.g. 60°C.

### 5.2.1.2 PI controllers for Heat Pump and Boiler

- For heat pump, with a user-defined  $T_{sp}$ , like 21 °C,  $U_{hp} = K_p e(t) + K_i \int e(t) dt$ .

Heat pump is turned on when  $U_{hp}$  is greater than 0, while it is switched off when

Uhp is equal to 0.

- For circulating pump 1, *if*  $U_{hp} > 0$ ,  $U_{p1} = 1$ ; *elseif*  $U_{hp} = 0$ ,  $U_{p1} = 0$ .

Circulating pump1 is turned on only when heat pump is on. Otherwise, it is off.

- For pump 2, *if*  $(U_{hp} > 0 \ \& \ T_z \leq T_{sp} - \Delta T/2)$  OR  $T_w \leq T_{w,sp}$ ,  $U_{p2} = 1$ ; *else*  $U_{p2} = 0$ .

Circulating pump2 is turned on only when heat pump is on and zone air temperature

$T_z$  is still less than 20.5°C, or entering water temperature to heat pump is less than or equal to setpoint temperature. Otherwise, it is turned off.

- For boiler, with a moderate  $T_{sp}$ , like 50 °C ,  $U_f = K_p e(t) + K_i \int e(t) dt$  .

Boiler is turned on when  $U_f$  is greater than 0, while it is switched off when  $U_f$  is equal to 0.

### 5.2.1.3 PI control for Heat Pump and On/off control for Boiler

- For heat pump, with a known user-defined  $T_{sp}$ ,  $U_{hp} = K_p e(t) + K_i \int e(t) dt$  .

Heat pump is turned on when  $U_{hp}$  is greater than 0, while it is switched off when  $U_{hp}$  is equal to 0.

- For circulating pump 1, *if*  $U_{hp} > 0$ ,  $U_{p1} = 1$ ; *elseif*  $U_{hp} = 0$ ,  $U_{p1} = 0$ .

Circulating pump1 is turned on only when heat pump is on. Otherwise, it is off.

- For pump 2, *if*  $(U_{hp} > 0 \ \& \ T_z \leq T_{sp} - \Delta T/2)$  OR  $T_w \leq T_{w,sp}$ ,  $U_{p2} = 1$ ; *else*  $U_{p2} = 0$ .

Circulating pump2 is turned on only when heat pump is on and zone air temperature

$T_z$  is still less than 20.5°C, or entering water temperature to heat pump is less than or equal to setpoint temperature. Otherwise, it is turned off.

- For boiler, if  $U_{p2}=1$  &  $T_w \leq T_{sp1}$ ,  $U_f=1$ ; else if  $T_w \geq T_{sp2}$ ,  $U_f=0$ .

Boiler is turned on when circulating pump2 is on and its outlet water temperature is less than  $T_{sp1}$ , e.g. 40°C, whereas it is switched off when water temperature is greater than  $T_{sp2}$ , e.g. 60°C.

## 5.2.2 Heating Mode Simulation Results

In order to examine whether or not the control strategies work well for the whole HGSHP system, a realistic single day rather than the design day, e.g. a day in February, is used in the simulation. The hourly outdoor air temperatures are listed in the following Table 5.1 (From Environment Canada).

**Table 5.1 Hourly Outdoor Air Temperatures of a specific day in winter**

Hr	To (°C)	Hr	To (°C)	Hr	To (°C)	Hr	To (°C)
<b>0:00</b>	-17.5	<b>6:00</b>	-14.8	<b>12:00</b>	-10.1	<b>18:00</b>	-3.7
<b>1:00</b>	-18.1	<b>7:00</b>	-14.9	<b>13:00</b>	-9.1	<b>19:00</b>	-3.4
<b>2:00</b>	-16.9	<b>8:00</b>	-14.8	<b>14:00</b>	-5.1	<b>20:00</b>	-3.8
<b>3:00</b>	-16.0	<b>9:00</b>	-14.4	<b>15:00</b>	-4.4	<b>21:00</b>	-5.4
<b>4:00</b>	-15.2	<b>10:00</b>	-13.2	<b>16:00</b>	-4.0	<b>22:00</b>	-4.9
<b>5:00</b>	-14.8	<b>11:00</b>	-12.2	<b>17:00</b>	-4.7	<b>23:00</b>	-5.6

As the design indoor temperature for the office building is set 21°C, the hourly heating load of the building can be calculated. The load profile of the office building on the specific day is presented in Figure 5.5.

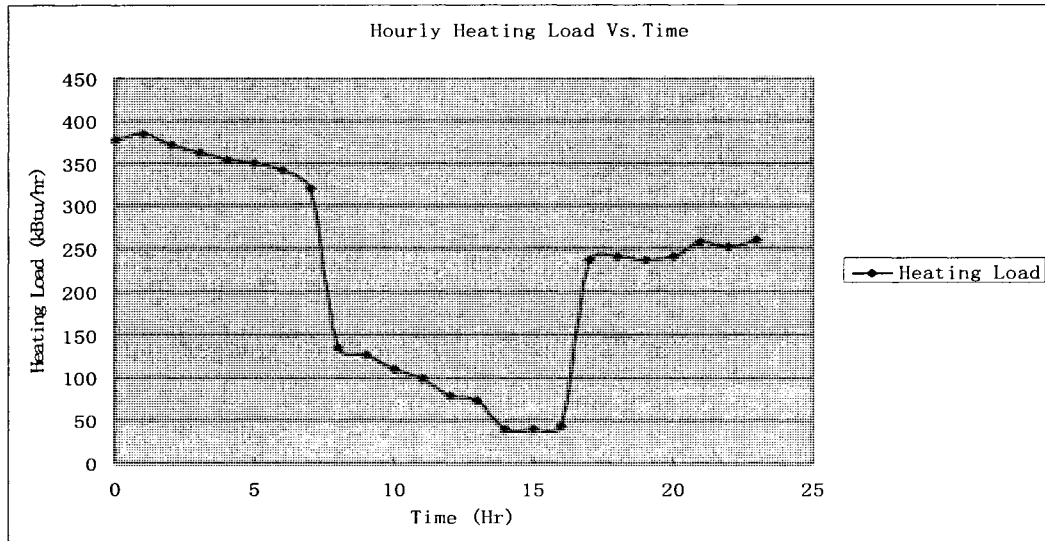


**Figure 5.5 Hourly Heating Load Profile on a Specific Day**

➤ **Case 1: On/off Controllers for HP and Boiler**

After performing the simulations of whole HGSHP system with the control strategies on the specific day, the simulation results are shown in Figures 5.6 to 5.12, of which Figures 5.6, 5.7 and 5.11 are shown only a few hours simulation in order to improve the clarity of the figures.

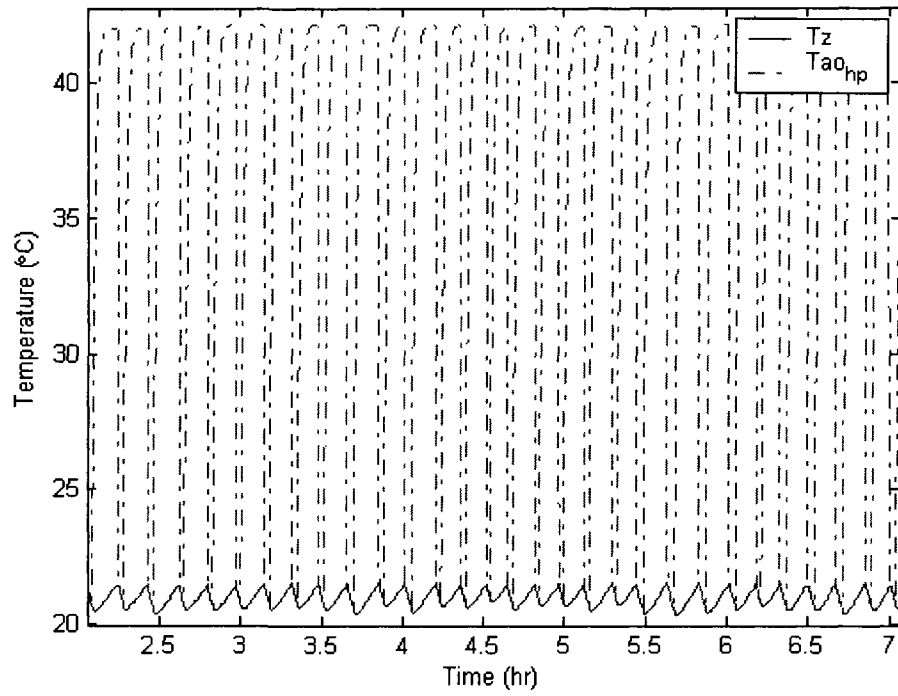


**Figure 5.6 Air Temperature responses of One Day Simulations**

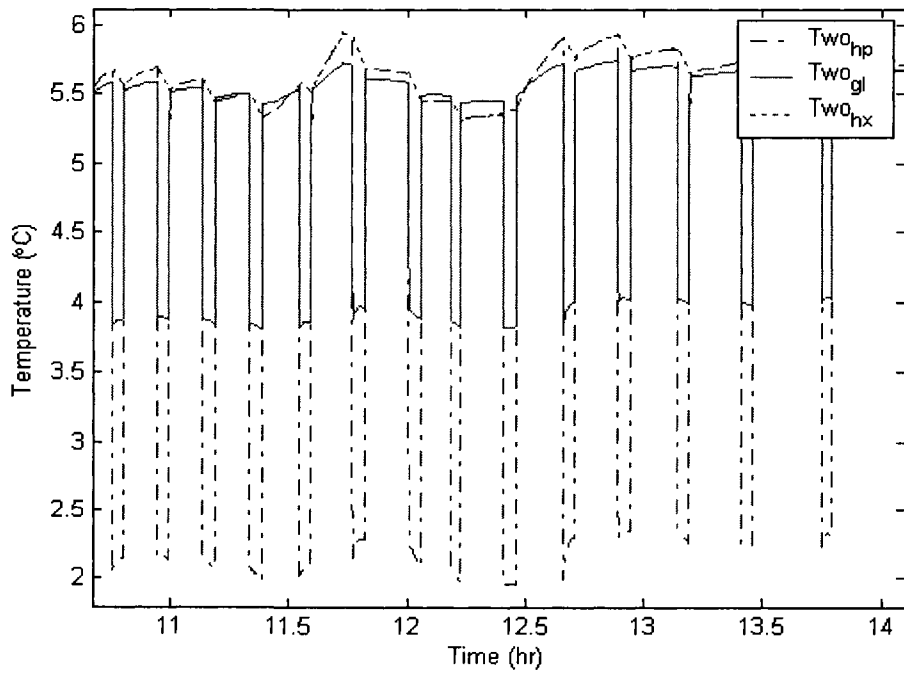


**Figure 5.7 Outlet Water Temperature responses of HP, GL and HX**

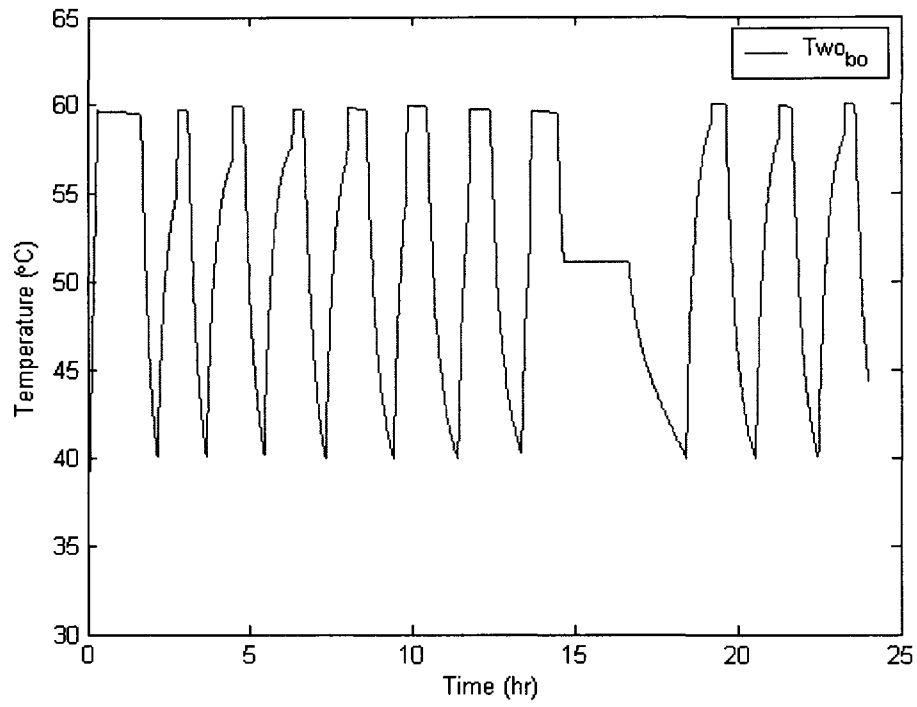


**Figure 5.8 Outlet Water Temperature response of Boiler**

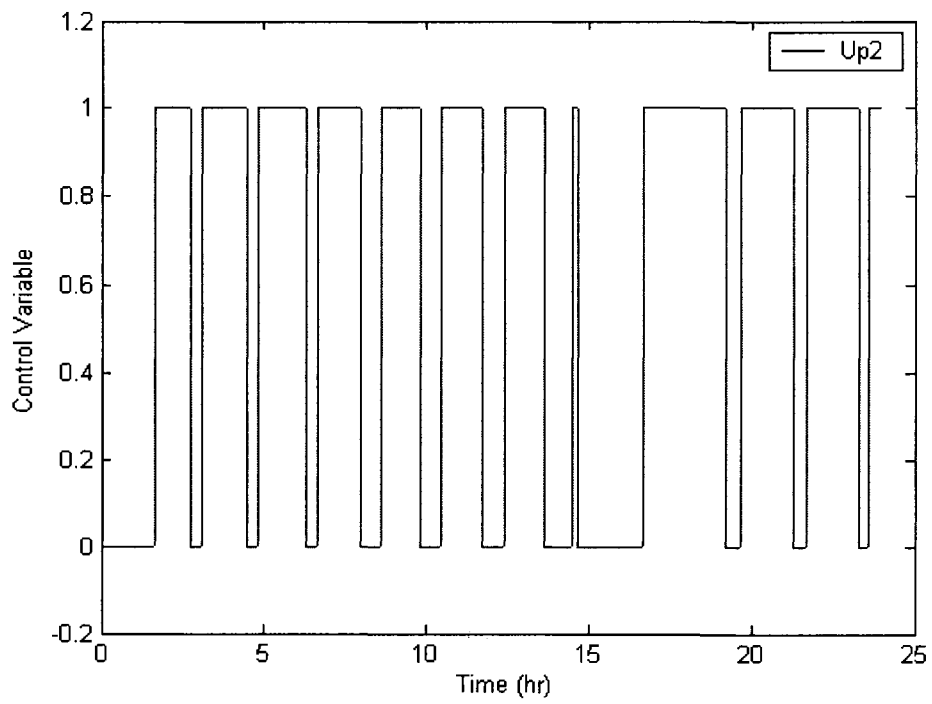


**Figure 5.9 Control Variable of Pump 2**

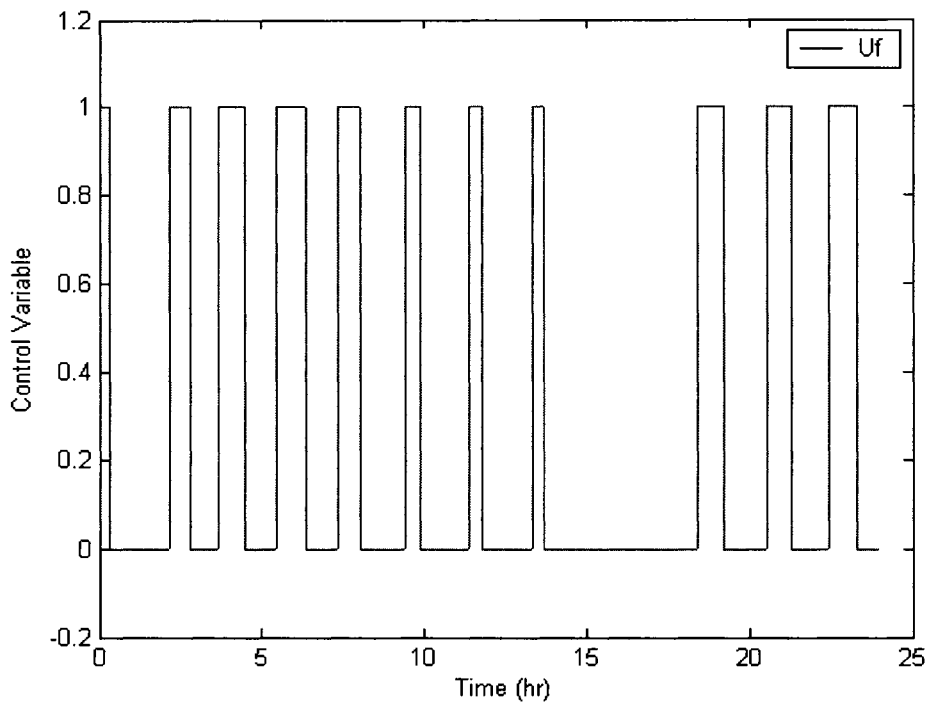


**Figure 5.10 Control Variable of Boiler Burner**

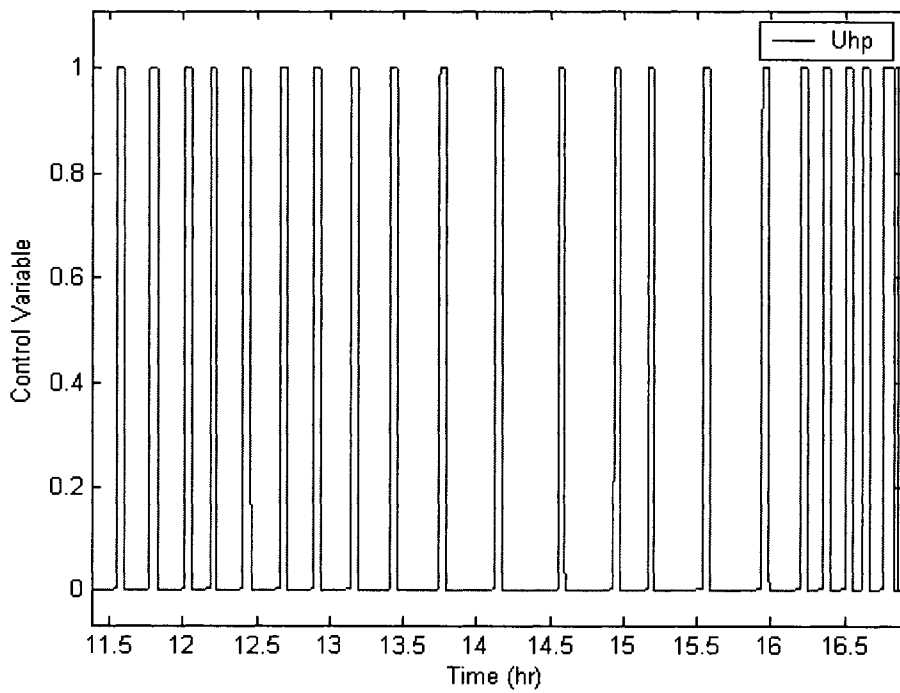


**Figure 5.11 Control Variable of Heat Pump**

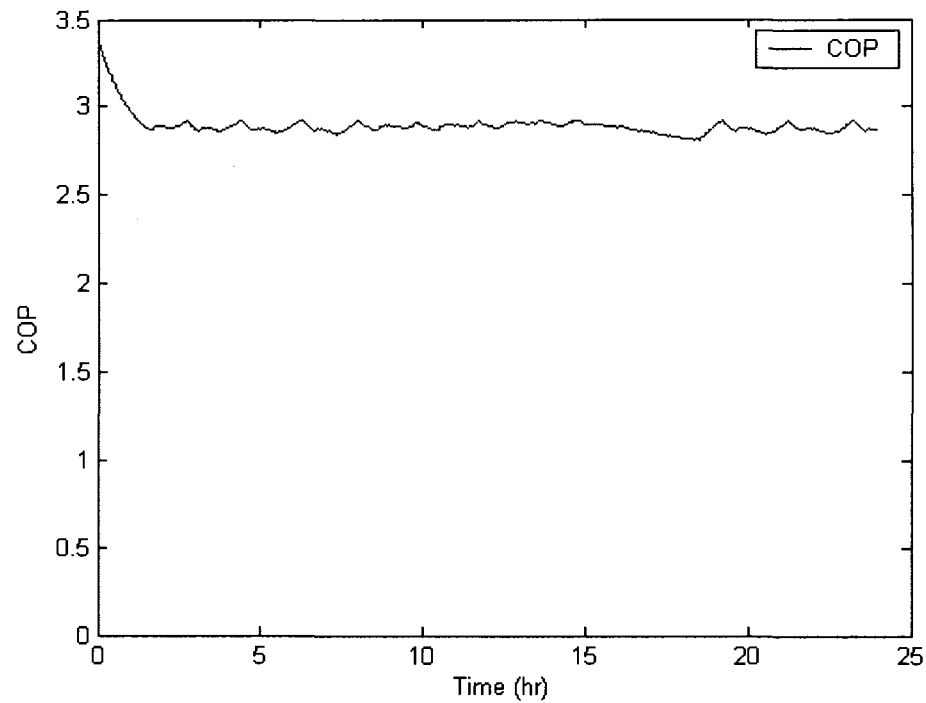


**Figure 5.12 COP of Heat Pump**

From Figures 5.6 to 5.12, it is noted that:

- a) Zone air temperature response was controlled within the desired range, 20.5°C to 21.5°C, on the specific day, while the temperature response of heat pump outlet air was controlled in either on or off mode.
- b) When heat pump is on, the water temperature responses of heat pump, ground loop, and heat exchanger are around 2.1°C, 3.8°C, and 5.5°C respectively. Conversely, when heat pump is off, the corresponding temperatures of heat pump, ground loop and heat exchanger are around 5.5°C, 5.5°C, and 5.7°C respectively.
- c) Boiler water temperature response was controlled within the desired range, 40°C to 60°C, using On-off control.

- d) Circulating pump 2 and boiler burner were controlled in either on or off mode based on corresponding temperature setpoints.

➤ **Case 2: PI Controllers for HP and Boiler**

The simulation of whole HGSHP system with the PI control strategies was done on the same specific day. The simulation results are shown in Figures 5.13 to 5.18.

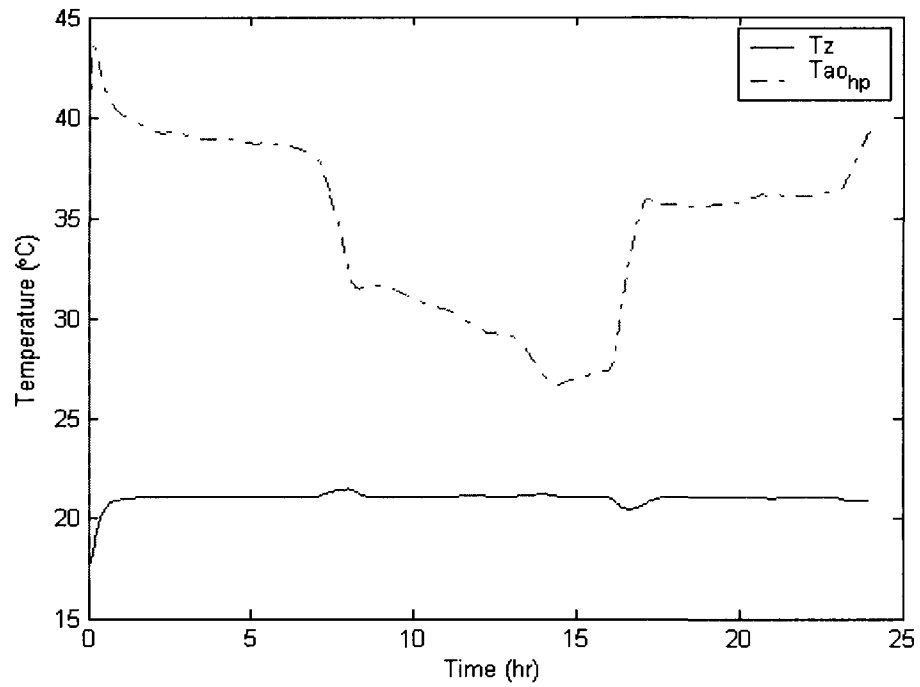


**Figure 5.13 Air Temperature responses of One Day Simulation**

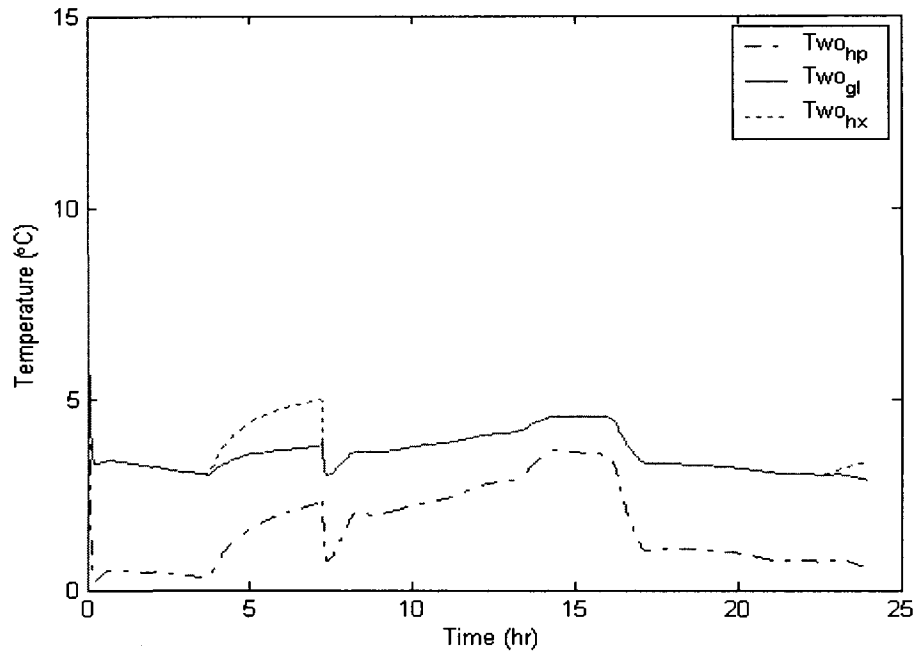


**Figure 5.14 Outlet Water Temperature responses of Heat Pump, Ground Loop and Heat Exchanger**

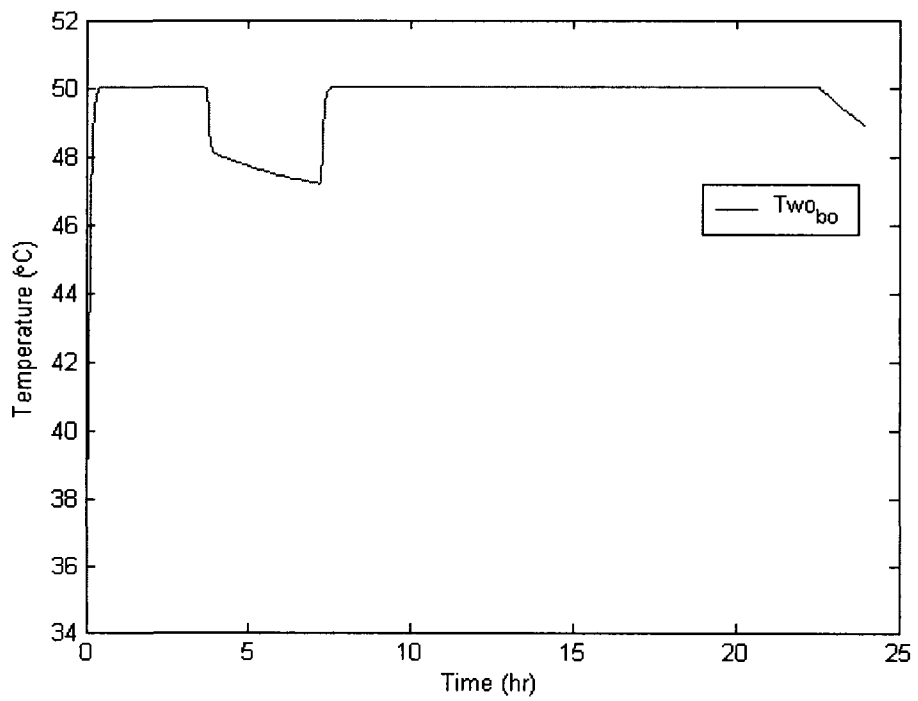


**Figure 5.15 Outlet Water Temperature response of Boiler**

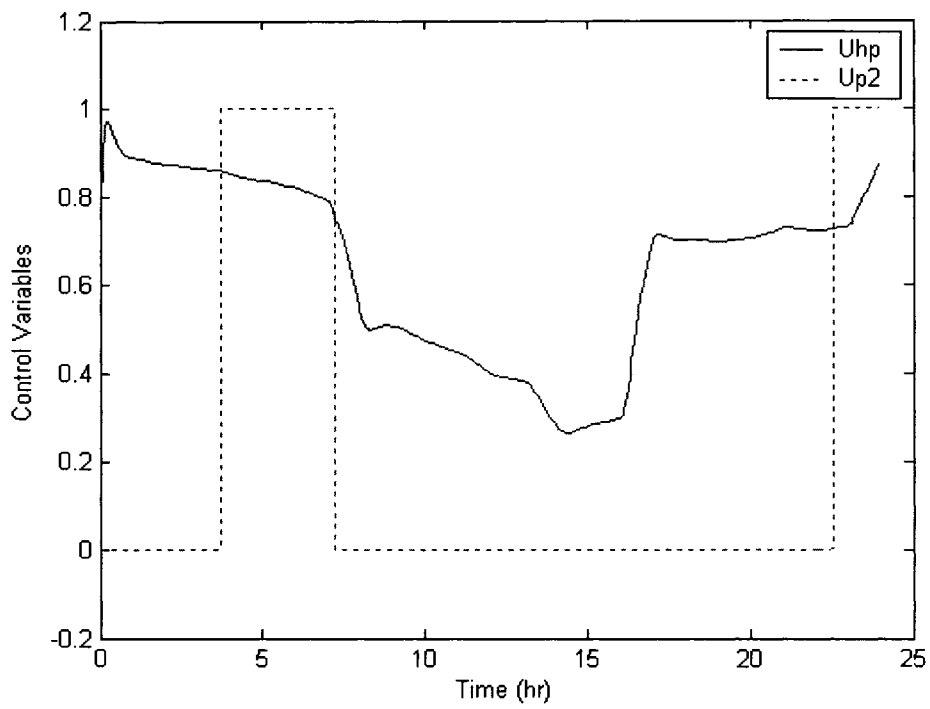


**Figure 5.16 Control Variables of HP and Pump 2**

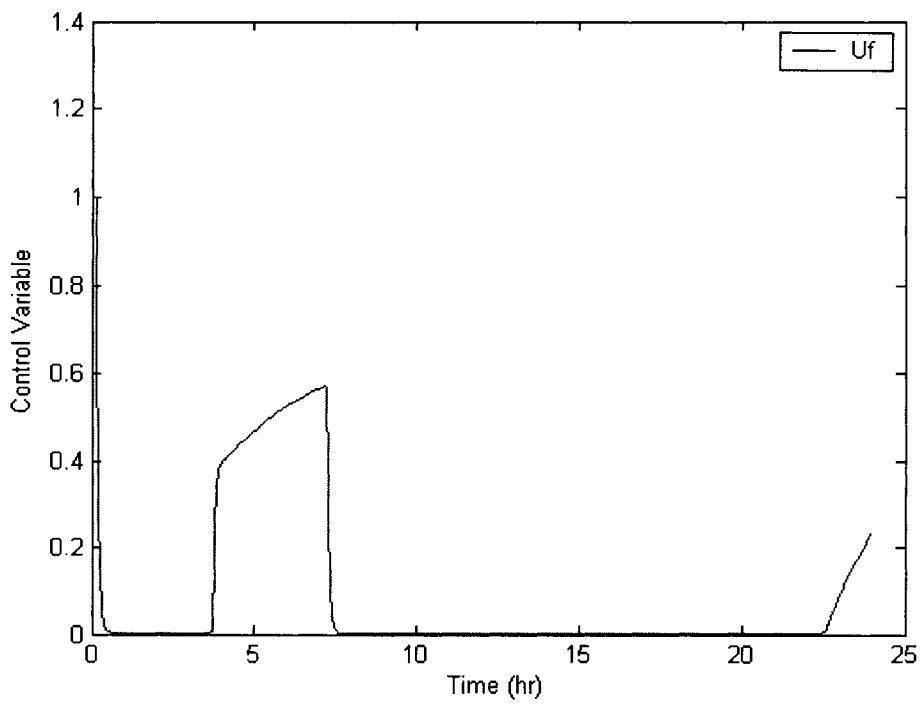


**Figure 5.17 Control Variable of Boiler Burner**

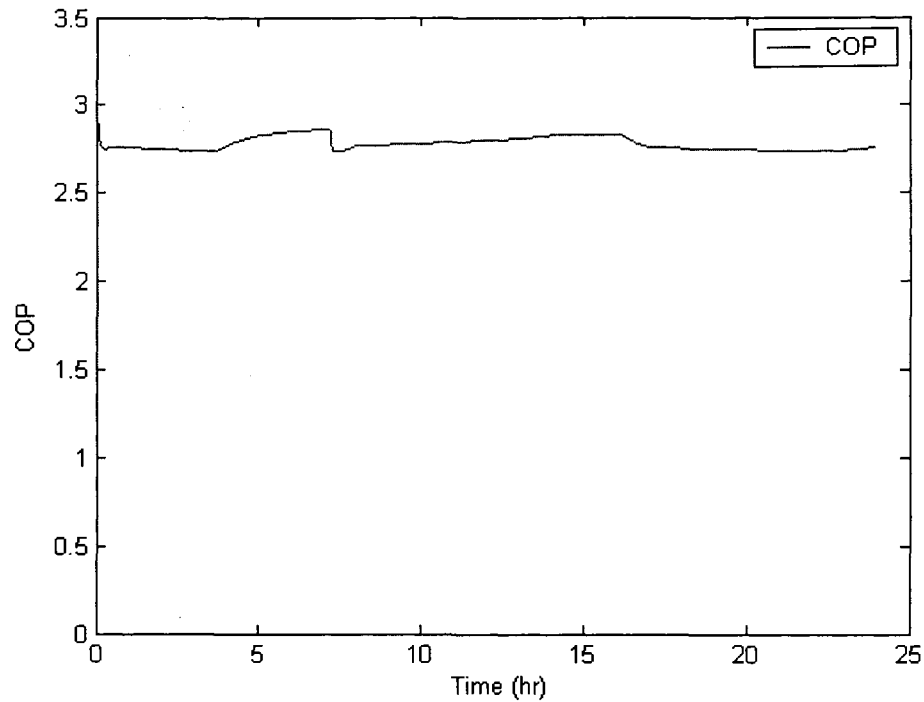


**Figure 5.18 COP of Heat Pump**

From Figures 5.13 to 5.18, the following observations can be made:

- a) Zone air temperature response was controlled at its set point, 21°C, throughout the day. Note that the temperature response of heat pump outlet air follows the building load profile.
- b) The outlet water temperature response of heat pump ranges between 0.1°C to 4°C due to variation in building load; that of ground loop is relatively constant with a range of around 4°C to 5°C, so is that of heat exchanger.
- c) Boiler water temperature response was controlled to keep near its set point, 50°C, throughout the day.
- d) Circulating pump 2 was controlled in either on or off mode based on corresponding

setpoint temperature.

➤ **Case 3: PI Controller for HP and On/off for Boiler**

In this strategy, the whole HGSHP system with PI control for the HP and On/off control for the boiler was simulated. The simulation results are shown in Figures 5.19 to 5.24.

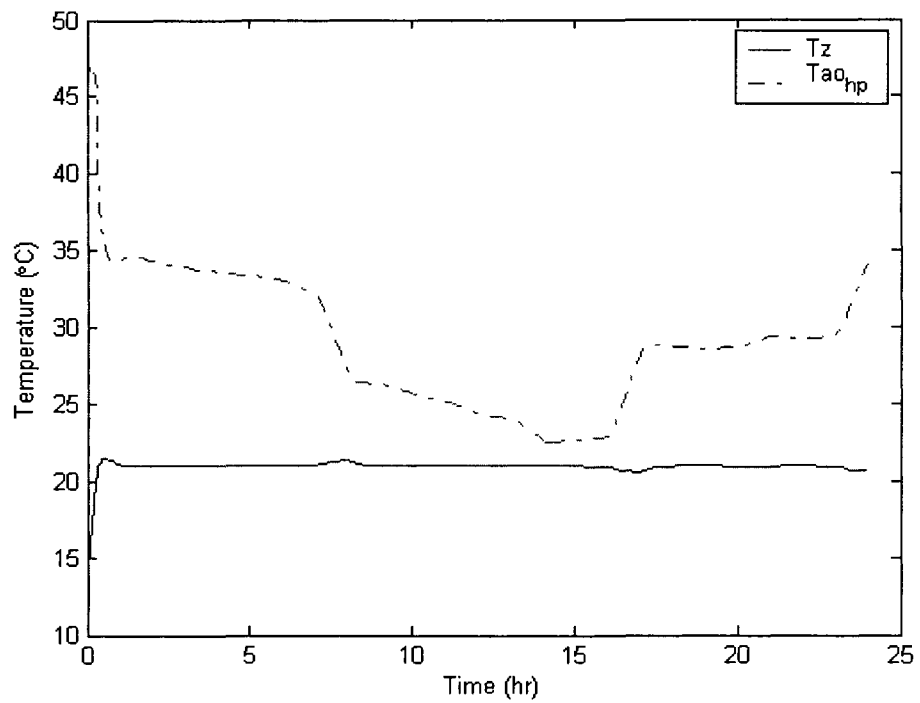


**Figure 5.19 Air Temperature responses of One Day Simulation**

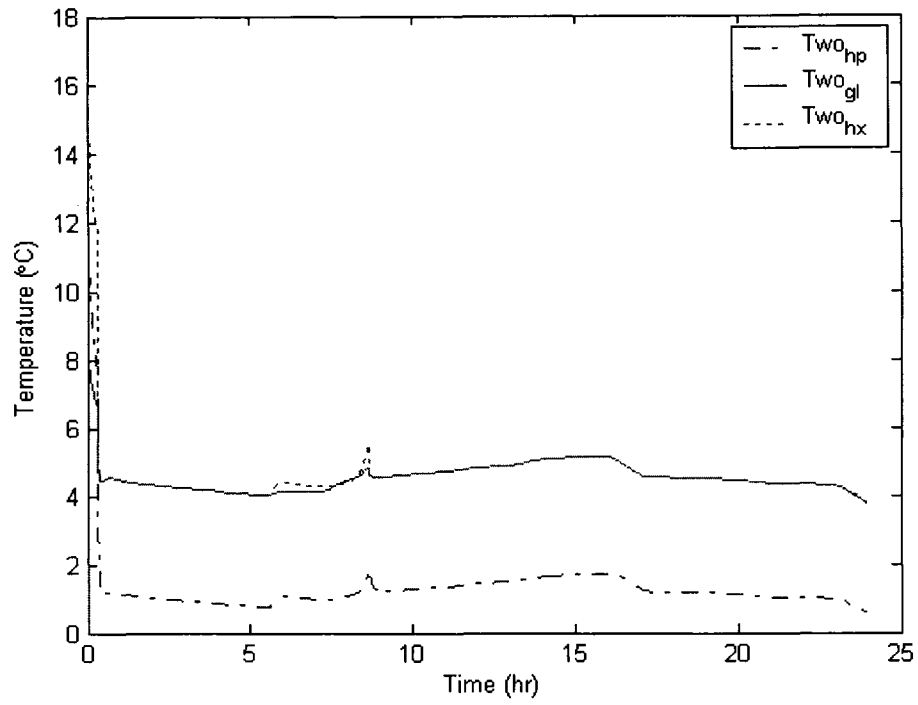


**Figure 5.20 Outlet Water Temperature responses of HP, GL and HX**

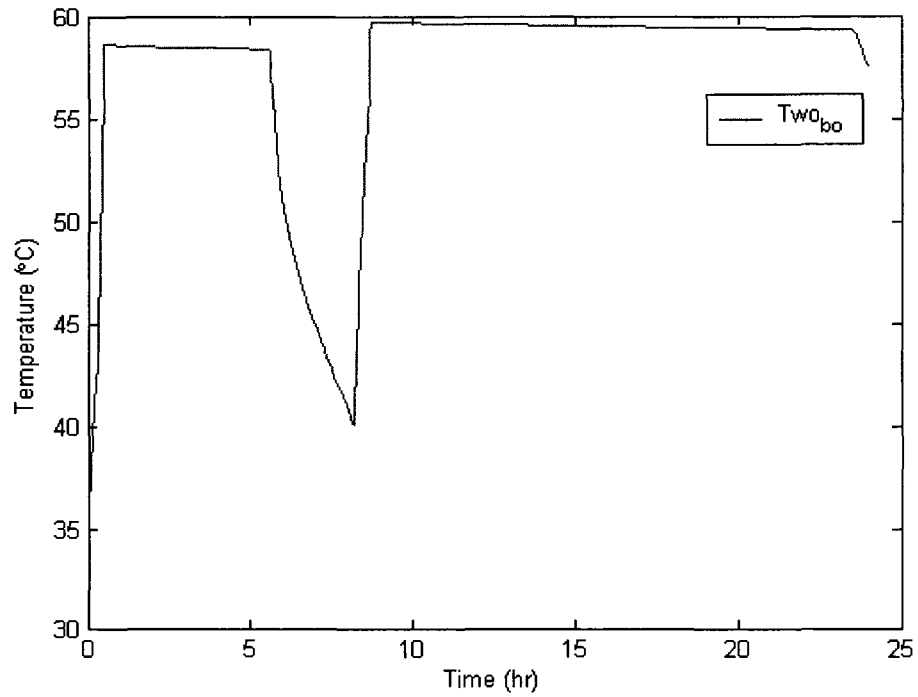


**Figure 5.21 Outlet Water Temperature response of Boiler**

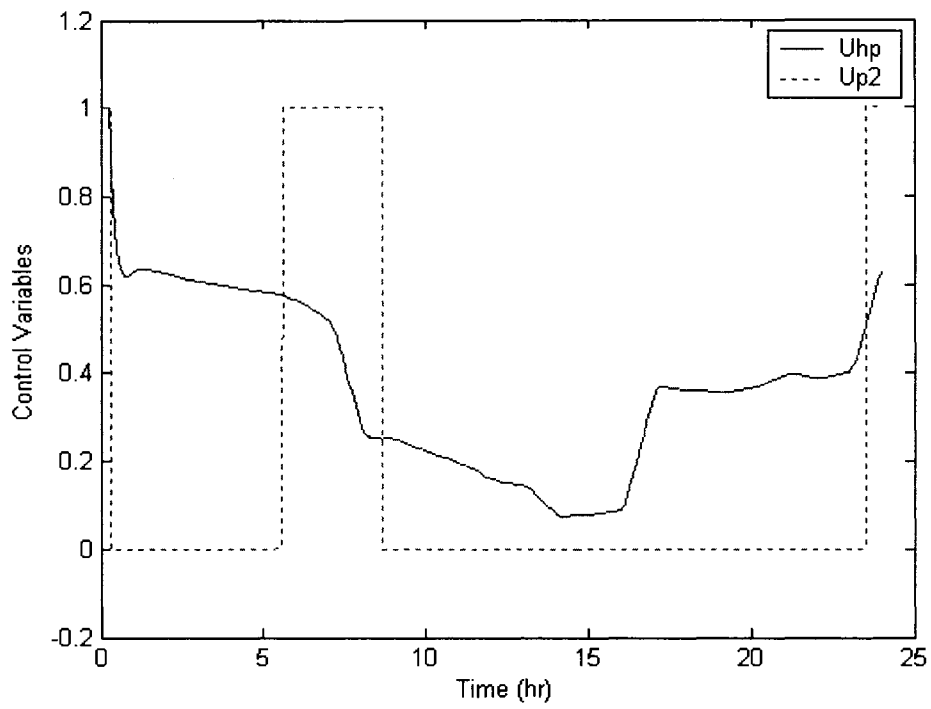


**Figure 5.22 Control Variables of HP and Pump 2**

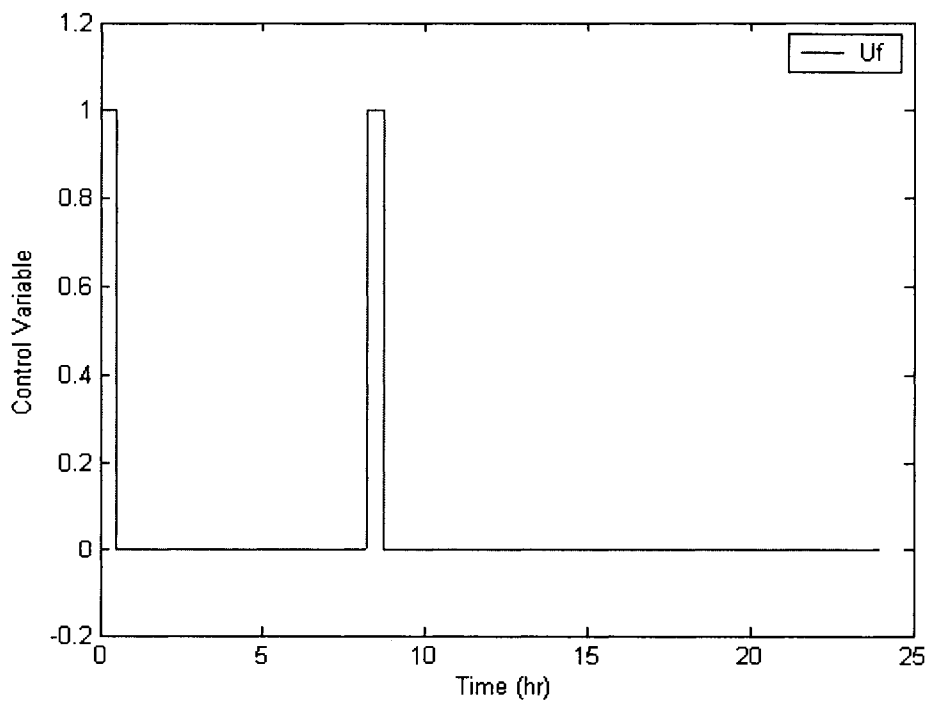


**Figure 5.23 Control Variable of Boiler Burner**

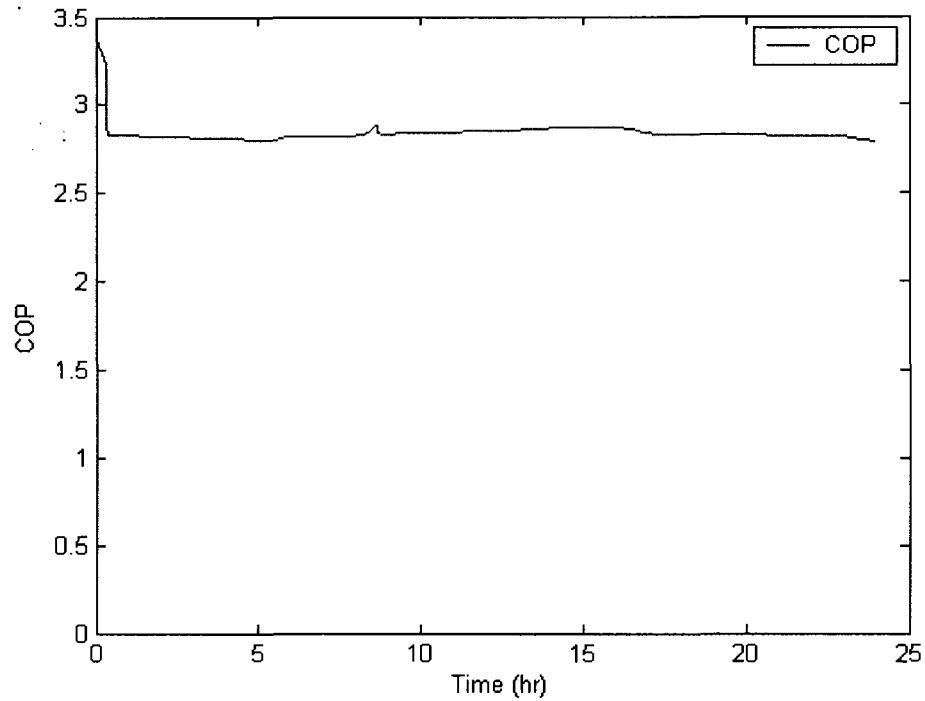


**Figure 5.24 COP of Heat Pump**

From Figures 5.19 to 5.24, it can be seen that:

- a) Zone air temperature response was controlled at its set point, 21°C, throughout the day, while the temperature response of heat pump outlet air follows the building load profile to keep zone air temperature at the setpoint.
- b) Boiler burner was turned on for a relatively short period of time as shown in Figure 5.23.

### **5.2.3 Heating Mode Cases Energy Comparison**

For the above 3 cases, when performing the simulations of whole HGSHP system with the control strategy on the specific day, the total energy consumption was also calculated.

They are 1175.9 kW-h, 1013.5 kW-h and 637.2 kW-h, respectively.

When comparing each case performance, one of the most important indexes is total energy consumption of whole system. From such point of view, it follows therefore that case 3, with PI controller for heat pump and On/off controller for boiler, achieves significant energy savings, 45% and 37.1%, respectively, compared to cases 1 and 2, under the same setpoint of indoor temperature.

However, for most office buildings, there can be two indoor temperature set points, one for office hours (e.g. 21°C for daytime) and the other non-office hours (e.g. 15°C for nighttime). Accordingly, this can result in a noticeable energy savings for a whole heating season, which will be discussed later. In the following case, two setting temperatures, 21°C for office hours from 8:00 to 17:00 and 15°C for the rest hours, are applied to check the feasibility of the control strategy as well. For the same office building on the same day as the above case, the hourly heating profile of the office building is shown in Figure 5.25.

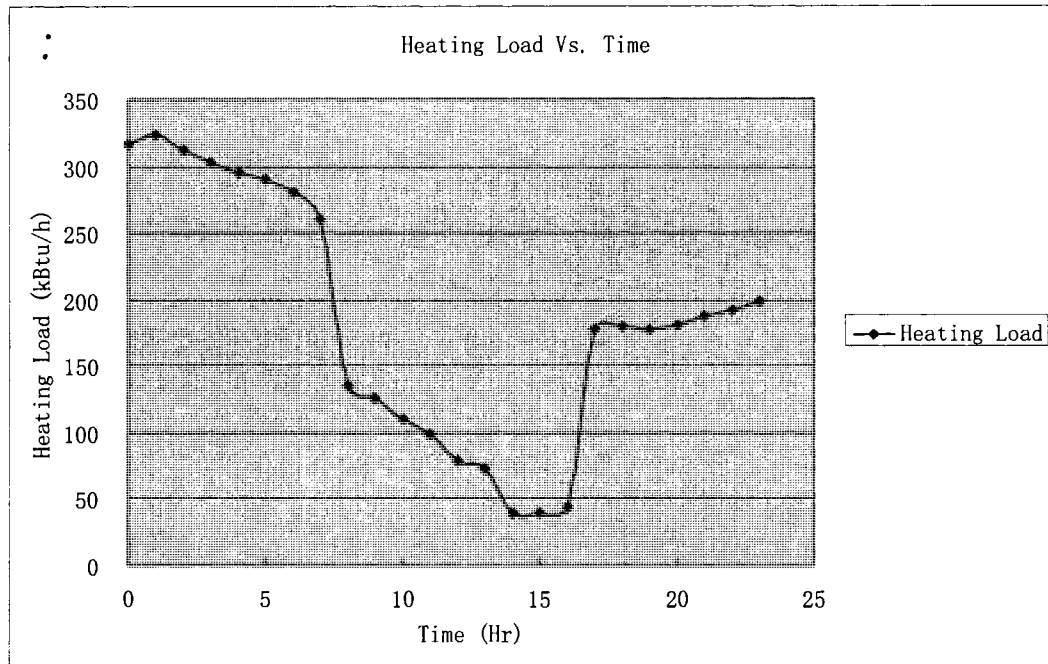


**Figure 5.25 Hourly Heating Load Profile (Tsp=15/21 °C)**

As Case 3 seems to be the most energy efficient compared to the other cases, the following will further discuss with such control strategy in case 3. Likewise, after performing the simulations of whole HGSHP system with the same control strategy on the same day at the dual setpoint indoor temperature, the simulation results are shown in Figures 5.26 to 5.31.

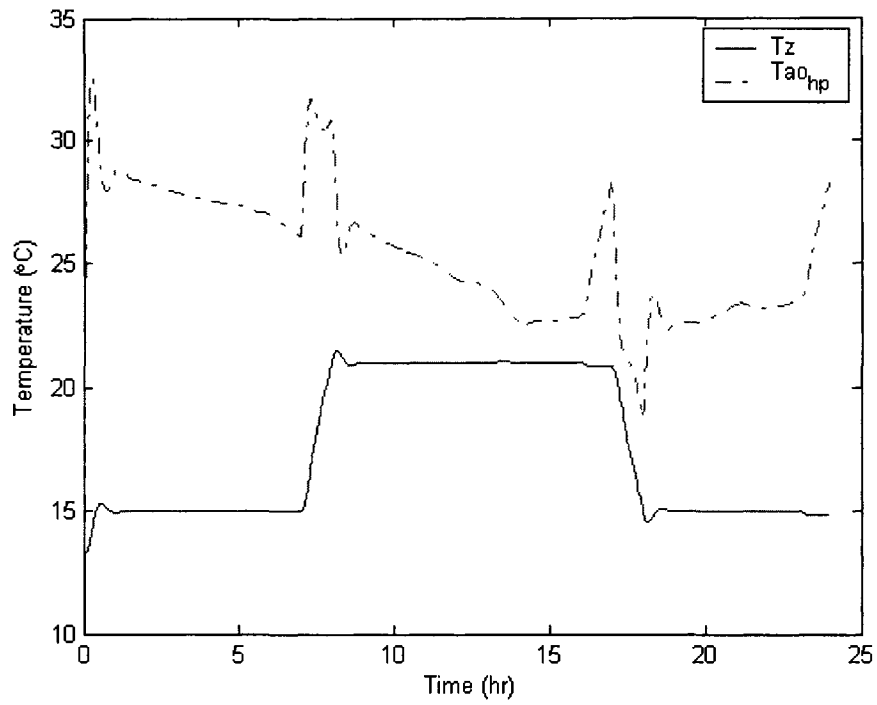


**Figure 5.26 Air Temperature responses of One Day Simulations (Tsp=15/21 °C)**

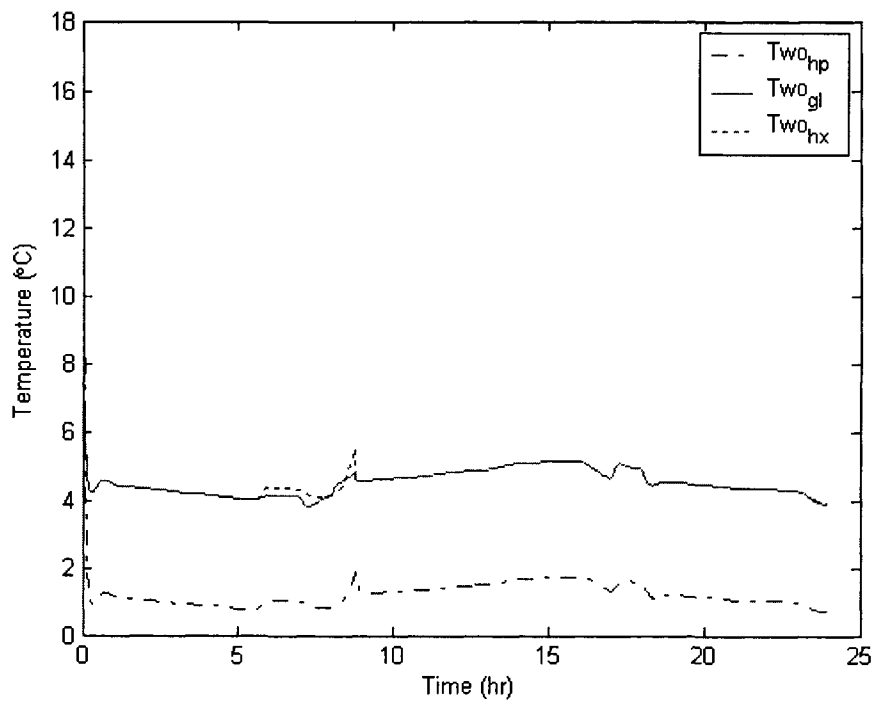


**Figure 5.27 Outlet Water Temperature responses of HP, GL and HX**

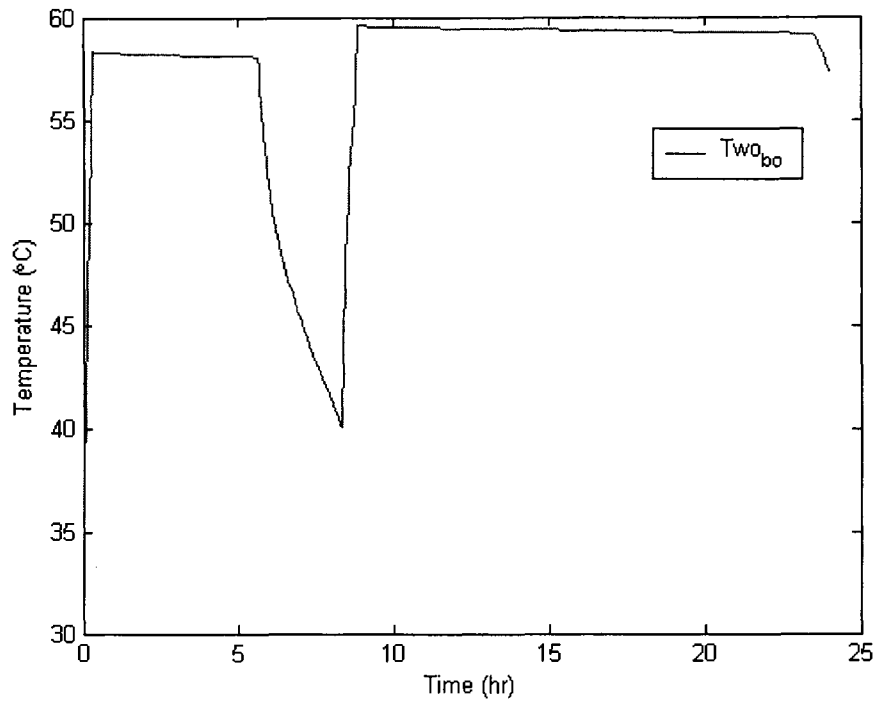


**Figure 5.28 Outlet Water Temperature response of Boiler ( $T_{sp}=15/21^{\circ}\text{C}$ )**

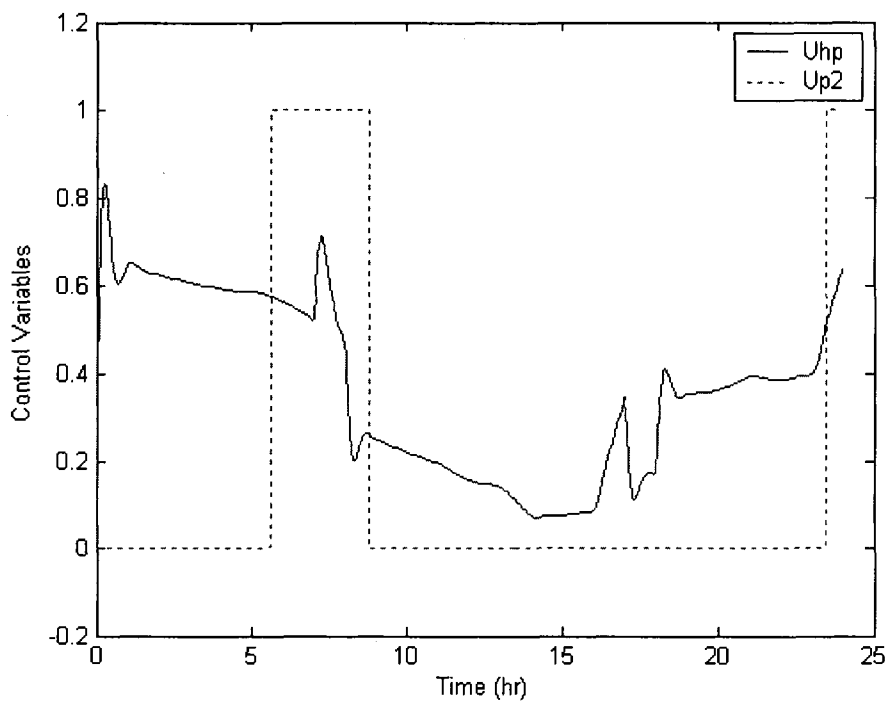


**Figure 5.29 Control Variables of HP and Pump2 ( $T_{sp}=15/21^{\circ}\text{C}$ )**

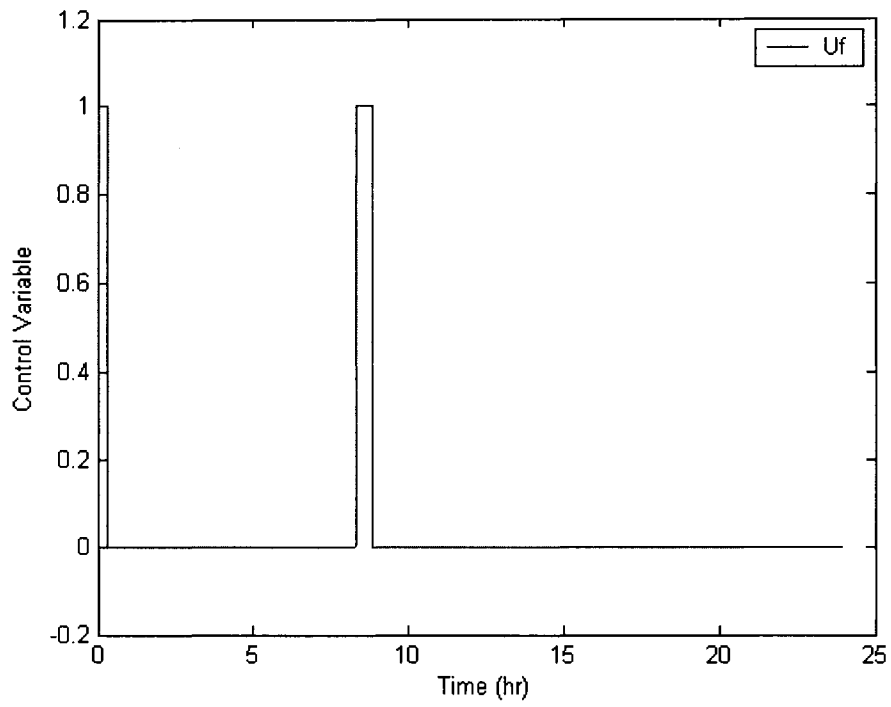


**Figure 5.30 Control Variable of Boiler Burner ( $T_{sp}=15/21^{\circ}\text{C}$ )**

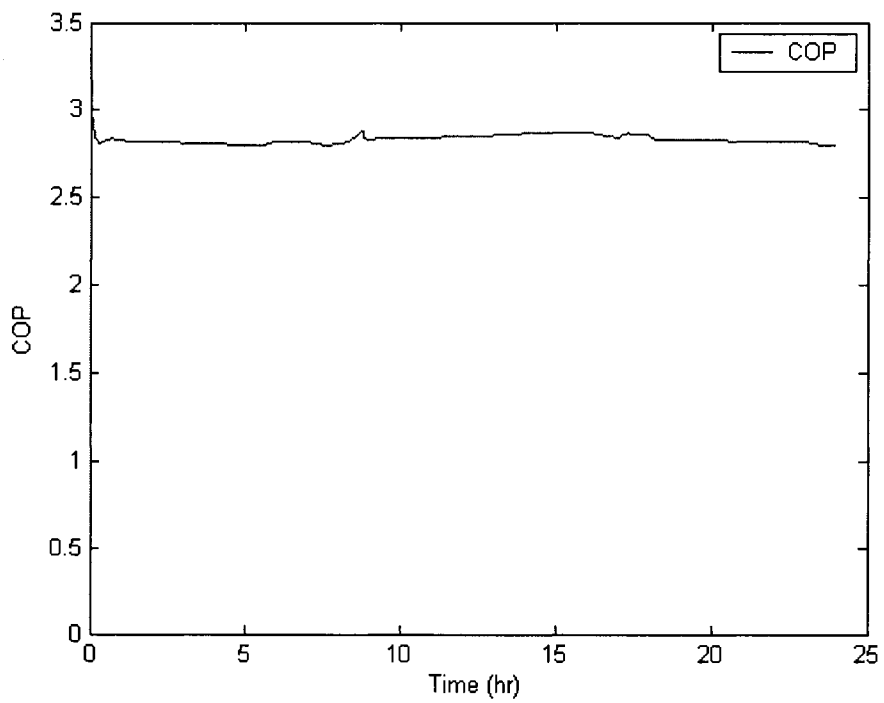


**Figure 5.31 COP of Heat Pump ( $T_{sp}=15/21^{\circ}\text{C}$ )**

From Figures 5.26 to 5.31, the following observations can be made:

a) Zone air temperature response was controlled at its set points, 21°C for office hours from 8:00 to 17:00 and 15°C for the rest non-office hours on the specific day, while the temperature response of heat pump outlet air was controlled to keep zone air temperature at the setpoints.

b) The heat pump modulation rate follows the dual setpoint and building load profile.

The total energy consumption for this case was 574.9 kW-h; that is, an energy saving of 9.7% can be obtained, compared to single setpoint of indoor temperature.

The design parameters of the PI controllers used throughout the simulations for heat pump and boiler operating in heating mode are listed in Table 5.2.

**Table 5.2 Design parameters of PI controllers**

Symbol	Magnitude	Units	Symbol	Magnitude	Units
$K_p$ (HP)	0.2	-	$K_p$ (BO)	0.15	-
$K_i$ (HP)	0.0002	-	$K_i$ (BO)	0.0003	-

5.2  
.4  
Co

### oling Mode of Operation

The following two control strategies were used to simulate cooling mode of simulation.

#### 5.2.4.1 On/off controllers for Heat Pump and Cooling Tower

- For heat pump, if  $T_z \geq T_{sp} + \Delta T/2$ ,  $U_{hp}=1$ ; elseif  $T_z \leq T_{sp} - \Delta T/2$ ,  $U_{hp}=0$ .

Heat pump is turned on only when zone air temperature,  $T_z$ , is greater than  $T_{sp}$

+  $\Delta T/2$ , e.g. 23.5°C, while it is switched off when  $T_z$  is less than  $T_{sp} - \Delta T/2$ , e.g. 22.5°C.

- For circulating pump 1, *if*  $U_{hp}=1$ ,  $U_{p1}=1$ ; *elseif*  $U_{hp}=0$ ,  $U_{p1}=0$ .  
Circulating pump1 is turned on only when heat pump is on. Otherwise, it is off.
- For circulating pump 2, *if* ( $U_{hp}=1$  &  $T_z \geq T_{sp} + \Delta T/2$ ) *OR*  $T_w > T_{w,sp}$ ,  $U_{p2}=1$ ; *else*  $U_{p2}=0$ . Circulating pump 2 is turned on only when heat pump is on and zone air temperature  $T_z$  is still greater than 23.5°C, or entering water temperature of heat pump is greater than set point water temperature. Otherwise, it is off.
- For closed-circuit cooling tower, *if*  $U_{p2}=1$ ,  $U_{ct}=1$ ; *elseif*  $U_{p2}=0$ ,  $U_{ct}=0$ .  
Cooling tower is turned on when circulating pump 2 is on. Otherwise, it is off.

#### 5.2.4.2 PI Control for HP and On/off Control for Cooling Tower

- For heat pump, with a known user-defined  $T_{sp}$ ,  $U_{hp} = K_p e(t) + K_i \int e(t) dt$ .  
Heat pump is turned on when  $U_{hp}$  is greater than 0, while it is switched off when  $U_{hp}$  is equal to 0.
- For circulating pump 1, *if*  $U_{hp} > 0$ ,  $U_{p1}=1$ ; *elseif*  $U_{hp}=0$ ,  $U_{p1}=0$ .  
Circulating pump1 is turned on only when heat pump is on. Otherwise, it is off.
- For circulating pump 2, *if* ( $U_{hp}=1$  &  $T_z \geq T_{sp} + \Delta T/2$ ) *OR*  $T_w > T_{w,sp}$ ,  $U_{p2}=1$ ; *else*  $U_{p2}=0$ . Circulating pump 2 is turned on when heat pump is on and zone air temperature  $T_z$  is still greater than 23.5°C, or when entering water temperature of heat pump is greater than set point water temperature. Otherwise, it is turned off.

- For closed-circuit cooling tower, *if*  $Up2=1$ ,  $Uct=1$ ; *elseif*  $Up2=0$ ,  $Uct=0$ .

Cooling tower is turned on when circulating pump 2 is on. Otherwise, it is turned off.

### 5.2.5 Cooling Mode Simulation Results

In order to examine whether or not the control strategy works well for the whole HGSHP system in cooling mode of operation, a realistic single day rather than the design day, e.g. a day in August, is studied in this case. The hourly outdoor air temperatures are listed in the following Table 5.3 (From Environment Canada).

**Table 5.3 Hourly Outdoor Air Temperatures of a specific day in summer**

Hr	To (°C)	Hr	To (°C)	Hr	To (°C)	Hr	To (°C)
<b>0:00</b>	19.6	<b>6:00</b>	17.4	<b>12:00</b>	27.1	<b>18:00</b>	27.4
<b>1:00</b>	18.6	<b>7:00</b>	19.7	<b>13:00</b>	27.4	<b>19:00</b>	25.4
<b>2:00</b>	18.2	<b>8:00</b>	22.3	<b>14:00</b>	28.1	<b>20:00</b>	24.5
<b>3:00</b>	18.2	<b>9:00</b>	22.0	<b>15:00</b>	28.4	<b>21:00</b>	22.9
<b>4:00</b>	17.2	<b>10:00</b>	24.5	<b>16:00</b>	28.3	<b>22:00</b>	23.4
<b>5:00</b>	16.6	<b>11:00</b>	26.1	<b>17:00</b>	27.9	<b>23:00</b>	22.0

As the design indoor temperature for the office building is set 23°C, the hourly cooling load of the building can be calculated. The load profile of the office building on the specific day is presented in Figure 5.32.

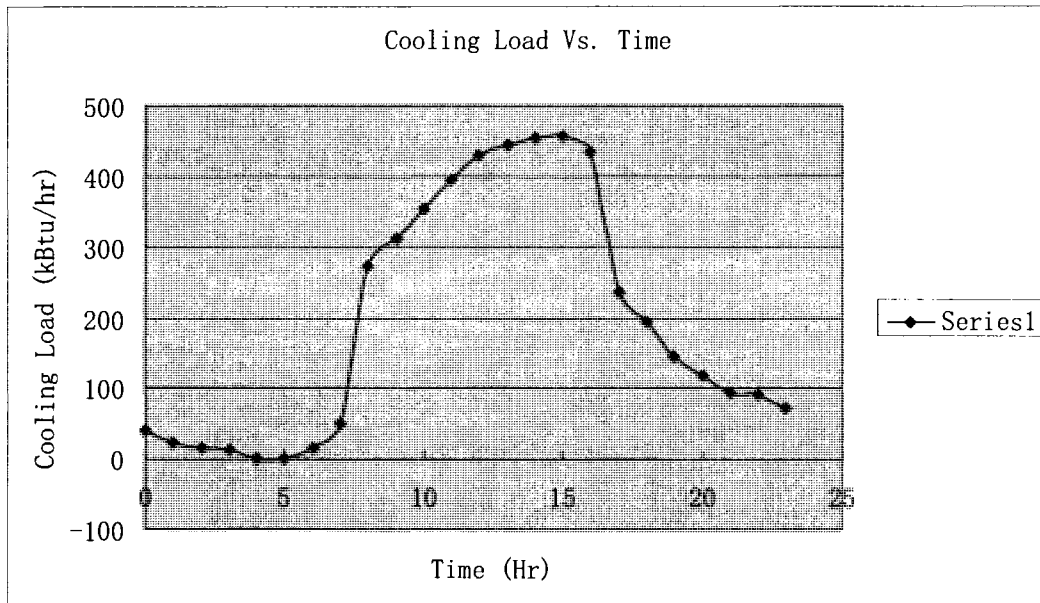


**Figure 5.32 Hourly Cooling Load Profile on a Specific Day**

➤ **Case 1: On/off Controllers for HP and Cooling Tower**

The simulation results for this case are shown in Figures 5.33 to 5.38, of which Figures 5.33, 5.34 and 5.36 show only a few hours simulation for clarity.

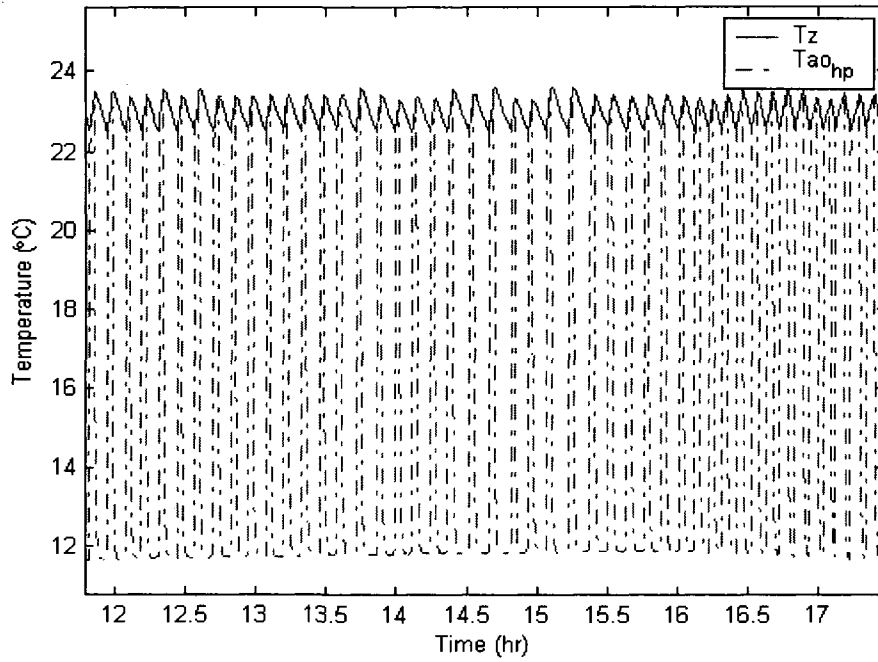


**Figure 5.33 Zone air and HP outlet air temperature responses**

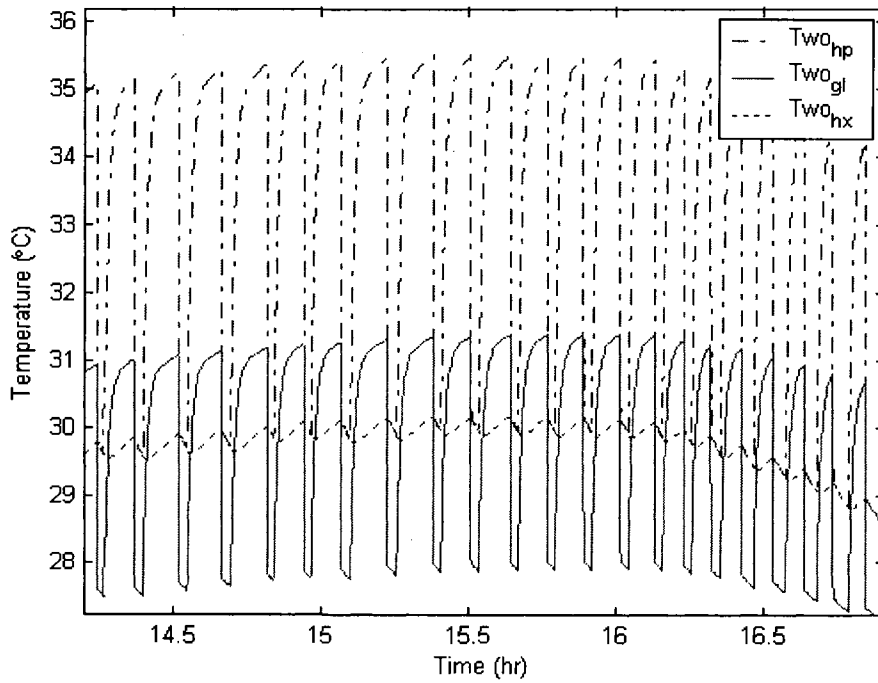


**Figure 5.34 Outlet water temperature responses of HP, GL and HX**

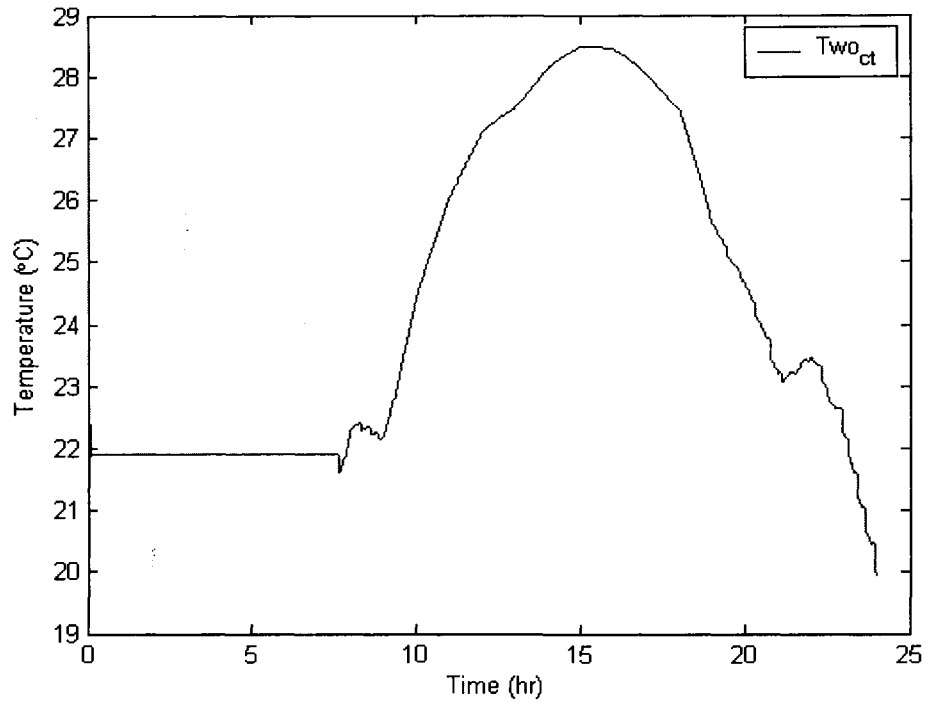


**Figure 5.35 Outlet water temperature response of cooling tower**

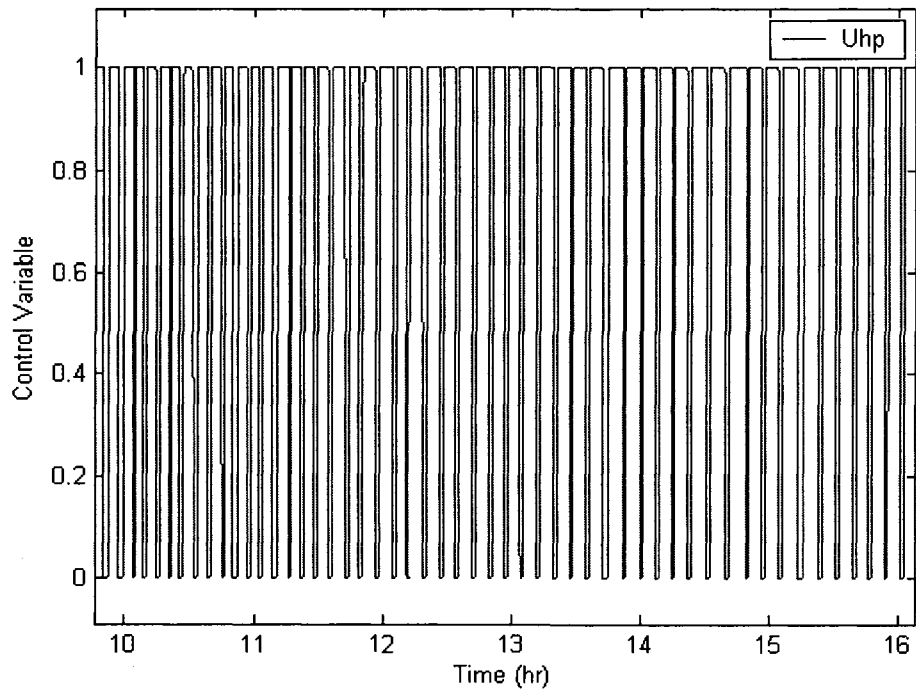


**Figure 5.36 Control variable of HP**

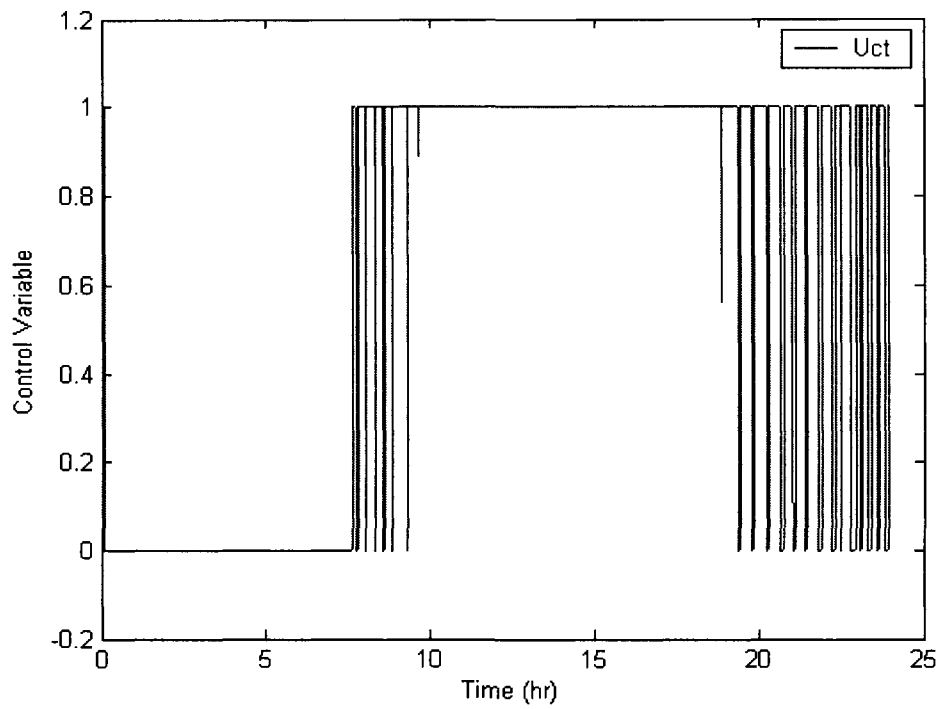


**Figure 5.37 Control variable of cooling tower**

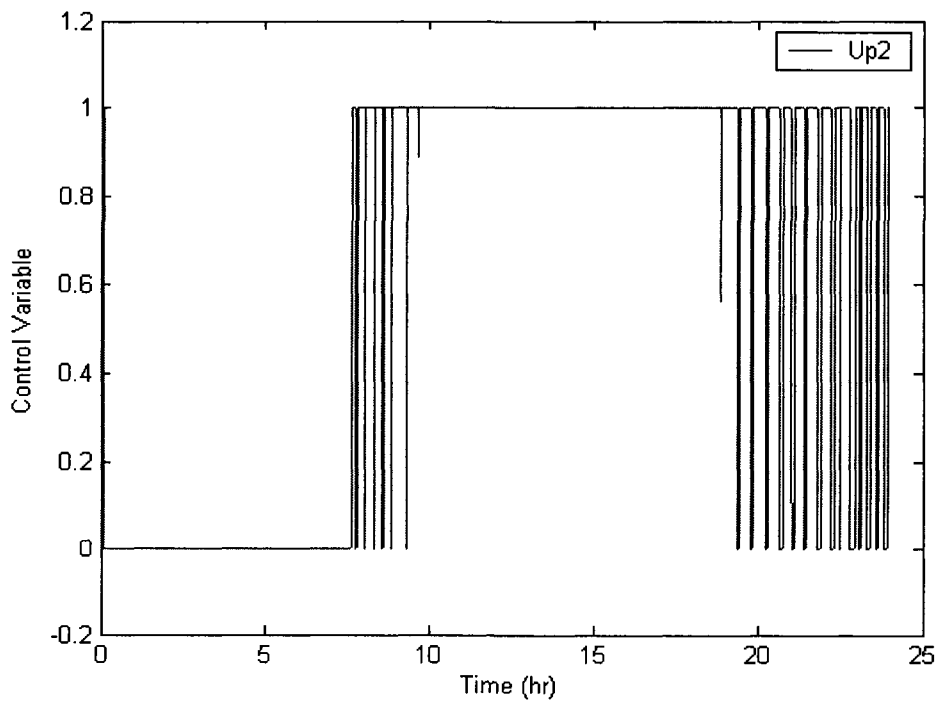


**Figure 5.38 Control variable of circulating pump 2**

From Figures 5.33 to 5.38, it is noted that:

- a) Zone air temperature response was controlled within the desired range, 22.5°C to 23.5°C, on the specific day. The temperature responses show cyclic on-off trends.
- b) When heat pump is on, the water temperature responses of heat pump, ground loop, and heat exchanger are around 35°C, 31°C, and 30°C respectively. Conversely, when heat pump is off, that of heat pump, ground loop and heat exchanger are around 28°C, 28°C, and 30°C respectively.

➤ **Case 2: PI Controller for HP and On/off for Cooling Tower**

This is a more realistic control strategy. The simulation results with this strategy are shown in Figures 5.39 to 5.43.

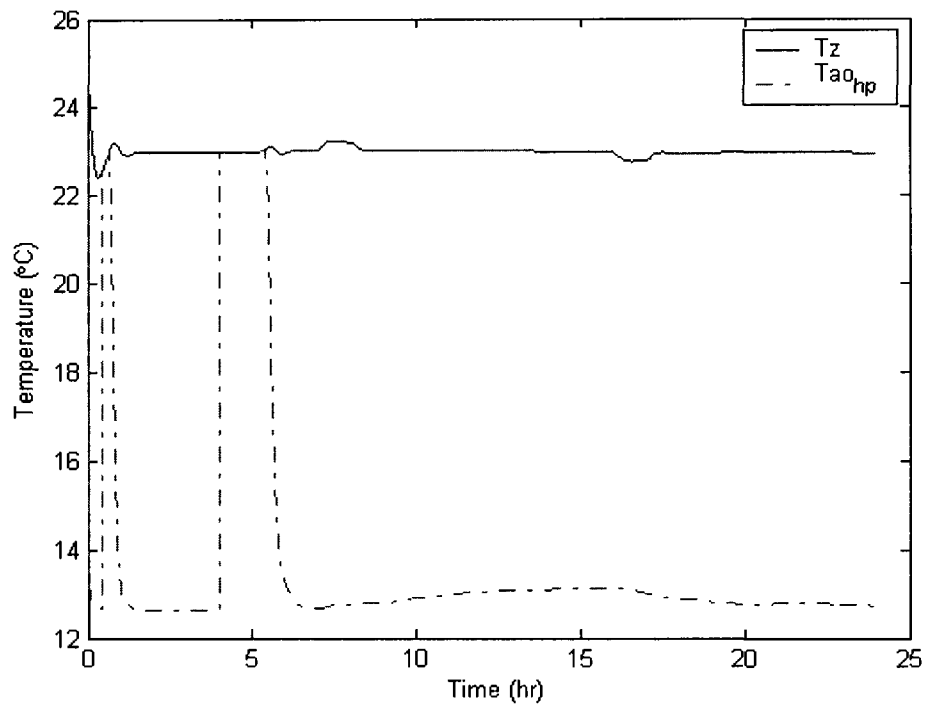


**Figure 5.39 Zone air and HP outlet air temperatures**

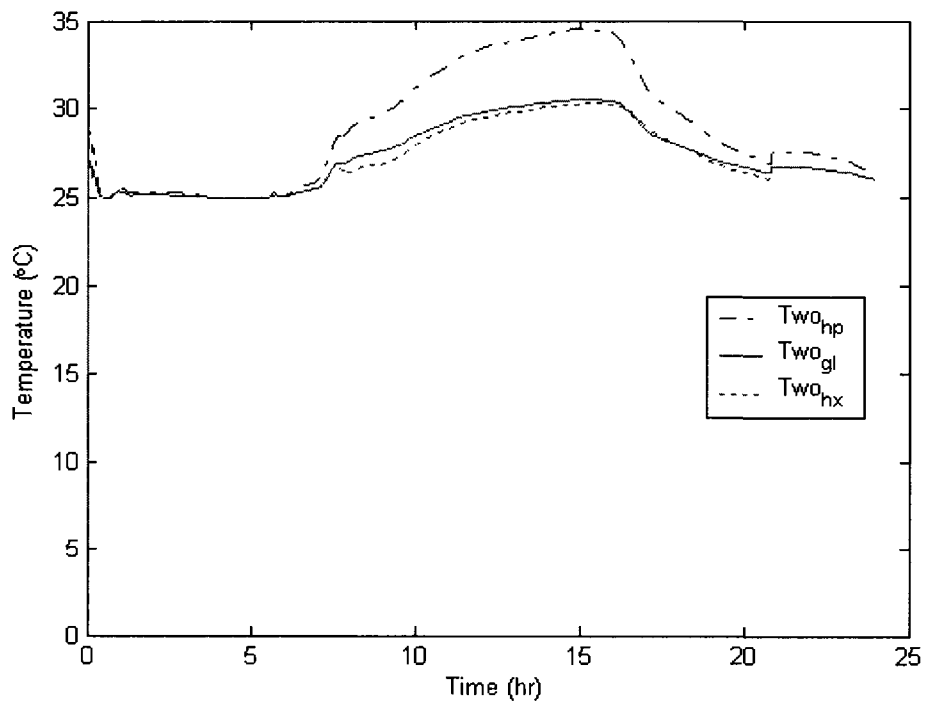


**Figure 5.40 Outlet water temperature responses of HP, GL and HX**

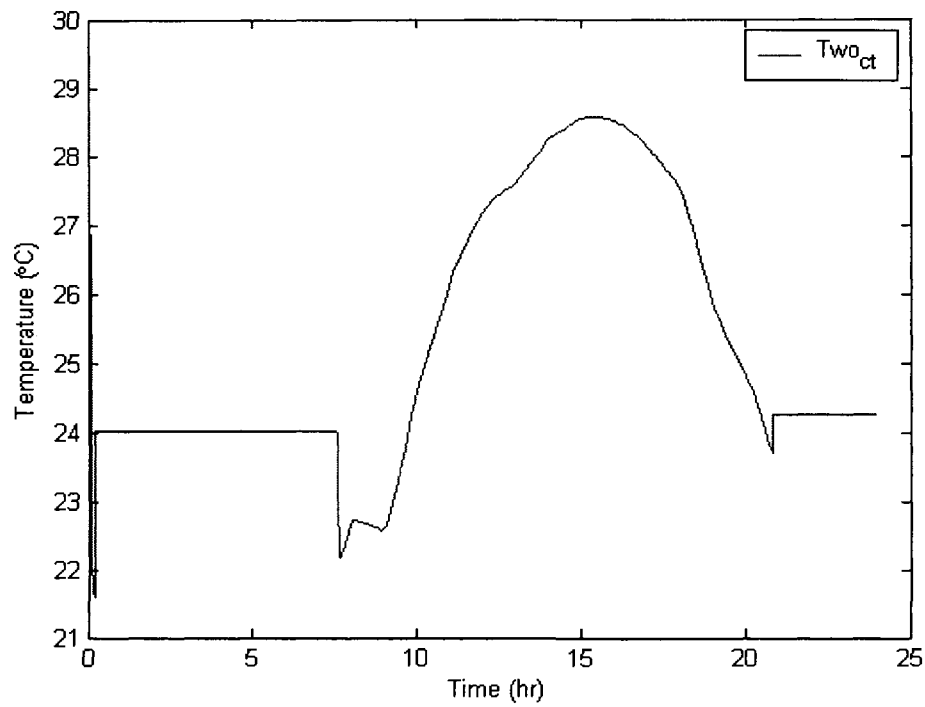


**Figure 5.41 Outlet water temperature response of cooling tower**

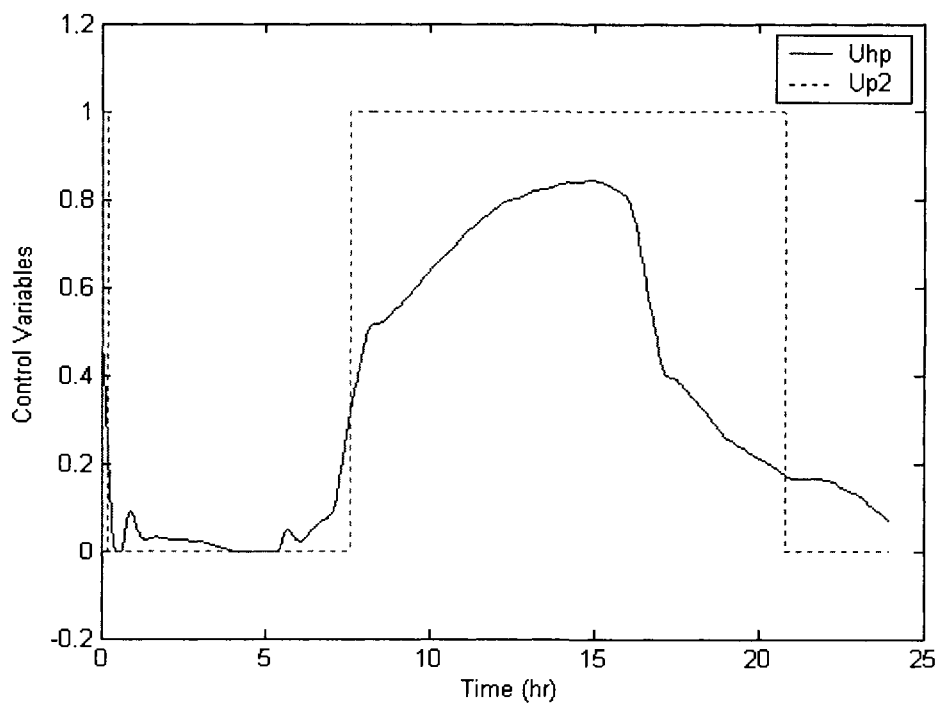


**Figure 5.42 Control variables of HP and pump 2**

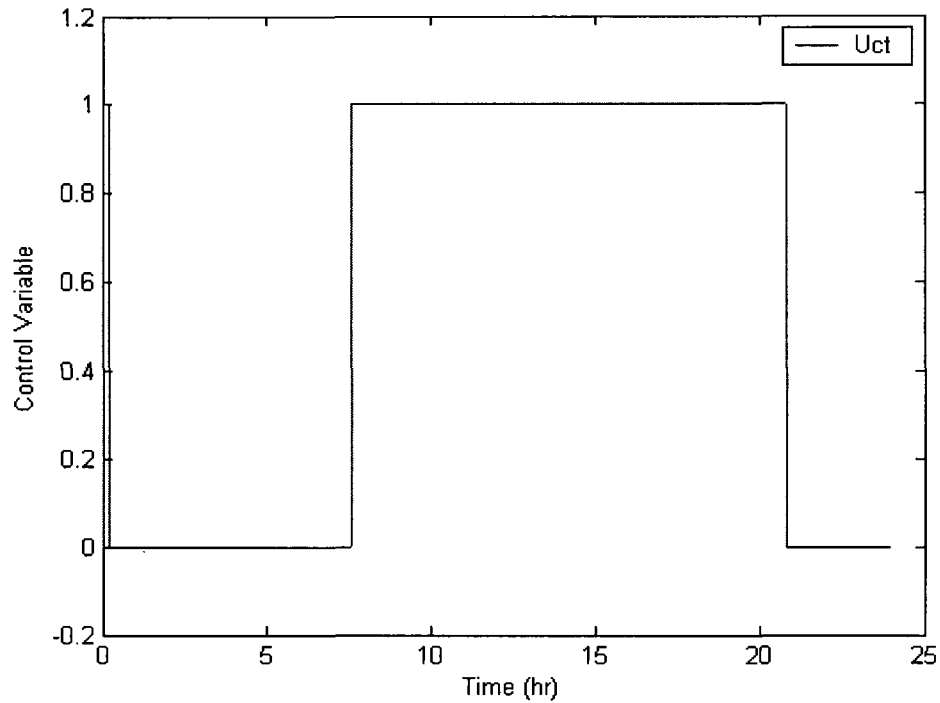


**Figure 5.43 Control variable of cooling tower**

From Figures 5.39 to 5.43, the following observations can be made:

- a) Zone air temperature response was controlled at its set point, 23°C, throughout the day.
- b) The cooling tower and ground loop water temperatures follow the cooling load profile.

➤ **Case 3: PI Controller for HP and On/off for CT without Heat Exchanger**

As in Case 2, with a plate heat exchanger between ground loop and cooling tower loop, the water temperature drop at the heat exchanger does not seem to be as adequate as expected.

As a result, a case like case 2 but without heat exchanger – which means ground loop outlet water goes directly into cooling tower and then heat pump – is studied in the following. The simulation results with this strategy are shown in Figures 5.44 to 5.48.

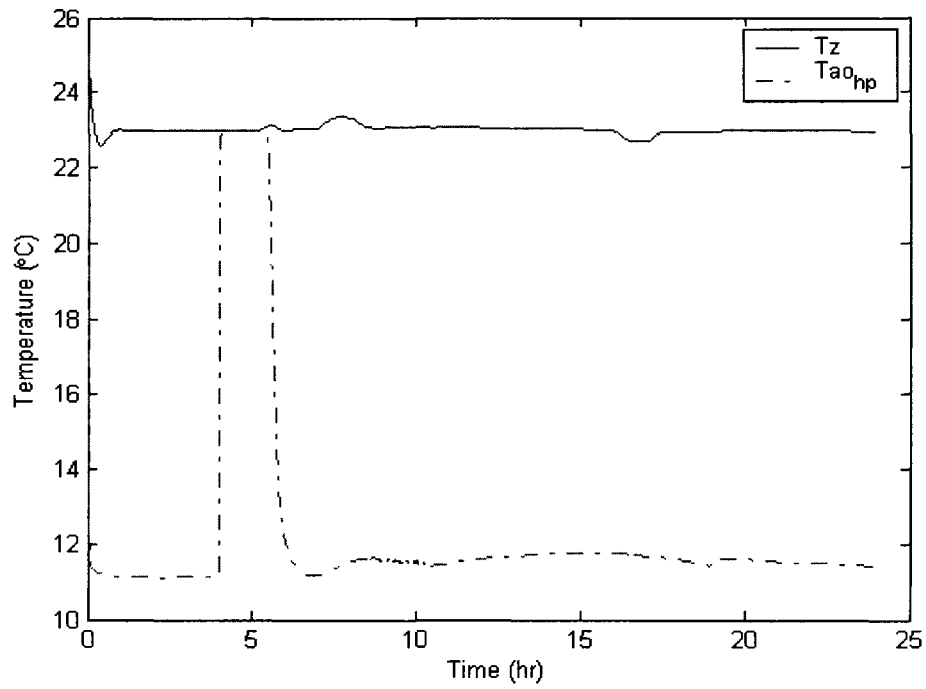


**Figure 5.44 Zone air and HP outlet air temperatures**

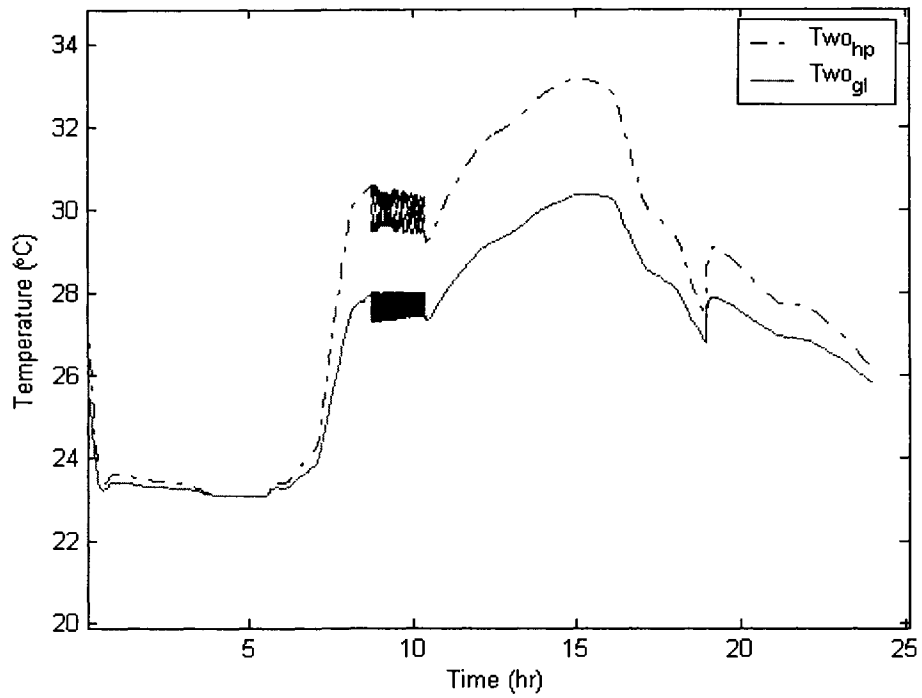


**Figure 5.45 Outlet water temperatures of HP and GL**

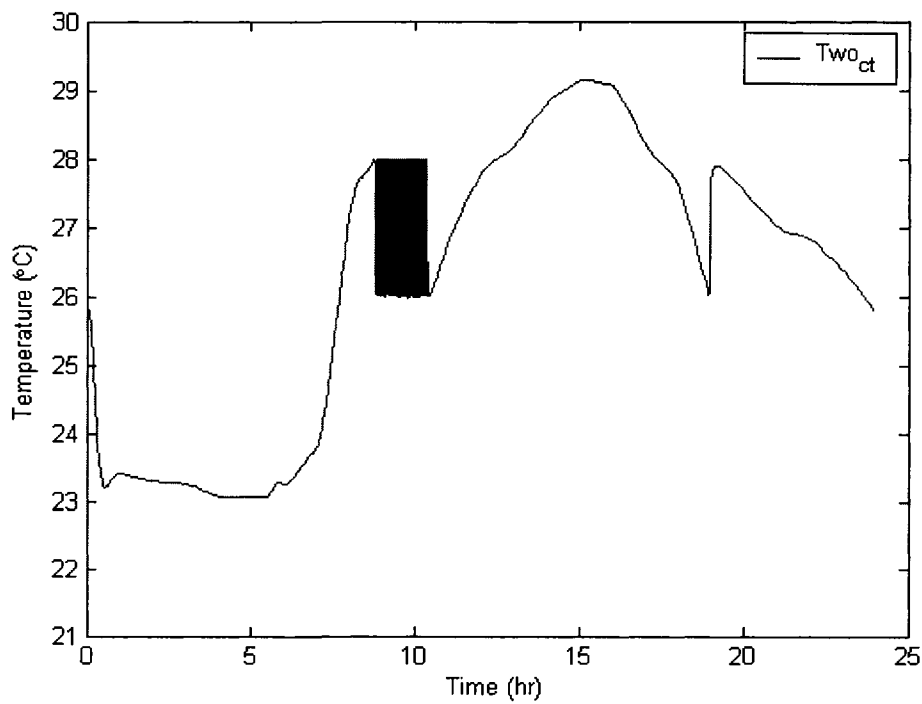


**Figure 5.46 Outlet water temperature of cooling tower**

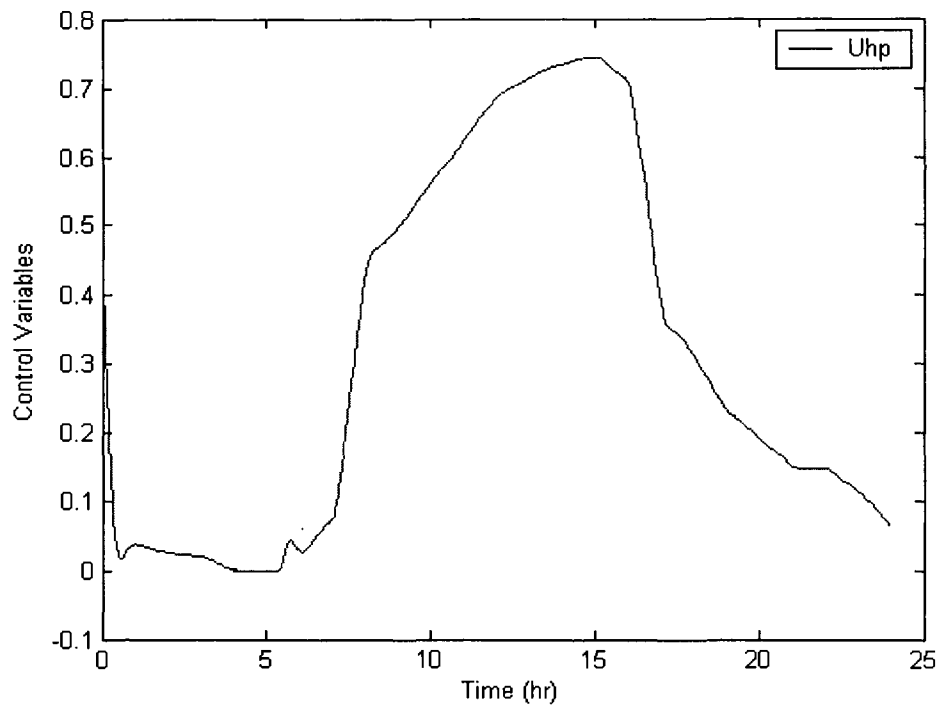


**Figure 5.47 Control variable of HP**

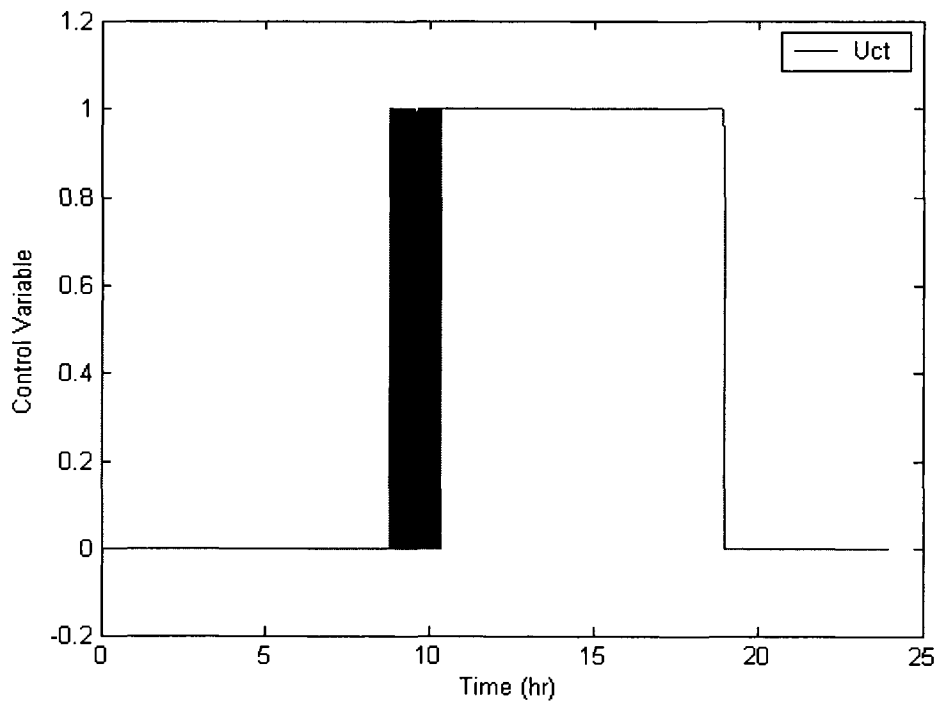


**Figure 5.48 Control variable of cooling tower**

From Figures 5.44 to 5.48, it can be seen that:

- a) Zone air temperature response was maintained close to its set point, 23 °C , throughout the day.
- b) The outlet water temperature response of heat pump ranges between 24°C to 32°C in response to building load; that of ground loop is relatively constant with a range of around 24°C to 30°C.
- c) Without the plate heat exchanger, circulating pump 2 and cooling tower were more sensitive to be turned on to cool outlet water of ground loop.

### **5.2.6 Cooling Mode Cases Energy Comparison**

The total energy consumption for the above three cases were calculated. These are 525.8 kW-h, 431.5 kW-h, and 437.2 kW-h respectively.

From the above energy consumption, it follows therefore that case 2, with PI controller for HP and On/off controller for cooling tower, achieves a significant energy saving of 21.9% compared to cases 1. Although case 2, compared to case 3 without heat exchanger, does not achieve as many energy savings as that to case 1, it, unlike case 3, has a relatively stable temperature drop with cooling tower. As a consequence, the whole HGSHP system has a relatively stable performance.

Considering two indoor temperature set points, one for office hours (e.g. 23°C for daytime) and the other non-office hours (e.g. 26°C for nighttime) as shown below can result in a noticeable energy savings. In the following two setting temperatures, 23°C for office

hours from 8:00 to 17:00 and 26°C for the rest hours, are applied to check the feasibility of the control strategy. For the same office building on the same day as the above case, the hourly heating profile of the office building is shown in Figure 5.49.

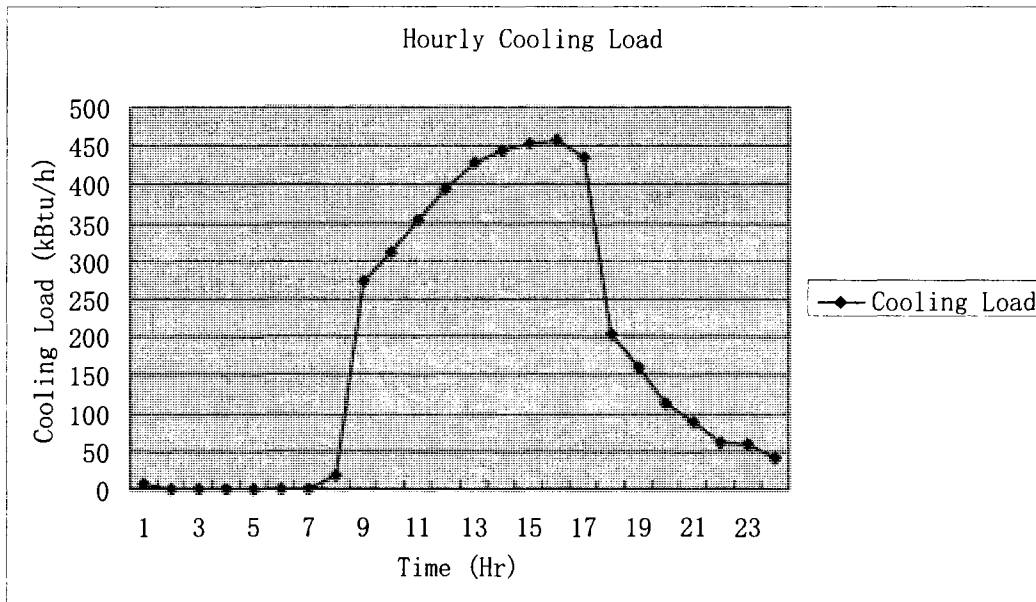


**Figure 5.49 Hourly Cooling Load Profile (Tsp=23/26°C)**

The simulation results with the dual setpoint indoor temperature are shown in Figures 5.50 to 5.54.

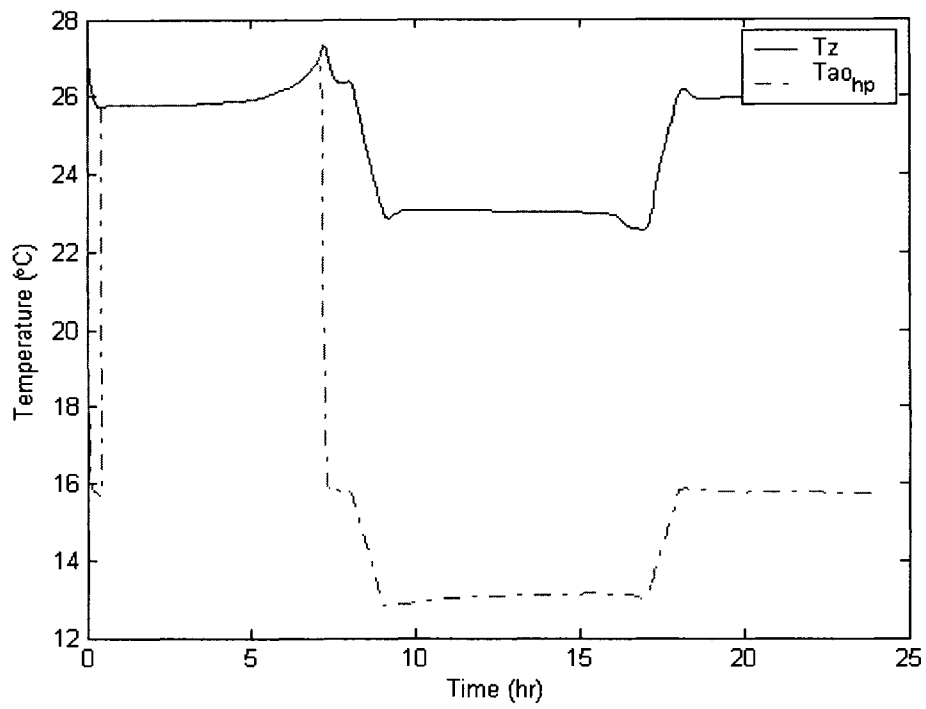


**Figure 5.50 Zone air and HP outlet air temperature responses**

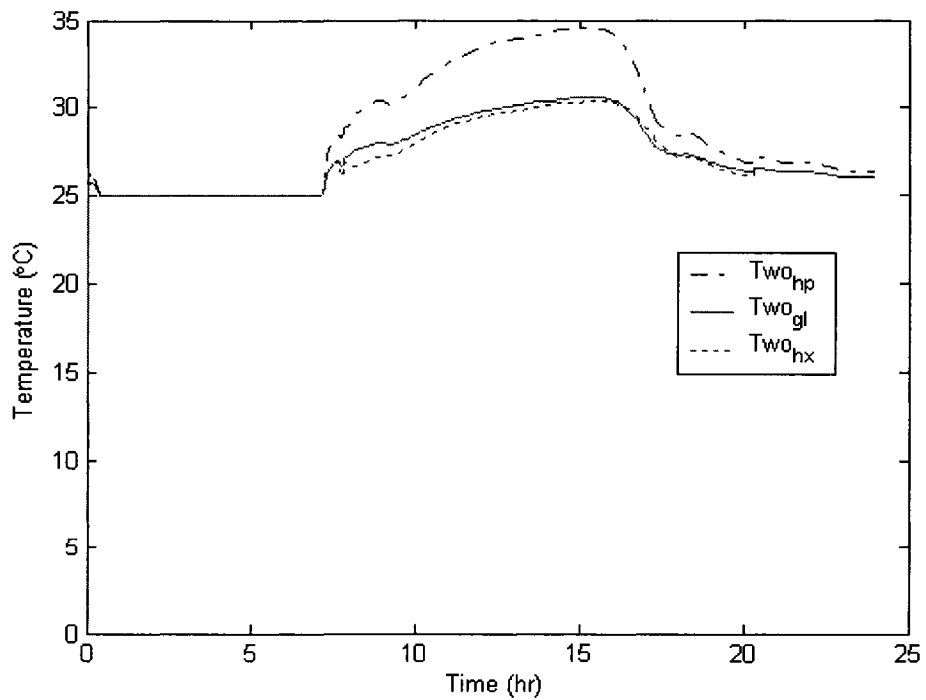


**Figure 5.51 Outlet water temperature responses of HP, GL and HX**

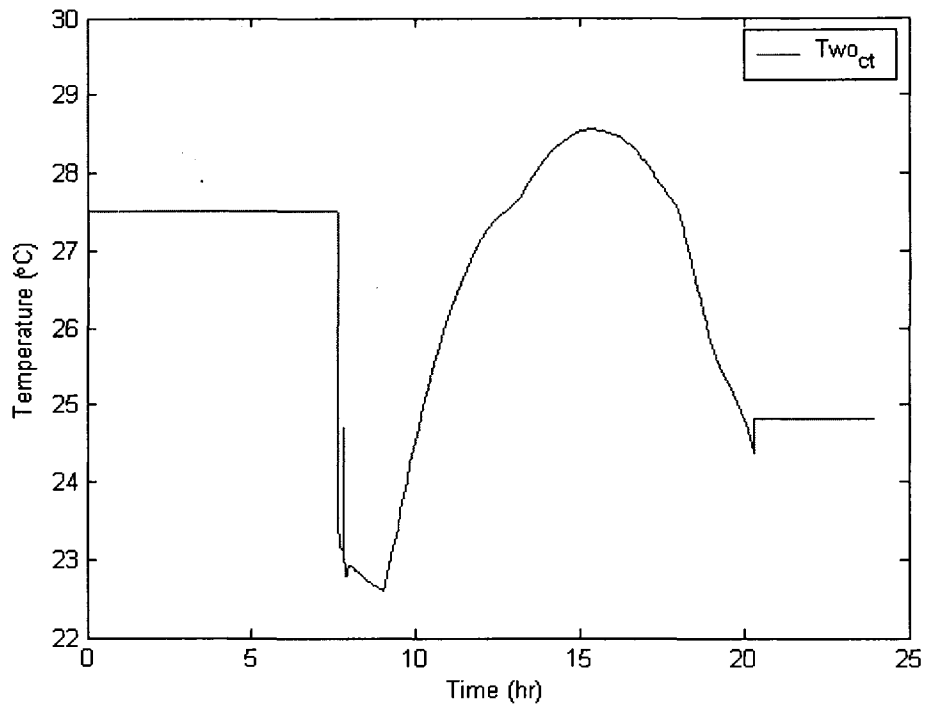


**Figure 5.52 Outlet water temperature response of cooling tower**

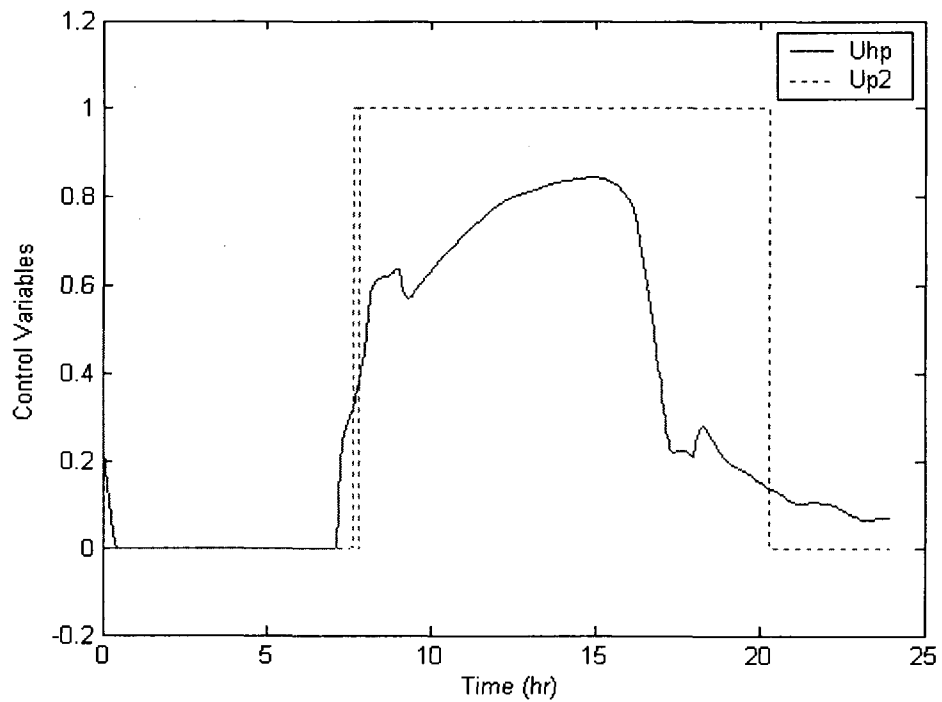


**Figure 5.53 Control variables of HP and pump 2**

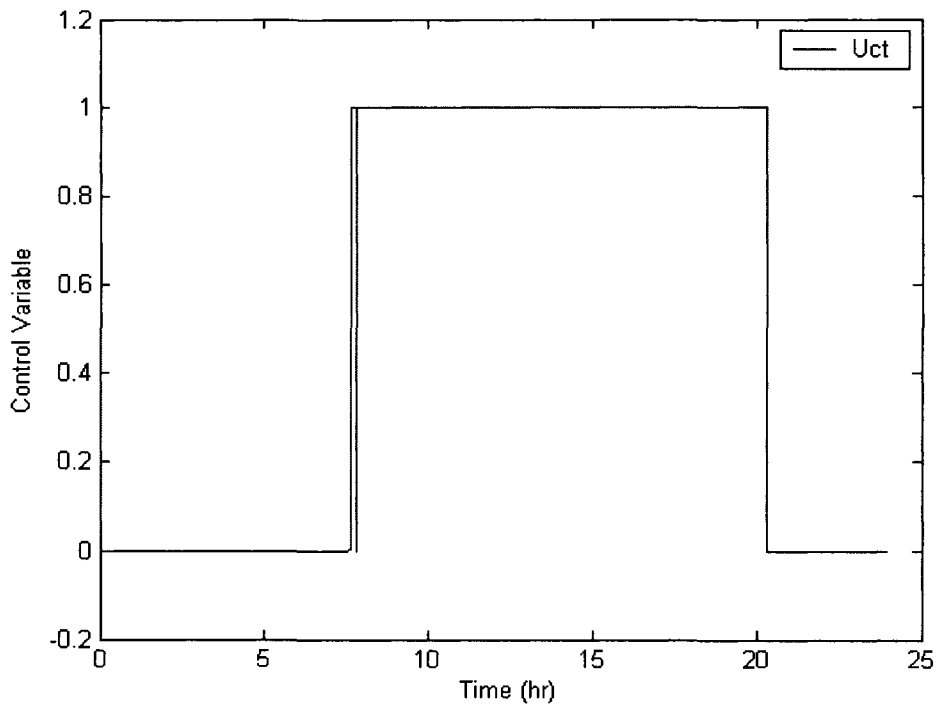


**Figure 5.54 Control variable of cooling tower**

From Figures 5.50 to 5.54, the following observations can be made:

- a) Zone air temperature response was controlled at its set points, 23°C for office hours from 8:00 to 17:00 and 26°C for the rest non-office hours on the specific day.
- b) Both the heat pump and circulating pump remain on during office hours.

The design parameters of the PI controller for heat pump in cooling mode are the same values as that in heating mode but with different sign.

### **5.3 Multiple Heat Pumps**

Thus far in the above simulations an aggregated single zone system model was used to simulate the system response with different control strategies. It is of interest to simulate

multiple zone /heat pump system and study its control performance. To this end, disaggregated multiple heat pumps systems were used to test the control strategies of the hybrid ground source heat pump system. A 2-heat-pump system and a 4-heat-pump system will be simulated to demonstrate that any multiple heat pumps system with the same control strategies could also be operated in the same manner.

### 5.3.1 Two Zone Disaggregated System Model

The single zone was subdivided into Zones 1 and 2 with heat pumps 1 and 2 serving each zone respectively. A 2-zone disaggregated 2-heat-pump system was used to simulate and test the control strategies. A schematic of the disaggregated 2-heat-pump system model is shown in Figure 5.55.

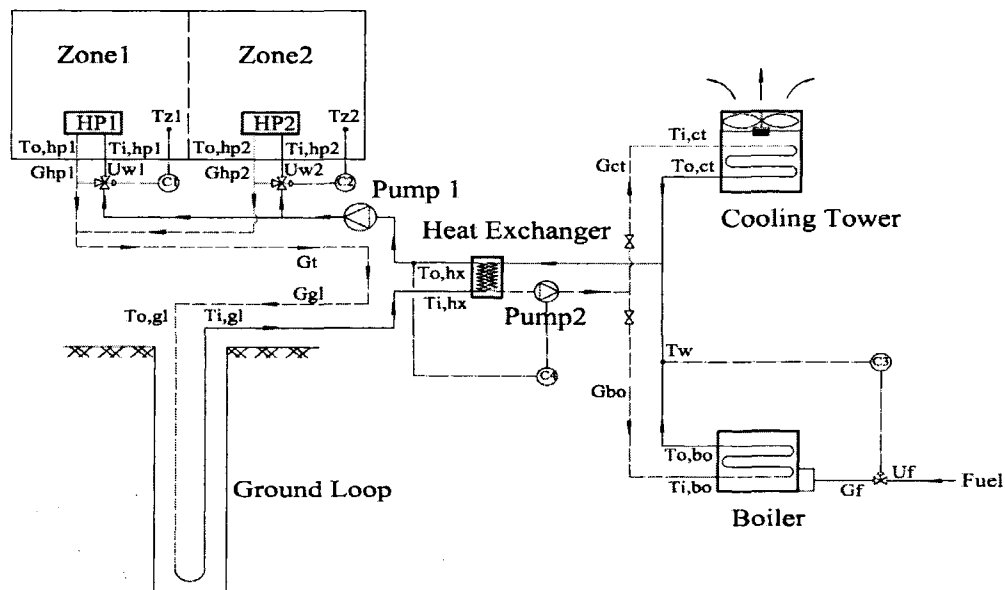


Figure 5.55 Control Schematic of 2-heat-pump HGSHSHP

### 5.3.1.1 Heating mode of operation

As the single zone was subdivided into Zones 1 and 2 by assuming that Zone 1 has 60 per cent of total building load and Zone 2 has 40 per cent. Zone air temperature set point in Zone 1 is set 21°C and that in Zone 2 is 22°C. The simulation results are shown in the following figures.

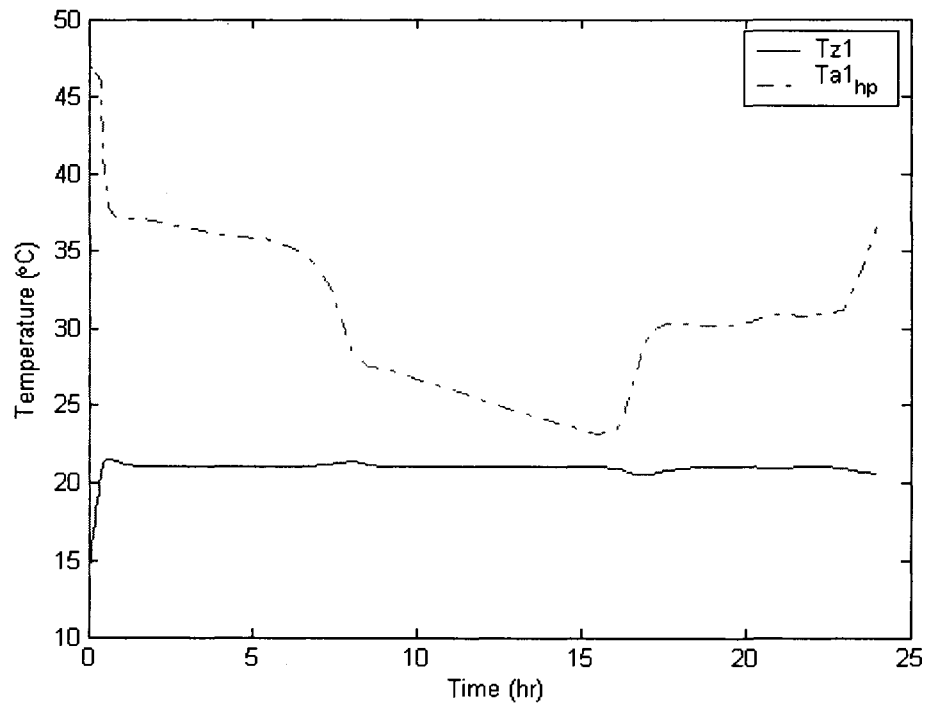
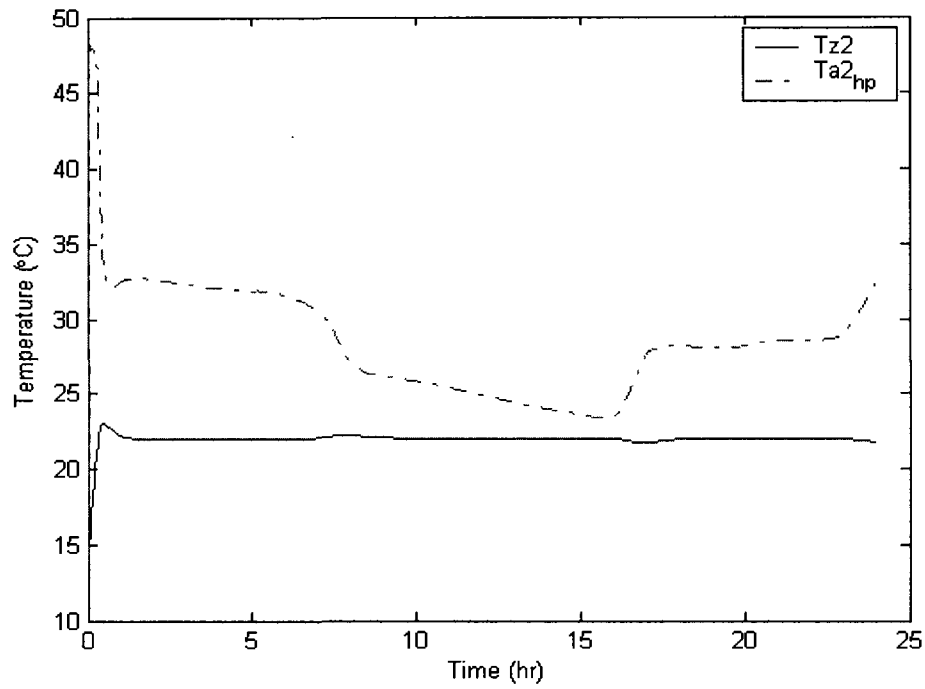
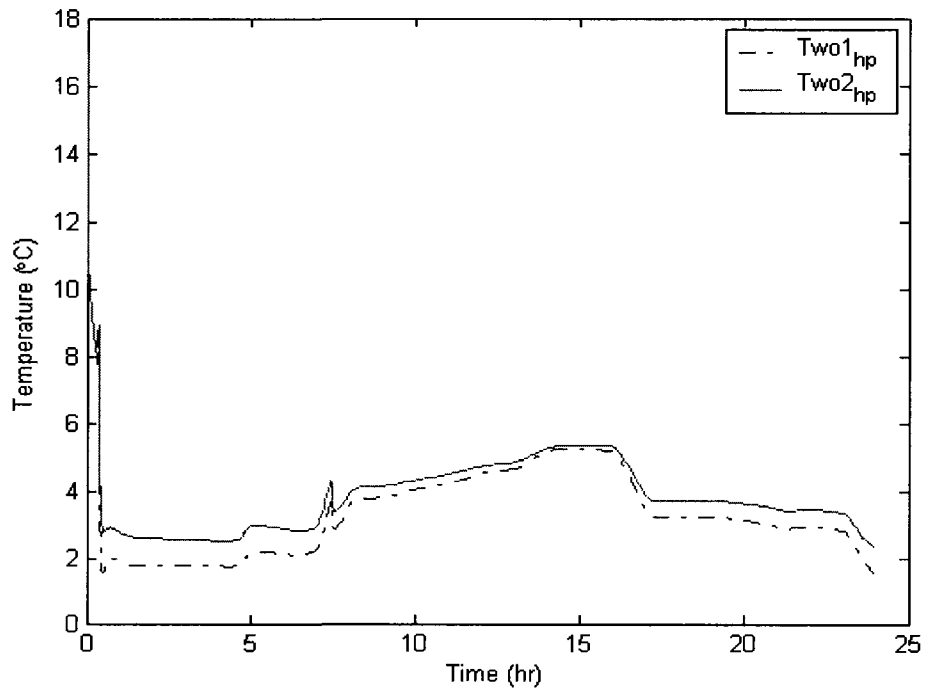


Figure 5.56 Air temperature responses of zone 1



**Figure 5.57 Air temperature responses of zone 2**



**Figure 5.58 Water temperature responses of heat pumps**

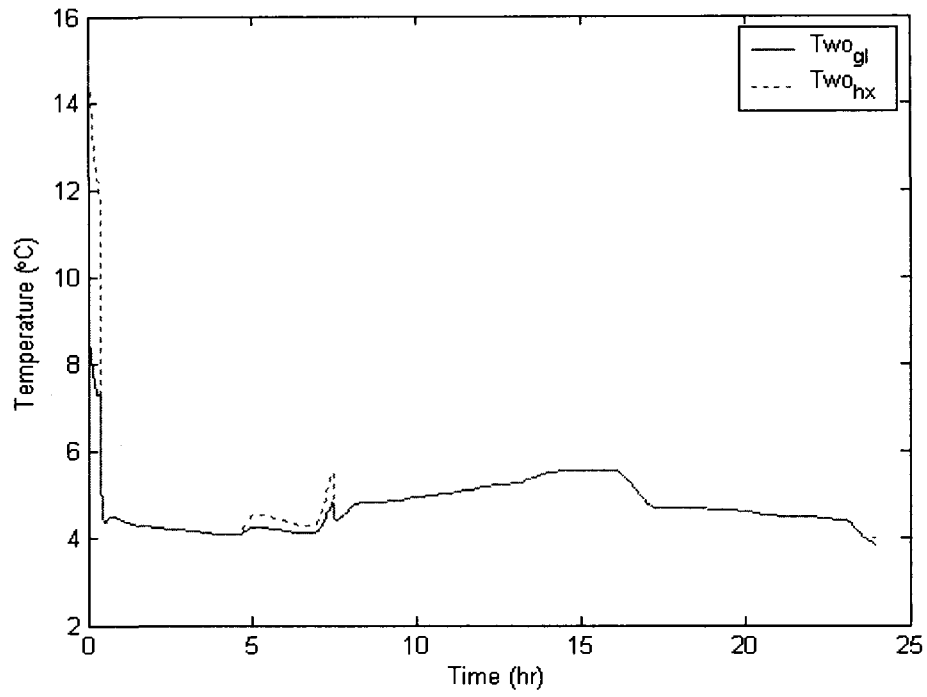


**Figure 5.59 Water temperature responses of GL and HX**

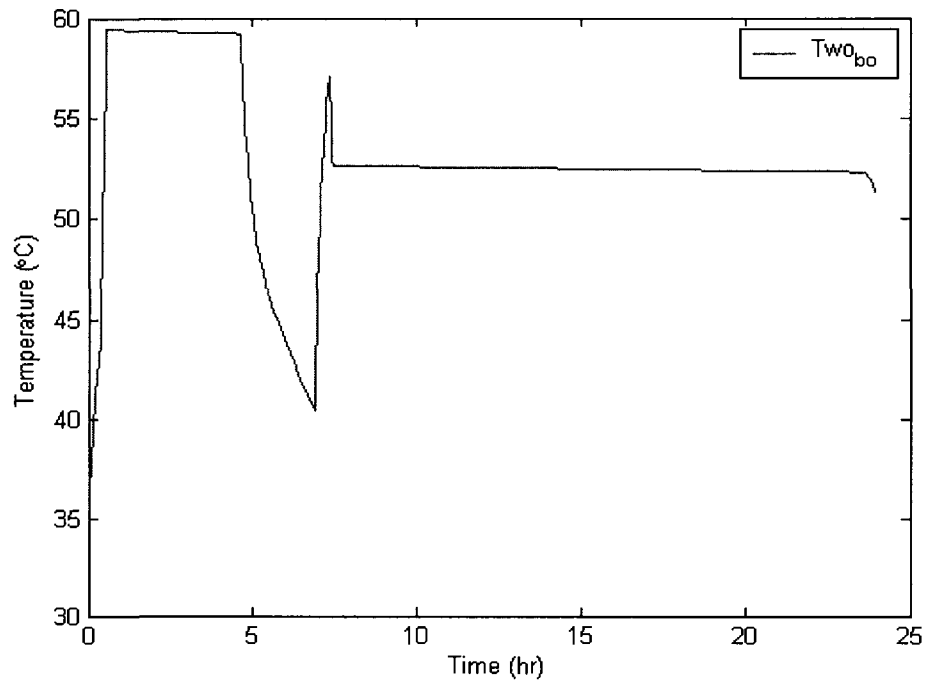


**Figure 5.60 Water temperature response of boiler**

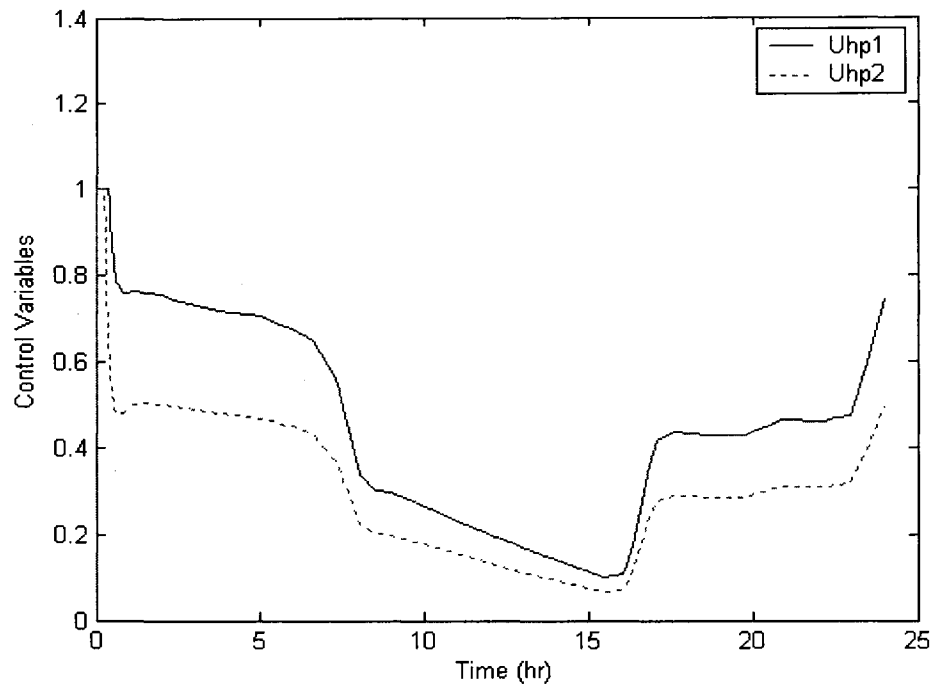


**Figure 5.61 Control variables of heat pumps**

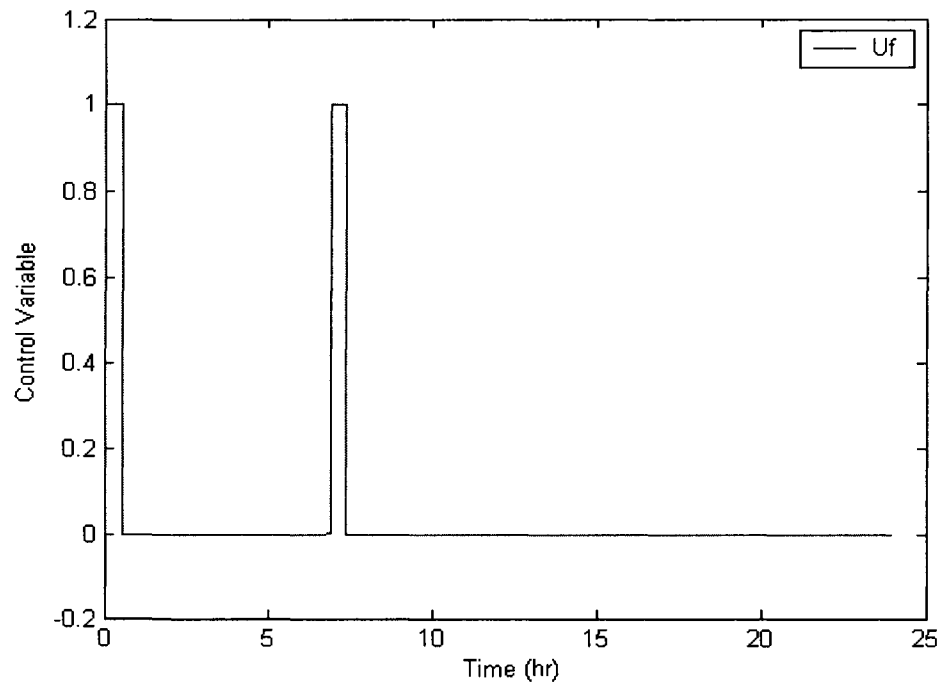


**Figure 5.62 Control variable of boiler**

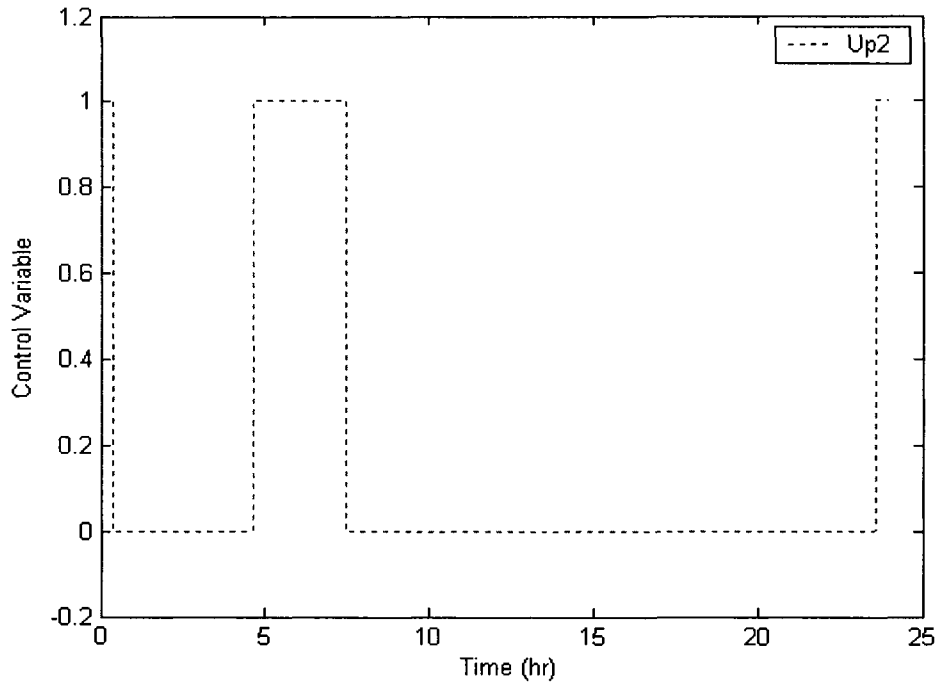


**Figure 5.63 Control variable of circulating pump 2**

From above Figures 5.56 to 5.63, it can be seen that:

- a) Both heat pumps are modulated at slightly different rates to compensate zone loads and individual zone setpoints.
- b) Initially higher boiler temperature is maintained which decreases by about 6°C during the rest of the day.

### 5.3.1.2 Cooling mode of operation

Similarly, by assuming that Zone 1 has 40% of total building load and Zone 2 has 60%, and zone air temperature set point in Zone 1 is set 23°C and that in Zone 2 is 22°C, simulation runs were made. The results are shown in Figures 5.64 to 5.71. The results show expected trends and good zone temperature setpoint tracking.

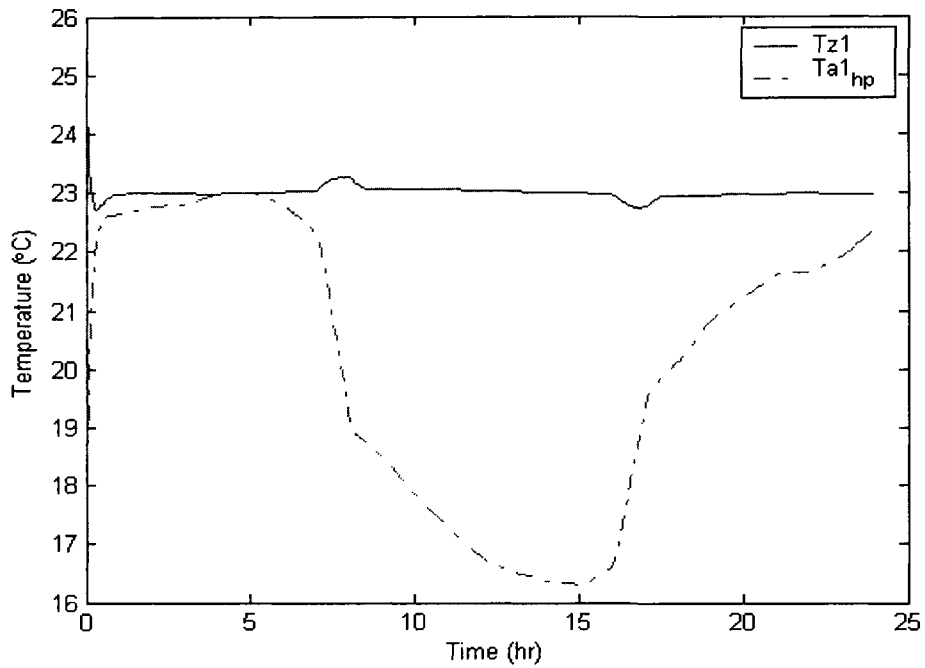


**Figure 5.64 Air temperature responses of zone 1**

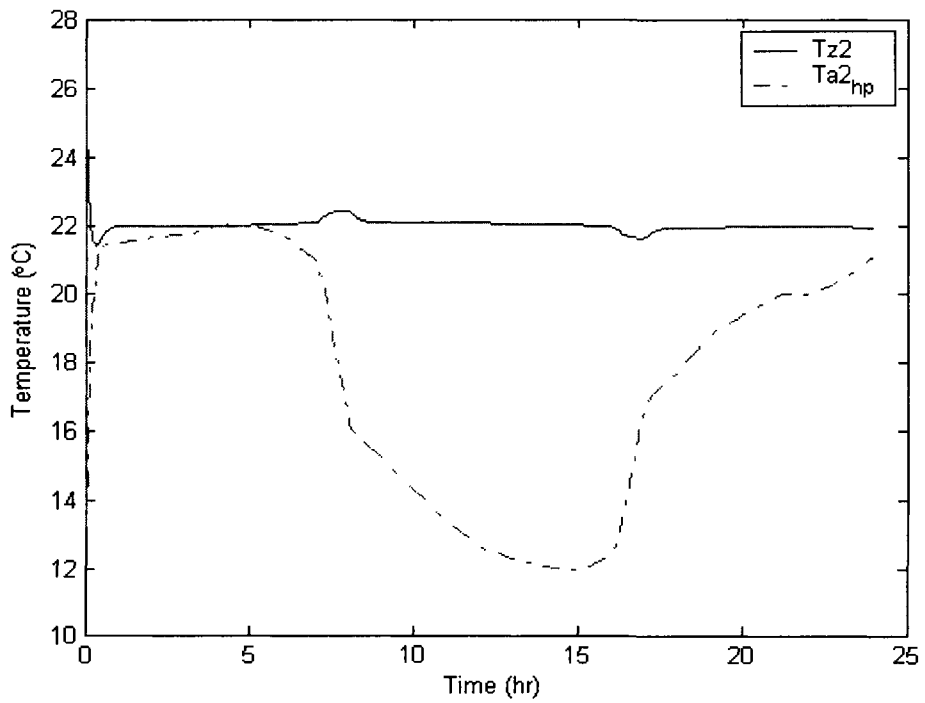


**Figure 5.65 Air temperature responses of zone 2**

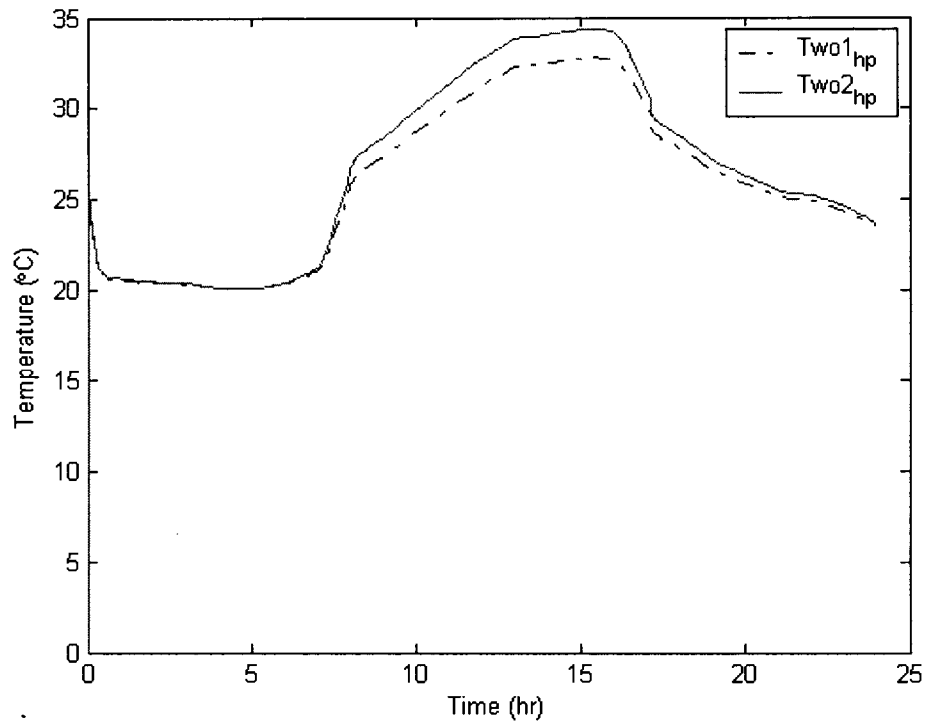


**Figure 5.66 Water temperature responses of HPs**

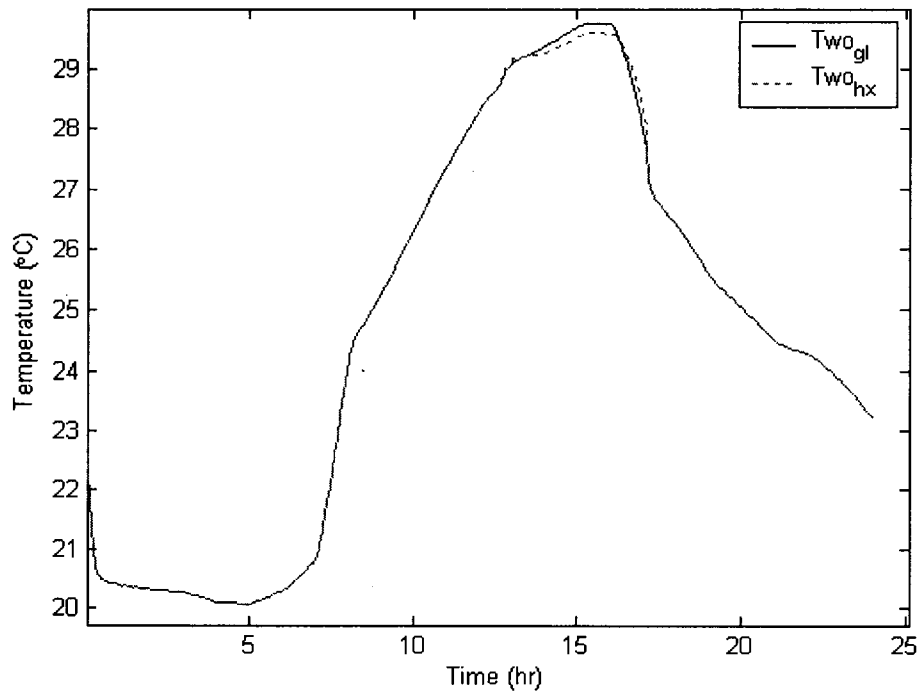


**Figure 5.67 Water temperature responses of GL and HX**

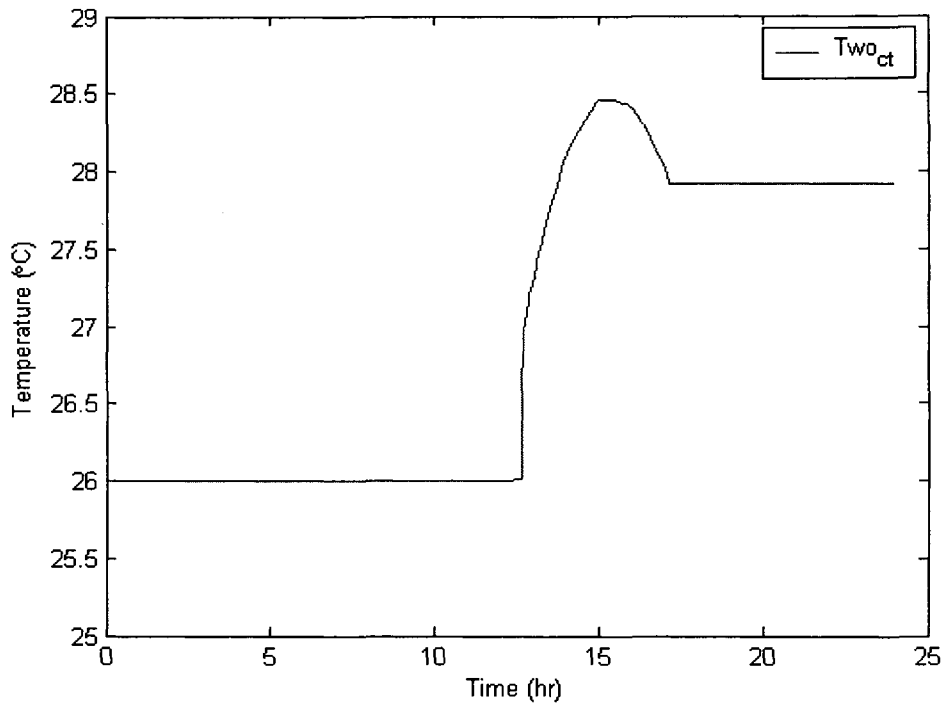


**Figure 5.68 Water temperature response of cooling tower**

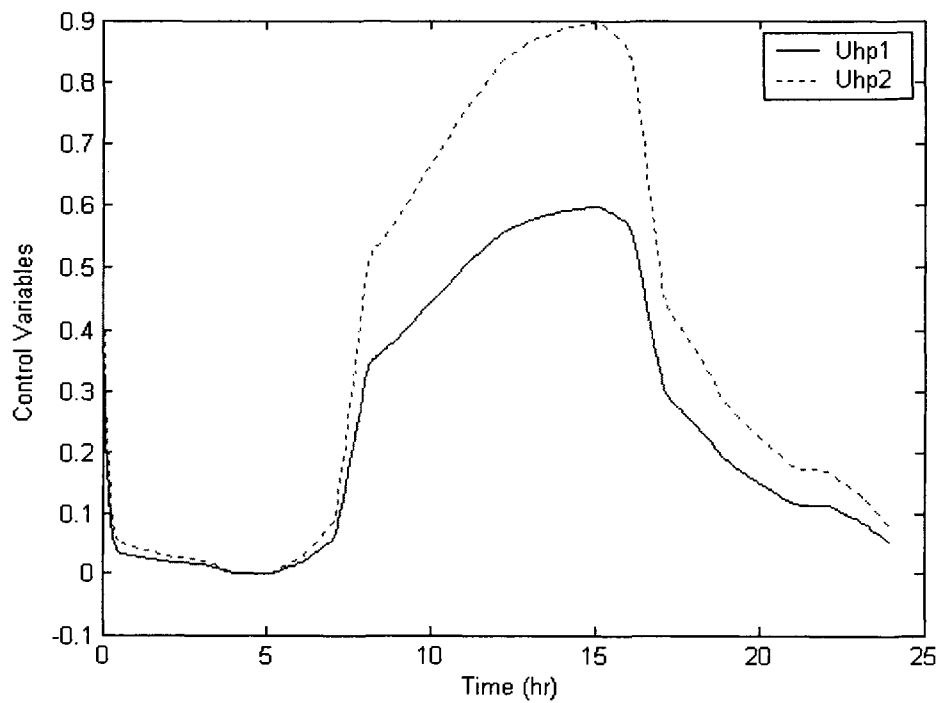


**Figure 5.69 Control variables of HPs**

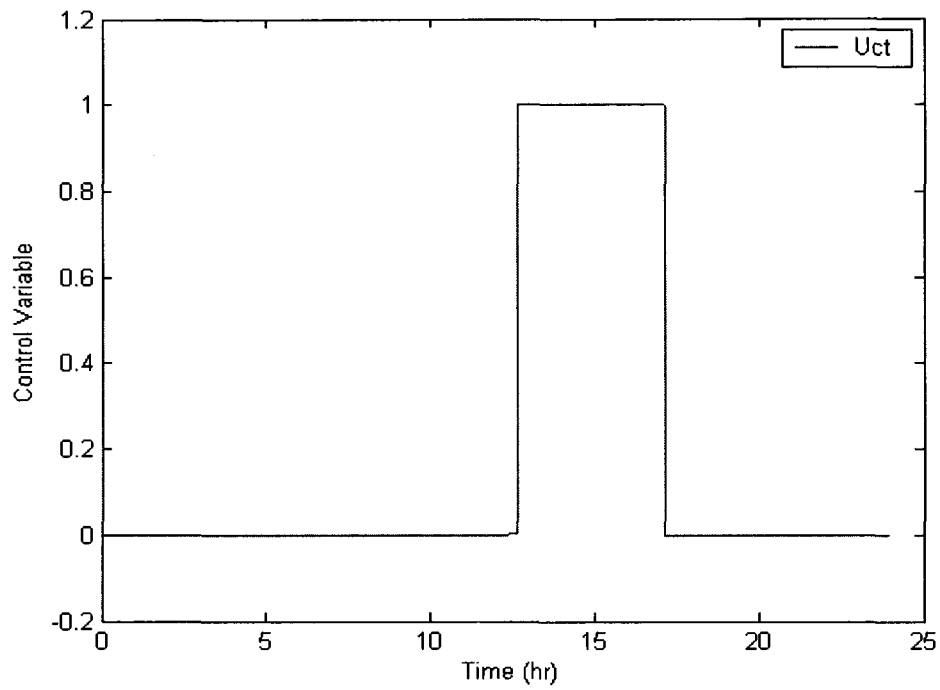


**Figure 5.70 Control variable of cooling tower**

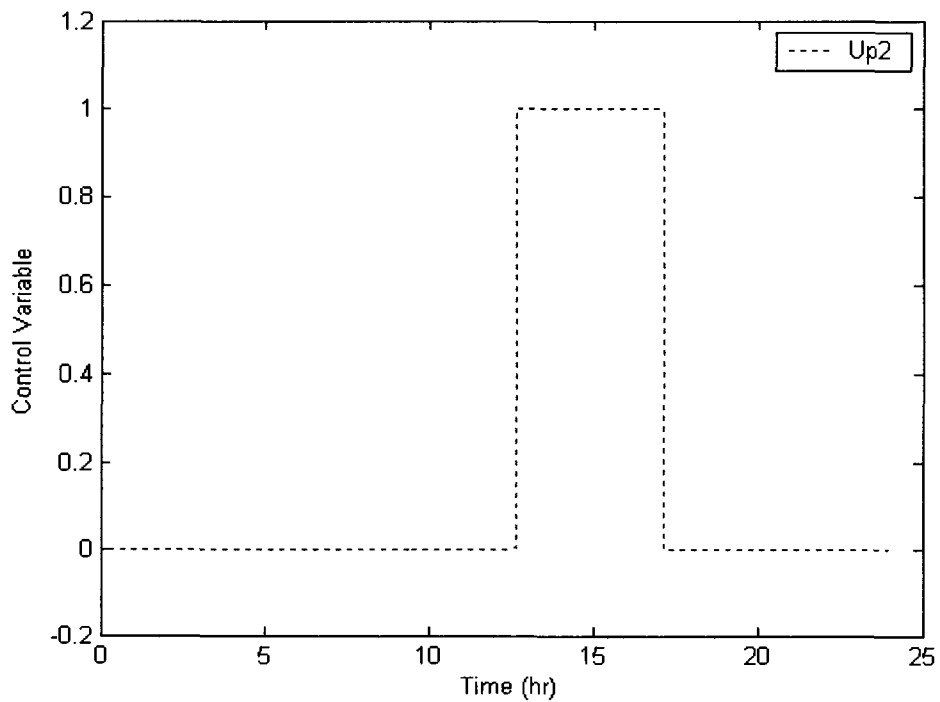


**Figure 5.71 Control variable circulating pump 2**

### 5.3.2 Four Zone Disaggregated System Model

The single zone was subdivided into 4 zones and each zone has its own heat pump. A schematic of the disaggregated 4-heat-pump system model is shown in Figure 5.72. At this point, note that the PI controllers for heat pumps used in aggregated one-zone or disaggregated 2-zone system models were with diverging 3-way valves to get variable flow rate but constant temperature differential. With such control strategy, when in very low load conditions, the system may need very little flow rate so that heat pumps may fail due to low heat transfer rates. Therefore, another control strategy with mixing 3-way valves, considered to be constant flow rate and variable temperature differential, is used in the system model.

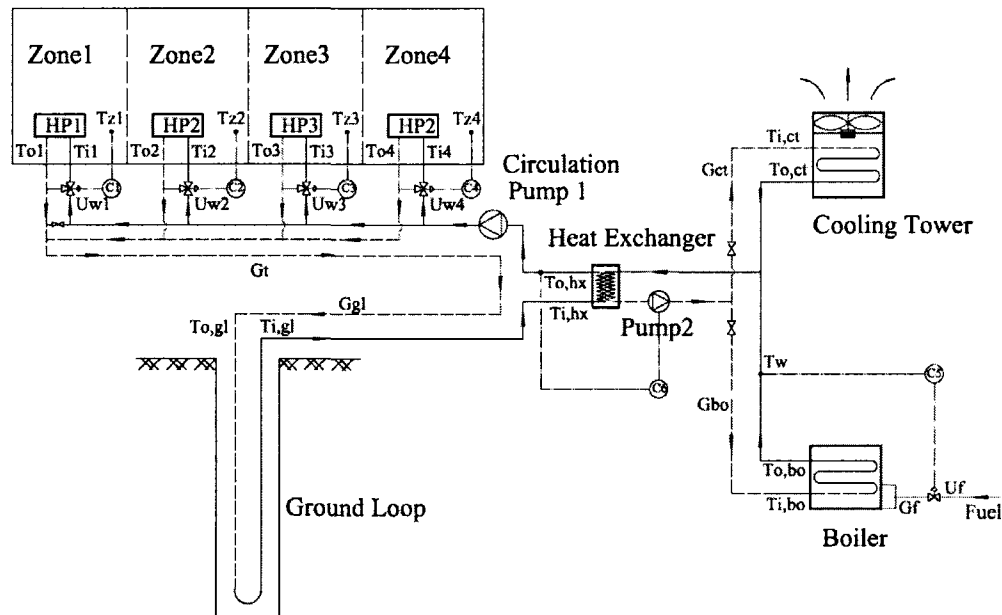


Figure 5.72 Schematic of 4-zone HGSHSHP system model

### 5.3.2.1 Heating mode of operation

The single zone was subdivided into 4 zones. The loads of zones 1 to 4 are 35%, 30%, 20% and 15% of total building load, respectively. Also assume that zone air temperature set point in Zones 1 to 4 are set at 22°C, 21°C, 20°C and 19°C, respectively. Due to the complexity of the system model and huge computational time, a period of 4 hours with two constant loads, e.g. 300 kBtu/h during first 2 hours and 150 kBtu/h later on, was assumed and used in the simulation. The simulation results are shown in Figures 5.73 to 5.82.

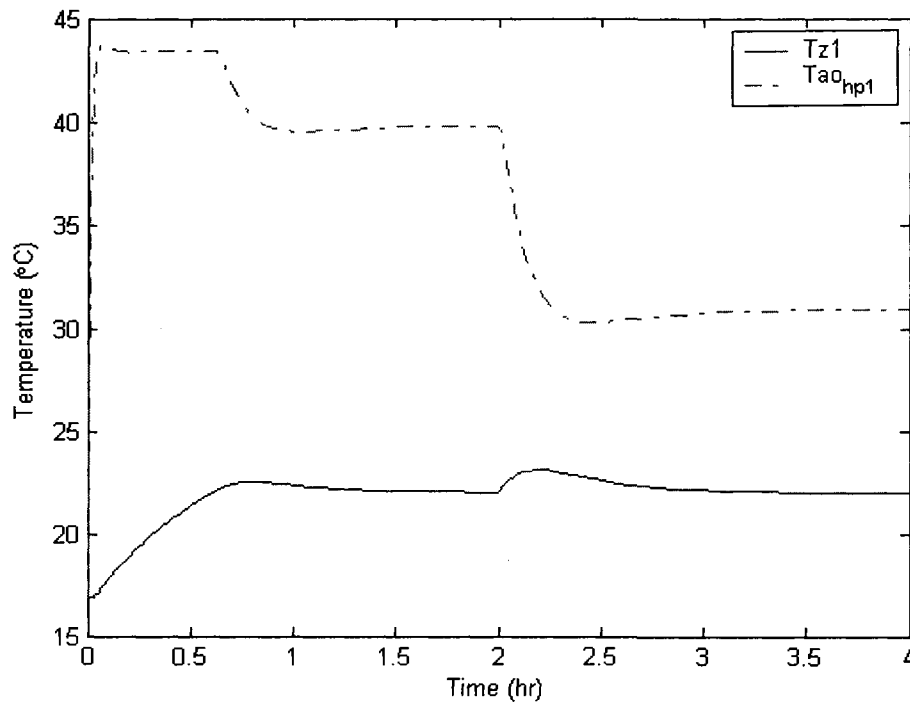
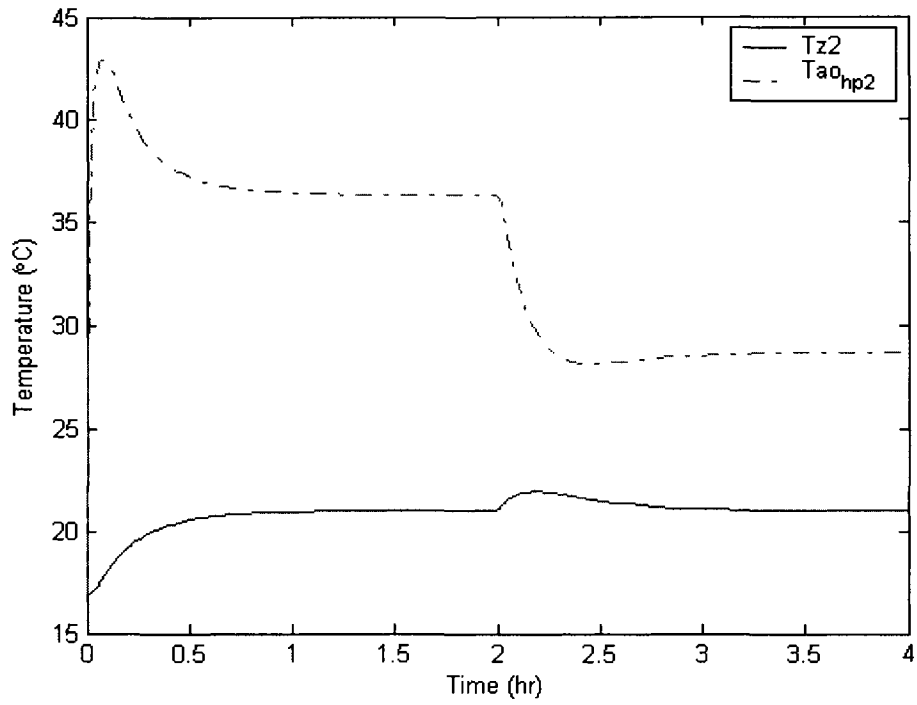
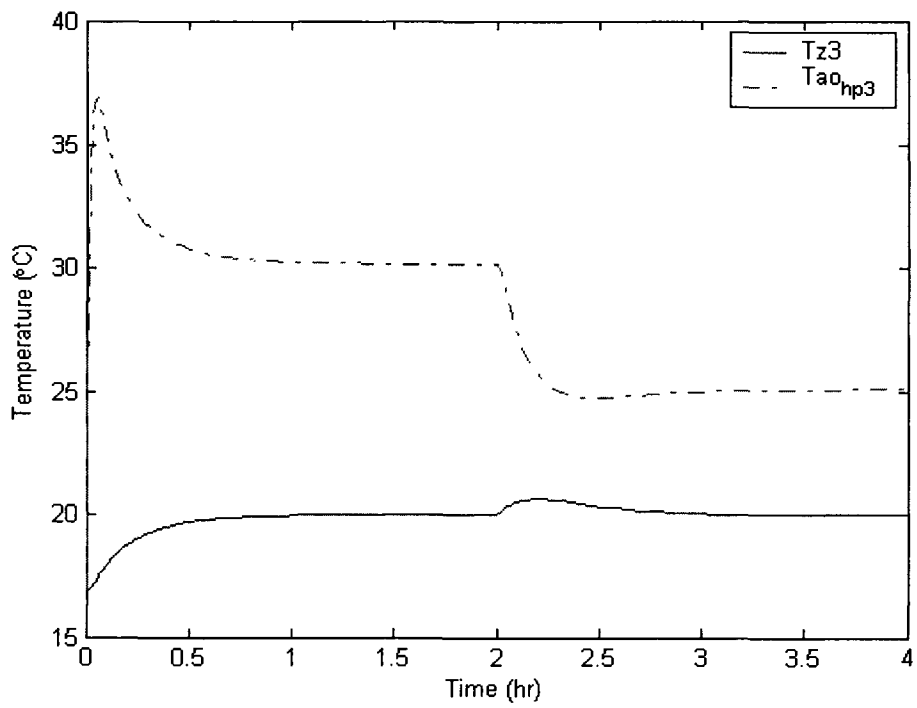


Figure 5.73 Air temperature responses of zone 1



**Figure 5.74 Air temperature responses of zone 2**



**Figure 5.75 Air temperature responses of zone 3**

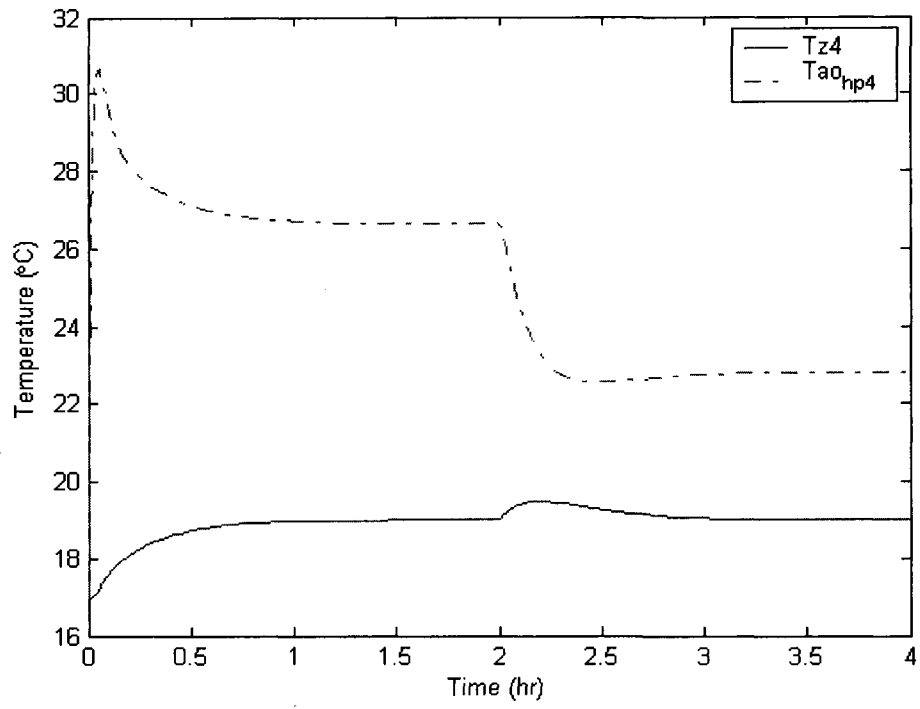


**Figure 5.76 Air temperature responses of zone 4**

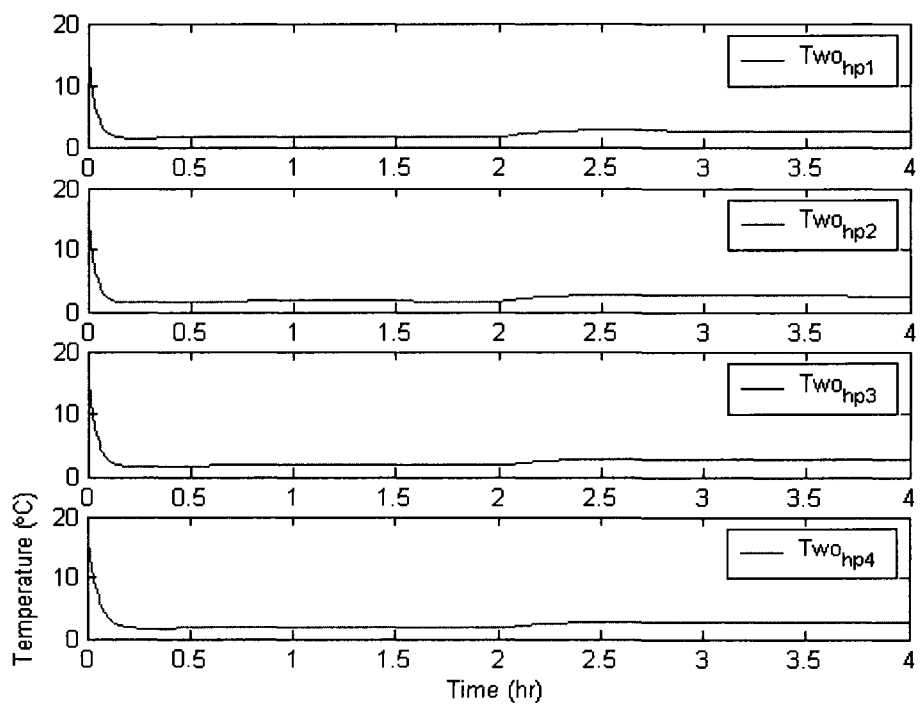


**Figure 5.77 Outlet water temperature responses of HPs**

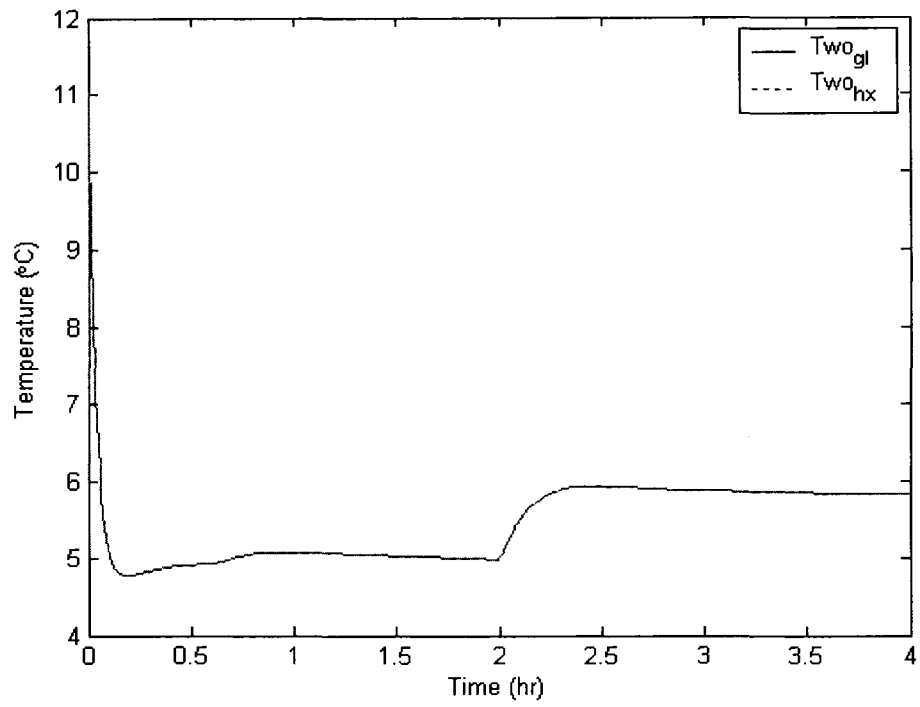


**Figure 5.78** Outlet water temperature responses of GL and HX

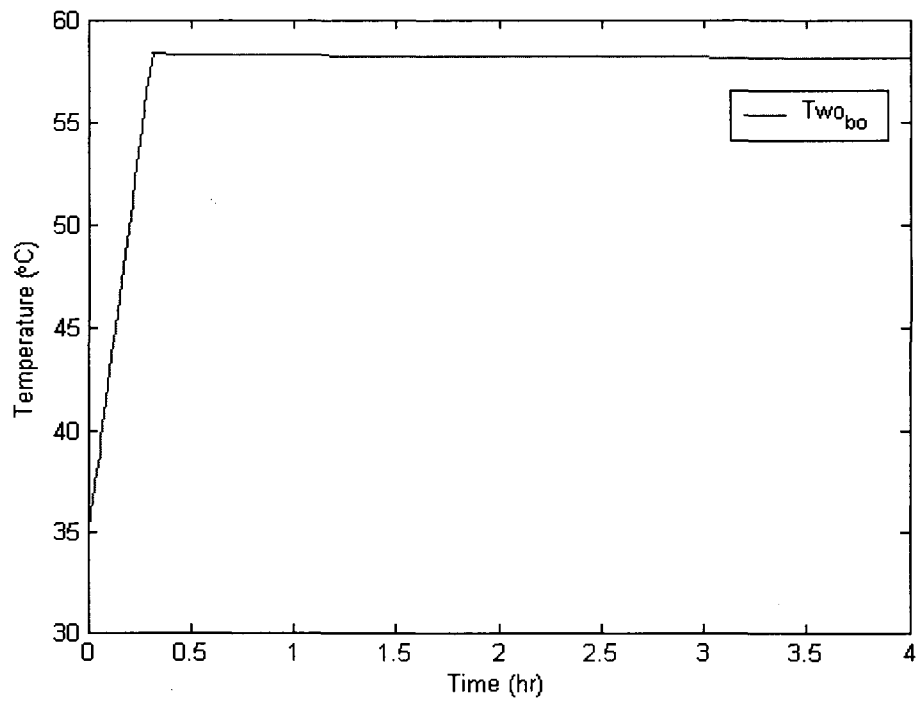


**Figure 5.79 Outlet water temperature response of boiler**

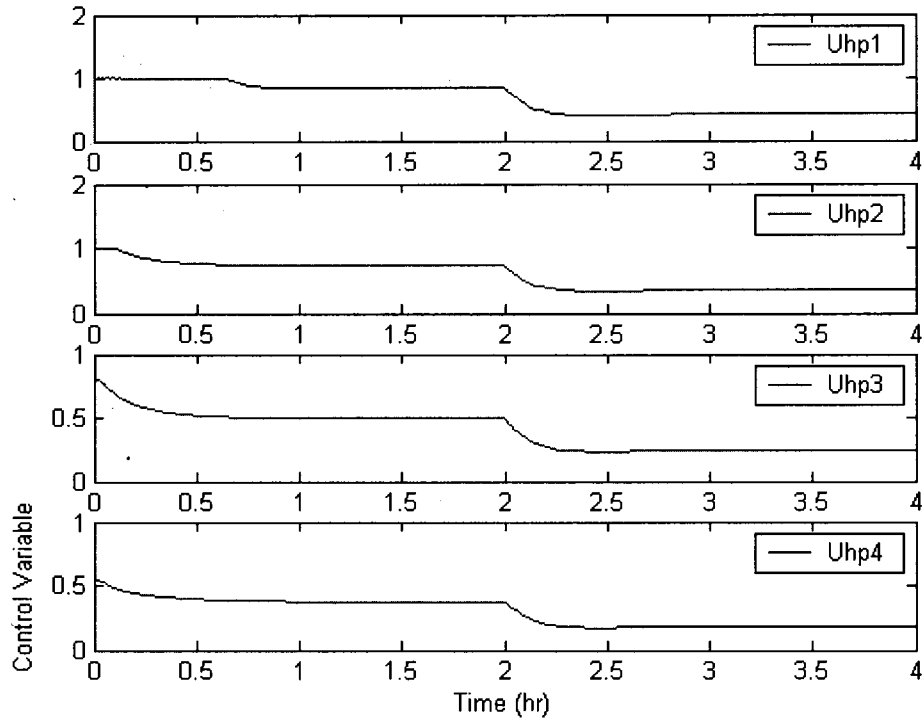


**Figure 5.80 Control variable of HPs**

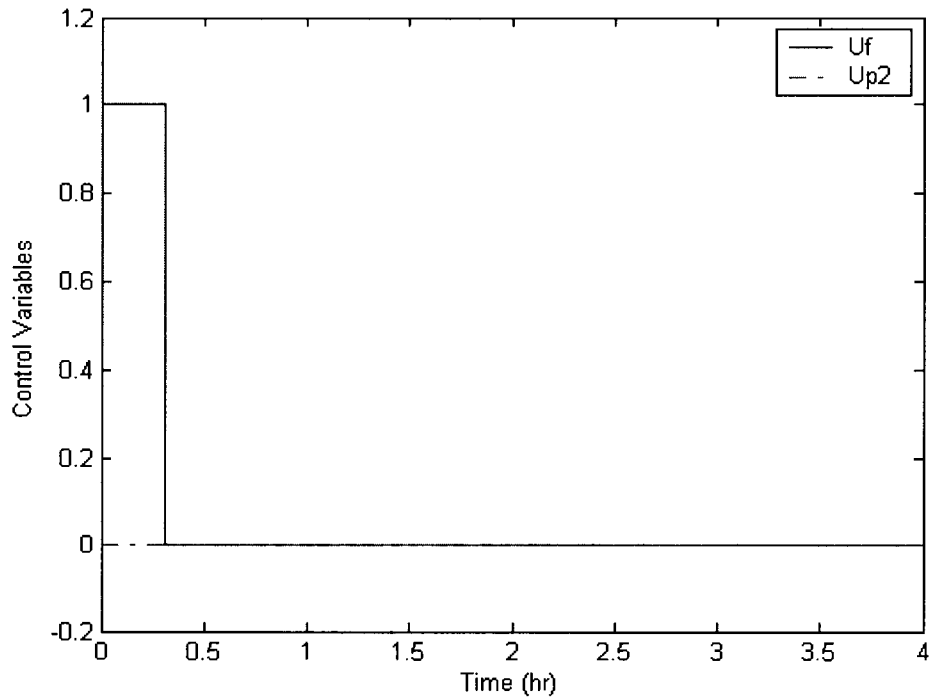


### **Figure 5.81 Control variables of Boiler and Pump 2**

From these results we can observe that all four heat pumps are heating at different capacity (Figure 5.80) to maintain corresponding zone temperature set points (Figures 5.73 to 5.76).

#### **5.3.2.2 Cooling mode of operation**

For the four zone cooling mode of operation the following zone temperature setpoints were chosen: 21°C, 22°C, 23°C and 24°C, respectively. Likewise, over a period of 4 hours the loads were 200 kBtu/h in first 2 hours and 400 kBtu/h later on. The simulation results under these operating conditions are shown in Figures 5.82 to 5.90.

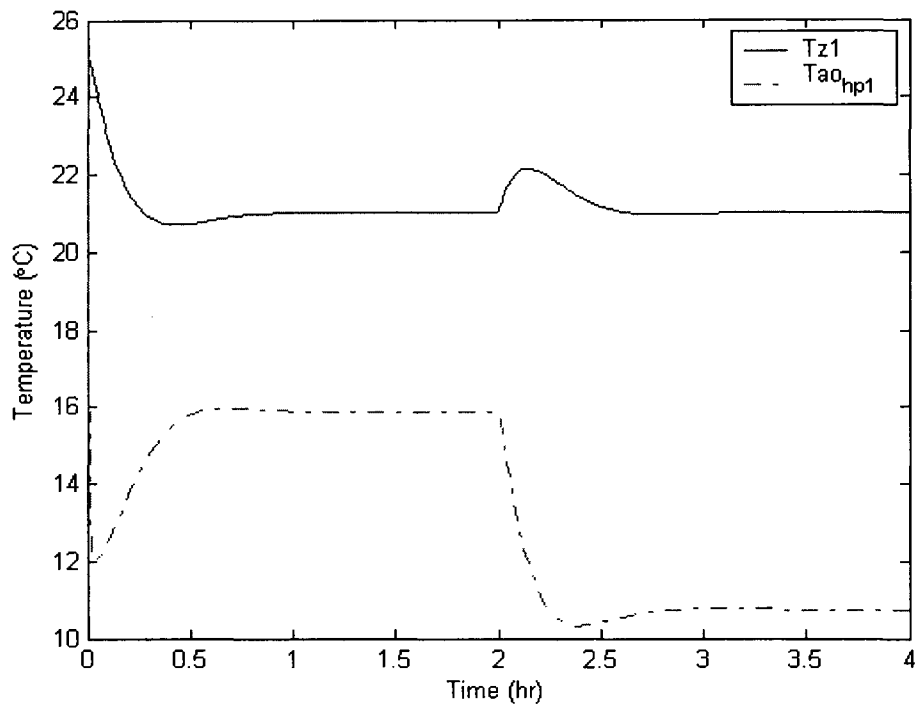


**Figure 5.82 Air temperature responses of zone 1**

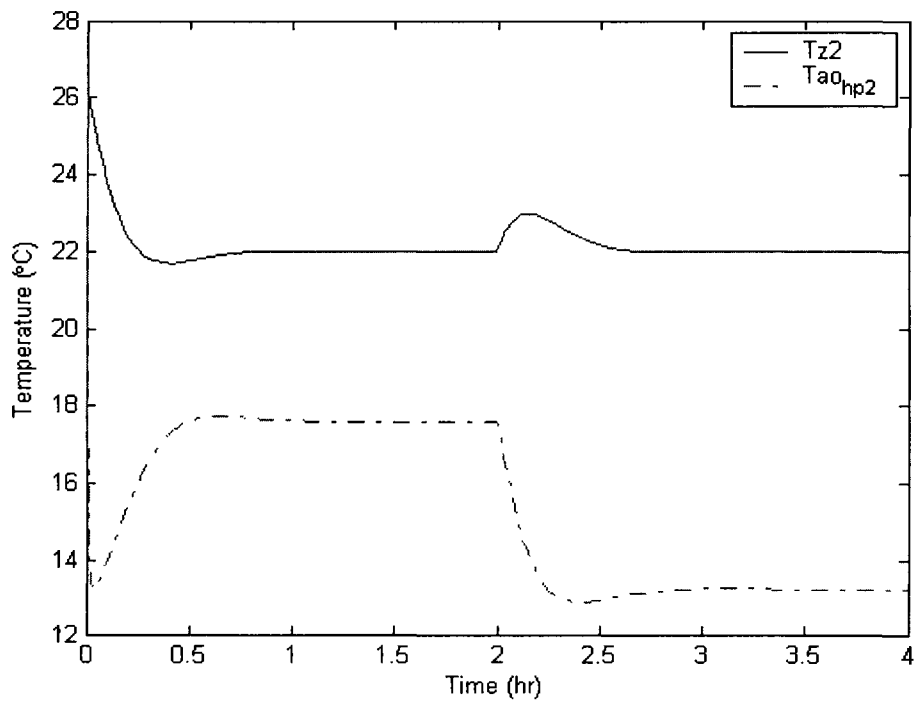


**Figure 5.83 Air temperature responses of zone 2**

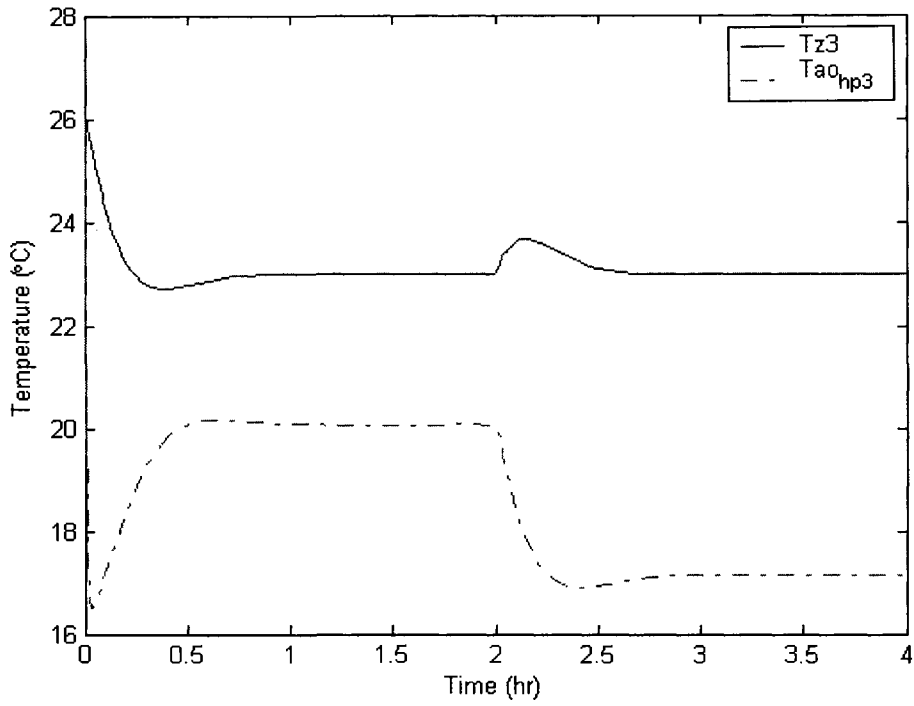


**Figure 5.84 Air temperature responses of zone 3**

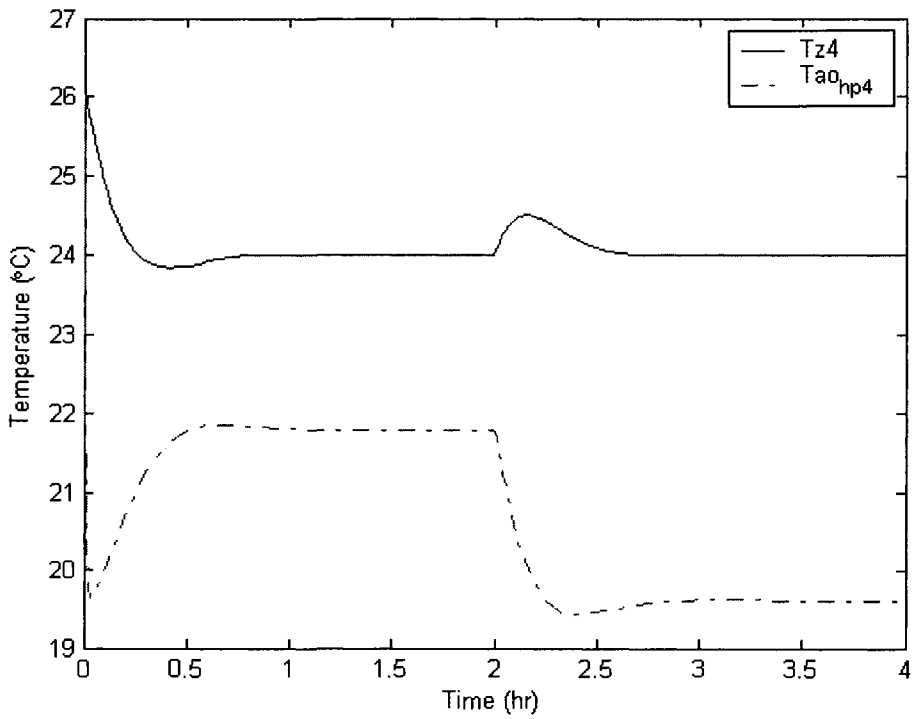


**Figure 5.85 Air temperature responses of zone 4**

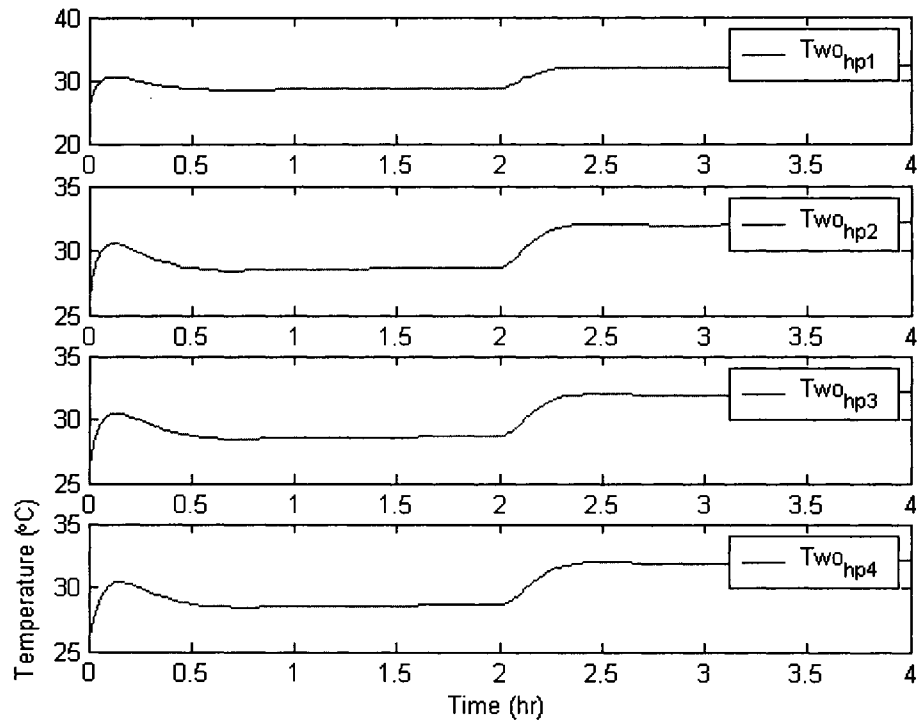


**Figure 5.86 Outlet water temperature responses of HPs**

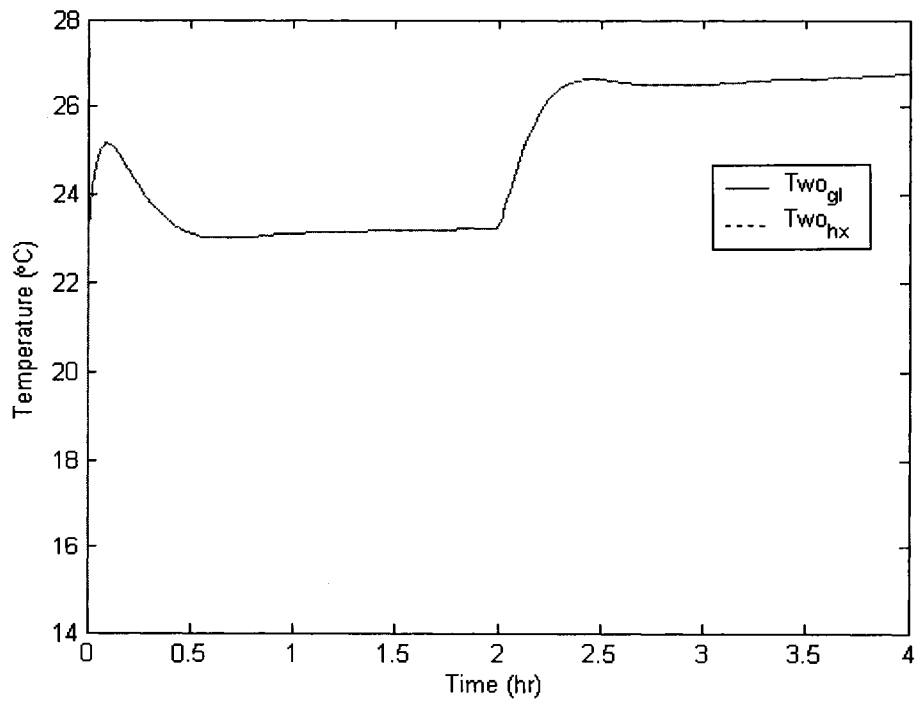


**Figure 5.87 Outlet water temperature responses of GL and HX**

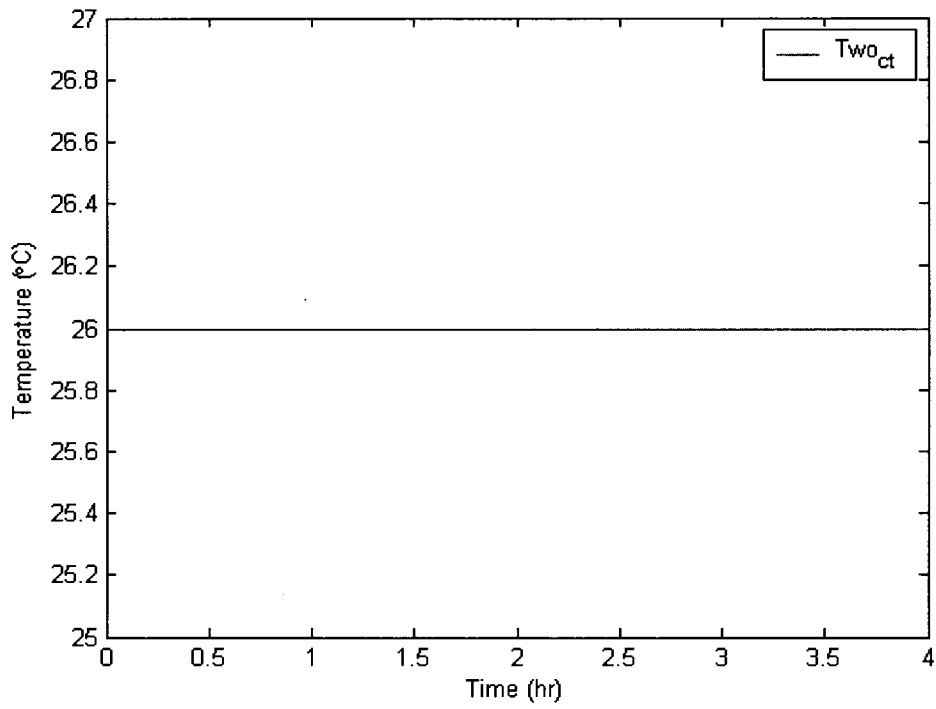


**Figure 5.88 Outlet water temperature response of cooling tower**

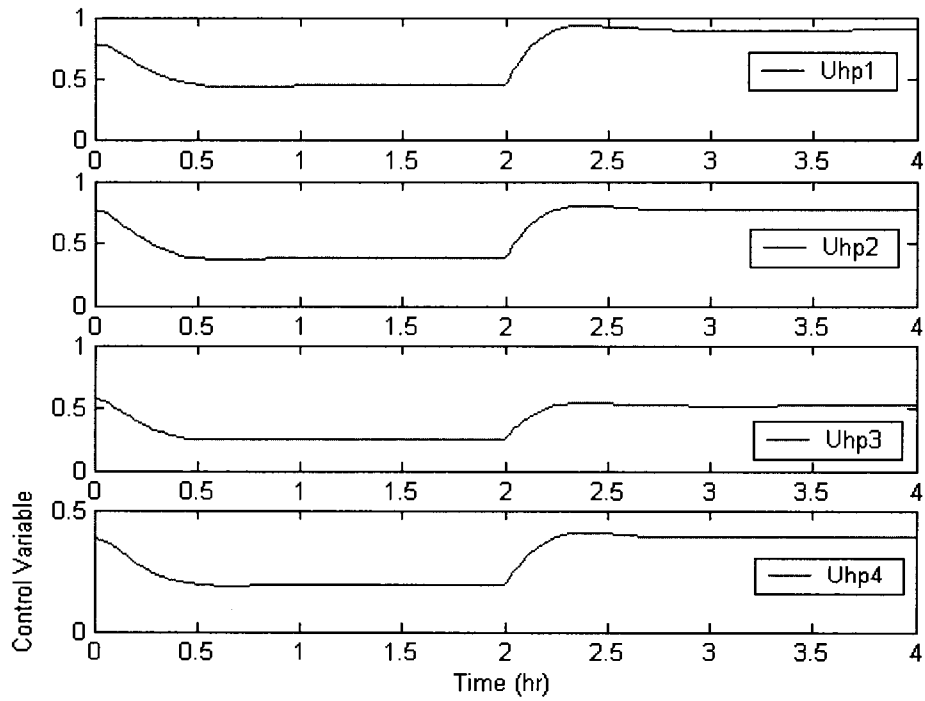


**Figure 5.89 Control variable of HPs**

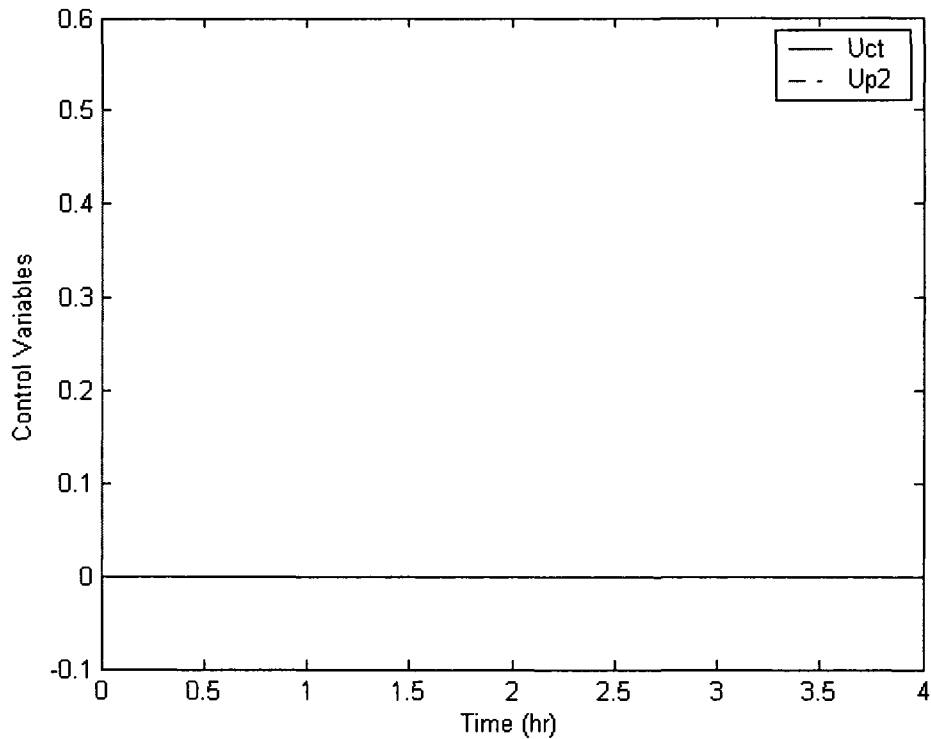


**Figure 5.90 Control variable of cooling tower**

These results demonstrate that multiple heat pump system responses are stable and exhibit good setpoint tracking properties under variable load conditions.

## 5.4 Optimization of HGSHP System

The aggregated single zone model is used to formulate and solve the optimization problem.

### 5.4.1 Heating mode of operation

As is known, significant energy is consumed by large hybrid ground source heat pump systems for operation all year round. Therefore, it is important to achieve energy savings by using optimal control strategies. To this end, a constrained optimization problem is

formulated and solved. The optimization approach contains defining an objective function and specifying the constraints. The method of multi-variable constraint optimization is used to solve such problem in MATLAB environment. Six variables, such as  $Q_{gl}$ ,  $U_{hp}$ ,  $U_f$ ,  $T_s$ ,  $T_{i,gl}$ , and  $T_{o,gl}$ , are chosen as variables to be determined in this optimization problem. The upper and lower bounds of the variables are given in Table 5.4.

**Table 5.4 Lower and upper bounds of variables in heating mode**

Variable	$Q_{gl}$	$U_{hp}$	$U_f$	$T_s$	$T_{igl}$	$T_{ogl}$
Units	W	--	--	°C	°C	°C
LB	13,000	0.1	0	3	-1.9	-1
UB	77,000	1	1	9	7	8

The objective function is the total power in terms of the variables to be optimized. Total power for whole HGSHP consists of power inputs to the heat pump, boiler, and circulating pumps. The objective function is given by:

$$f(x) = P_{hp} + P_{bo} + P_{pp} \quad (5-1)$$

where

$P_{hp}$  = Power input to heat pump, W

$P_{bo}$  = Power input to boiler, W

$P_{pp}$  = Power input to circulating pumps, W

$$P_{hp} = 8U_{hp}(6417 + 8.73T_s + 1.07T_s^2) \quad (5-2)$$

$$P_{bo}=U_f G_{f,max} h v \quad (5-3)$$

$$P_{pp}=g h_1 G_{hp} / \eta_1 + g h_2 G_{bo} / \eta_2 \quad (5-4)$$

The constraints of the optimization problem are equations of heat pump model, ground loop model, and boiler model. All the equations are taken as static state constraint equations and simplified to reduce the number of constraints. The resulting linear and nonlinear equalities are given as follows:

$$MLAA(t)+U_{i,i+1}(T_{i+1}-T_i)=0 \quad (5-5,8,\dots,62)$$

$$U_{i+1,i}(T_i-T_{i+1}) + U_{i+1,i+2}(T_{i+2}-T_{i+1})=0 \quad (5-6,9,\dots,63)$$

$$U_{i+2,i+1}(T_{i+1}-T_{i+2})+U_{i+2,j}(T_j-T_{i+2})+U_{i+2,k}(T_k-T_{i+2}) \\ + \dots + U_{i+2,n}(T_n-T_{i+2})=0 \quad (5-7,10,\dots,64)$$

$$U_{61,3}(T_3-T_{61})/2+U_{61,15}(T_{15}-T_{61})/2+U_{61,48}(T_{48}-T_{61})/2+U_{60,61}(T_{60}-T_{61})/2 \\ +U_{61,6}(T_6-T_{61})/4+U_{61,9}(T_9-T_{61})/4+U_{61,12}(T_{12}-T_{61})/4+U_{61,18}(T_{18}-T_{61})/4 \\ +U_{61,30}(T_{30}-T_{61})/4 + U_{61,33}(T_{33}-T_{61})/4 + U_{61,45}(T_{45}-T_{61})/4 + U_{61,51}(T_{51}-T_{61})/4 \\ +U_{61,54}(T_{54}-T_{61})/4 + U_{61,57}(T_{57}-T_{61})/4=0 \quad (5-65)$$

$$U_{62,61}(T_{61}-T_{62}) + U_{62,63}(T_{63}-T_{62})=0 \quad (5-66)$$

$$U_{63,62}(T_{62}-T_{63}) + U_{63,g}(T_g-T_{63})=0 \quad (5-67)$$

$$MLAA(t)=Q_{gl}G(Fo(3600)) \quad (5-68)$$

$$Q_{gl}=G_{hp}Cp(T_{ogl}- T_{igl}) \quad (5-69)$$

$$T_{wall}= (T_1 + T_4 + \dots + T_{58})/20 \quad (5-70)$$

$$(T_{igl}+T_{ogl})/2= T_{wall} - Q_{gl}R_b/L \quad (5-71)$$

$$U_f G_{f,max} h v = G_{hp}Cp(T_s- T_{ogl}) \quad (5-72)$$

$$8U_{hp}(16186+489.8T_s-2.88T_s^2)=Q_b \quad (5-73)$$

$$Q_b=8U_{hp}(6417+8.73T_s+1.07T_s^2)+Q_{gl}+U_f G_{f,max} h v \eta \quad (5-74)$$

When solving the optimization problem, the computer program searches feasible point that satisfies all of the linear and nonlinear constraints at the given initial guess of each variable. After some iteration, the solution converges and each variable takes its optimal value. The simulation results at design load of 435kBTu/h (127,455Watts) are shown in Table 5.5.

**Table 5.5 Optimal results at design load in heating mode**

Variable	$Q_{gl}$	$U_{hp}$	$U_f$	$T_s$	$T_{igl}$	$T_{ogl}$	$f_{min}(x)$
Units	W	--	--	°C	°C	°C	W
Magnitude	65,473	0.90	0.64	3.0	-0.57	1.65	51,463

Likewise, the simulation results at part loads were conducted, and optimal entering water temperatures of heat pump at different building loads (only when boiler is needed) are plotted as shown in Figure 5.91.

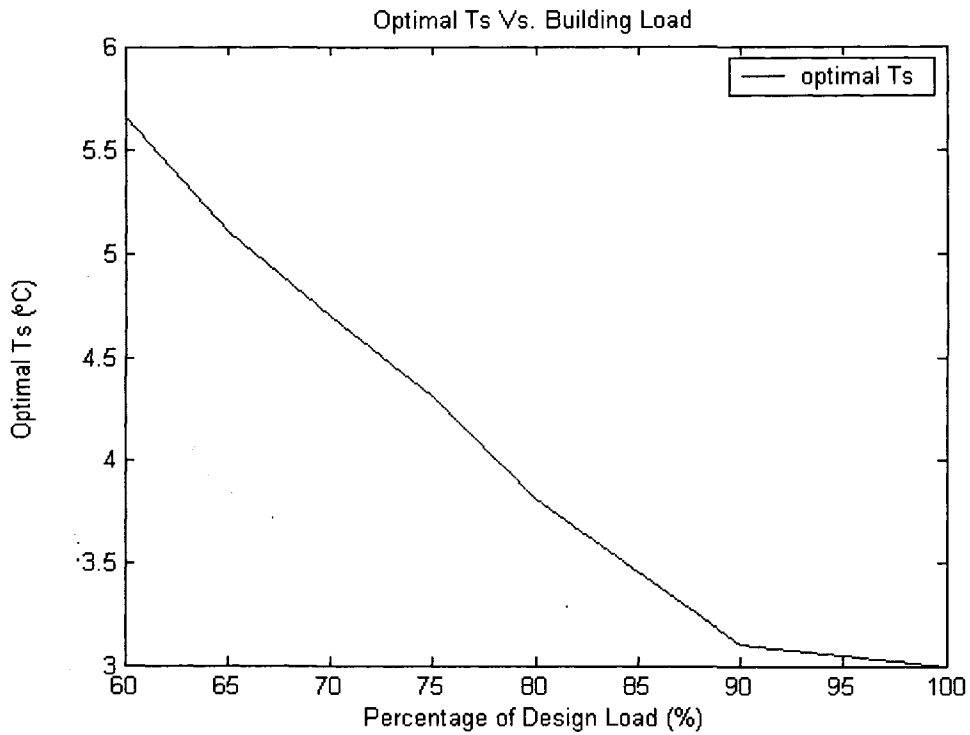


**Figure 5.91 Optimal entering water temperatures in heating mode**

From the above figure, it is noted that the optimal entering water temperature of heat pump depends on building load. The higher the building load, the lower the optimal entering water temperature. When the building load reaches its design value, optimal supply water temperature drops down to its lower bound of the heat pump model, 3°C. A value lower than that means the system always needs supplemental boiler to heat the entering water.

#### **5.4.2 Cooling mode of operation**

Similarly, the same methodology is applied to the system in cooling mode of operation. Six variables, such as  $Q_{gl}$ ,  $U_{hp}$ ,  $U_{ct}$ ,  $T_s$ ,  $T_{i,gl}$ , and  $T_{o,gl}$ , are chosen as variables to be

determined in the optimization problem. The upper and lower bounds of the variables are given in Table 5.6.

**Table 5.6 Lower and upper bounds of variables in cooling mode**

Variable	$Q_{gl}$	$U_{hp}$	$U_{ct}$	$T_s$	$T_{igl}$	$T_{ogl}$
Units	W	--	--	°C	°C	°C
LB	17,000	0.1	0	11	15	14
UB	90,000	1	1	30	35	29

The objective function is given by:

$$f(x) = P_{hp} + P_{ct} + P_{pp} \quad (5-75)$$

where

$P_{hp}$  = Power input to heat pump, W

$P_{ct}$  = Power input to cooling tower, W

$P_{pp}$  = Power input to circulating pumps, W

$$P_{hp} = 8U_{hp}(4472 + 73.10T_s + 0.08T_s^2) \quad (5-76)$$

$$P_{ct} = 1100U_{ct} \quad (5-77)$$

$$P_{pp} = gh_1G_{hp}/\eta_1 + gh_2G_{ct}/\eta_2 \quad (5-78)$$

The linear and nonlinear equalities constraints are given as follows:

$$MLAA(t) + U_{i,i+1}(T_{i+1} - T_i) = 0 \quad (5-79, 82, \dots, 136)$$

$$U_{i+1,i}(T_i - T_{i+1}) + U_{i+1,i+2}(T_{i+2} - T_{i+1}) = 0 \quad (5-80, 83, \dots, 137)$$

$$U_{i+2,i+1}(T_{i+1}-T_{i+2})+U_{i+2,j}(T_j-T_{i+2})+U_{i+2,k}(T_k-T_{i+2})$$

$$+\dots+U_{i+2,n}(T_n-T_{i+2})=0 \quad (5-81,84,\dots,138)$$

$$U_{61,3}(T_3-T_{61})/2+U_{61,15}(T_{15}-T_{61})/2+U_{61,48}(T_{48}-T_{61})/2+U_{60,61}(T_{60}-T_{61})/2$$

$$+U_{61,6}(T_6-T_{61})/4+U_{61,9}(T_9-T_{61})/4+U_{61,12}(T_{12}-T_{61})/4+U_{61,18}(T_{18}-T_{61})/4$$

$$+U_{61,30}(T_{30}-T_{61})/4 +U_{61,33}(T_{33}-T_{61})/4 +U_{61,45}(T_{45}-T_{61})/4 +U_{61,51}(T_{51}-T_{61})/4$$

$$+U_{61,54}(T_{54}-T_{61})/4 +U_{61,57}(T_{57}-T_{61})/4=0 \quad (5-139)$$

$$U_{62,61}(T_{61}-T_{62}) +U_{62,63}(T_{63}-T_{62})=0 \quad (5-140)$$

$$U_{63,62}(T_{62}-T_{63}) +U_{63,g}(T_g-T_{63})=0 \quad (5-141)$$

$$MLAA(t)=Q_{gl}G(Fo(3600)) \quad (5-142)$$

$$Q_{gl}=G_{hp}Cp(T_{igl}- T_{ogl}) \quad (5-143)$$

$$T_{wall}= (T_1 +T_4+\dots+T_{58})/20 \quad (5-144)$$

$$(T_{igl}+T_{ogl})/2= T_{wall} + Q_{gl}R_b/L \quad (5-145)$$

$$112,512U_{ct} =-G_{hp}Cp(T_s- T_{ogl}) \quad (5-146)$$

$$8U_{hp}(25993-180.6T_s-0.48T_s^2)=Q_b \quad (5-147)$$

$$Q_b=-8U_{hp}(4472+73.10T_s+0.08T_s^2)+Q_{gl}+112,512U_{ct} \quad (5-148)$$

The simulation results at design cooling load of 565kBtu/h (165,545Watts) are shown in Table 5.7.

**Table 5.7 Optimal results at design load in cooling mode**

Variable	$Q_{gl}$	$U_{hp}$	$U_{ct}$	$T_s$	$T_{igl}$	$T_{ogI}$	$f_{min}(x)$
Units	W	--	--	°C	°C	°C	W
Magnitude	82,773	0.791	0.763	27.07	30.86	28.99	42,007

At different part load ratios the optimal entering water temperatures of heat pump were determined (only when cooling tower is needed). These are plotted as shown in Figure 5.92.

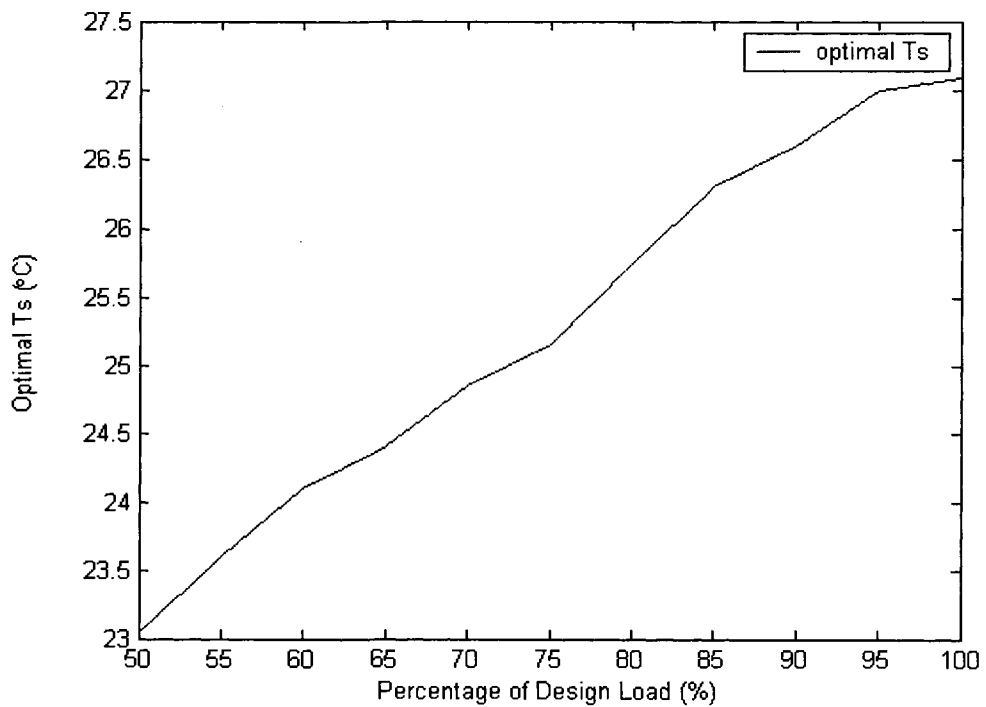


**Figure 5.92 Optimal entering water temperatures in cooling mode**

From the above figure, it can be seen that the higher the building load, the higher the optimal entering water temperature.

## 5.5 Overall Performance of HGSHP System

As mentioned in the preceding section, calculating and comparing total energy consumption during the same period and under the same condition can be useful method to rate heat pump performance and efficiency. In this section, total energy consumptions with and without optimal entering water temperature controlled during a long period in both heating and cooling modes of operation are presented. However, when trying to perform simulation for whole season in each mode is very time-consuming for computer programs to run through and get final simulation results. Therefore, a typical one-week simulations in design month of each mode are shown following.

### 5.5.1 Heating Mode of Operation

A realistic one-week outdoor condition in Montreal in design month of January was taken to study in this section. The hourly outdoor air temperatures of the week are listed in the following Table 5.8 (From Environment Canada). Note that the unit of all temperatures is degrees Celsius.

**Table 5.8 Hourly outdoor temperatures of a specific week in winter**

Hr	Day 1	Day 2	Day 3	Day 4	Day 5	Day 6	Day 7
0	-6.5	-15.0	-4.6	2.3	-10.9	-7.6	-9.7
1	-5.9	-15.0	-4.4	2.2	-11.1	-8.6	-10.0
2	-5.9	-15.0	-4.5	2.2	-11.2	-8.3	-9.8
3	-4.2	-15.1	-3.6	2.7	-11.1	-8.4	-10.5

4	-2.9	-15.7	-2.3	1.7	-11.1	-8.5	-10.8
5	-1.8	-15.0	-0.5	0.4	-10.9	-8.9	-11.2
6	-0.7	-15.0	0.2	-1.5	-10.7	-9.5	-11.9
7	-0.7	-15.3	0.1	-3.7	-10.5	-9.9	-12.5
8	-0.1	-14.8	0.1	-6.2	-10.2	-10.1	-12.4
9	0.1	-13.9	0.4	-7.4	-9.7	-10.7	-12.9
10	1.1	-12.1	0.7	-7.3	-8.7	-11.0	-12.6
11	1.9	-10.9	0.6	-7.0	-8.0	-11.0	-12.5
12	1.7	-9.7	0.7	-7.2	-6.8	-10.7	-12.0
13	1.0	-8.4	1.0	-7.0	-6.0	-10.8	-12.4
14	1.3	-7.6	1.4	-6.7	-5.4	-10.0	-12.5
15	0.9	-7.3	1.7	-6.6	-4.9	-10.0	-12.7
16	1.0	-8.0	1.9	-7.0	-4.8	-9.1	-13.7
17	0.7	-7.9	1.8	-8.3	-5.0	-9.0	-13.9
18	0.5	-7.5	2.4	-9.0	-5.0	-8.9	-16.9
19	0.9	-6.7	2.6	-9.3	-4.9	-8.8	-17.9
20	1.6	-6.1	2.3	-10.0	-4.9	-9.0	-18.9
21	2.0	-5.5	2.2	-10.7	-5.7	-9.2	-19.9
22	1.8	-5.1	2.2	-11.1	-6.5	-9.4	-20.2
23	2.0	-4.9	2.5	-10.9	-7.5	-9.1	-21.0

The design indoor temperature for the office building is set 21°C from 8:00 to 17:00 and 15°C for the rest of the hours each day, the hourly heating load of the building of the week can be calculated. The hourly loads of the office building of the specific week are presented in Table 5.9. Note that the unit of all hourly loads is kBtu/hr.

**Table 5.9 Hourly building heating loads of a specific week in winter**

Hr	Day 1	Day 2	Day 3	Day 4	Day 5	Day 6	Day 7
0	208.0	292.6	189.0	120.3	251.8	218.9	239.9
1	202.0	292.6	187.0	121.3	253.8	228.8	242.8
2	202.0	292.6	188.0	121.3	254.9	225.9	240.8
3	185.0	293.6	179.1	116.3	253.7	226.9	247.8
4	172.1	299.6	166.1	126.3	253.7	227.9	250.8
5	161.1	292.6	148.2	139.2	251.8	231.9	254.8

6	140.7	283.1	131.7	148.6	240.3	228.3	252.2
7	118.5	263.9	110.5	148.3	216.1	210.1	236.0
8	0.0	135.4	0.0	49.7	89.5	88.5	111.5
9	0.0	120.5	0.0	55.8	78.7	88.7	110.6
10	0.0	98.9	0.0	51.1	65.1	88.0	103.9
11	0.0	85.7	0.0	46.9	56.9	86.7	101.7
12	0.0	75.0	0.0	50.1	46.2	85.0	97.4
13	0.0	65.8	0.0	51.8	41.9	89.7	105.6
14	0.0	63.6	0.0	54.7	41.7	87.5	112.4
15	0.0	68.3	0.0	61.3	44.4	95.2	122.1
16	0.0	84.1	0.0	74.2	52.3	95.1	140.9
17	122.9	208.6	112.0	212.5	179.7	219.5	268.3
18	138.2	217.9	119.3	232.9	191.1	231.9	311.5
19	134.3	209.9	117.3	235.8	192.0	230.9	321.5
20	127.3	204.0	120.3	242.8	192.1	232.9	331.5
21	123.3	198.0	121.3	249.8	200.0	234.8	341.4
22	125.3	194.0	121.3	253.8	208.0	236.8	344.4
23	123.3	192.0	118.3	251.8	217.9	233.9	352.3

The one-week simulation results – with control strategy of PI control for heat pump and On/off for cooling tower – are shown in Figures 5.93 to 5.97.

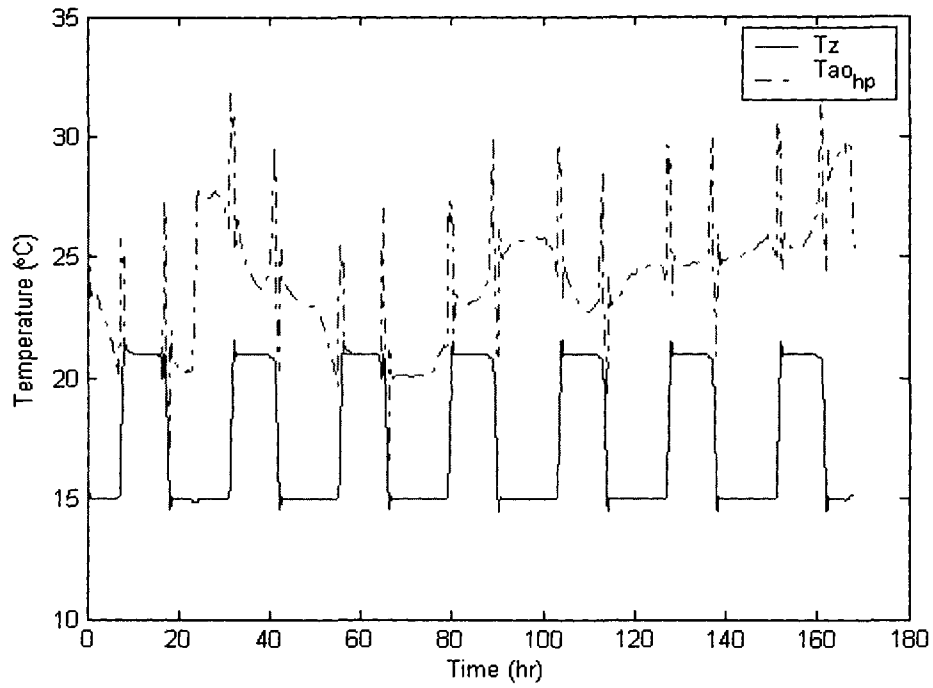


**Figure 5.93 Zone air and HP outlet air temperatures**

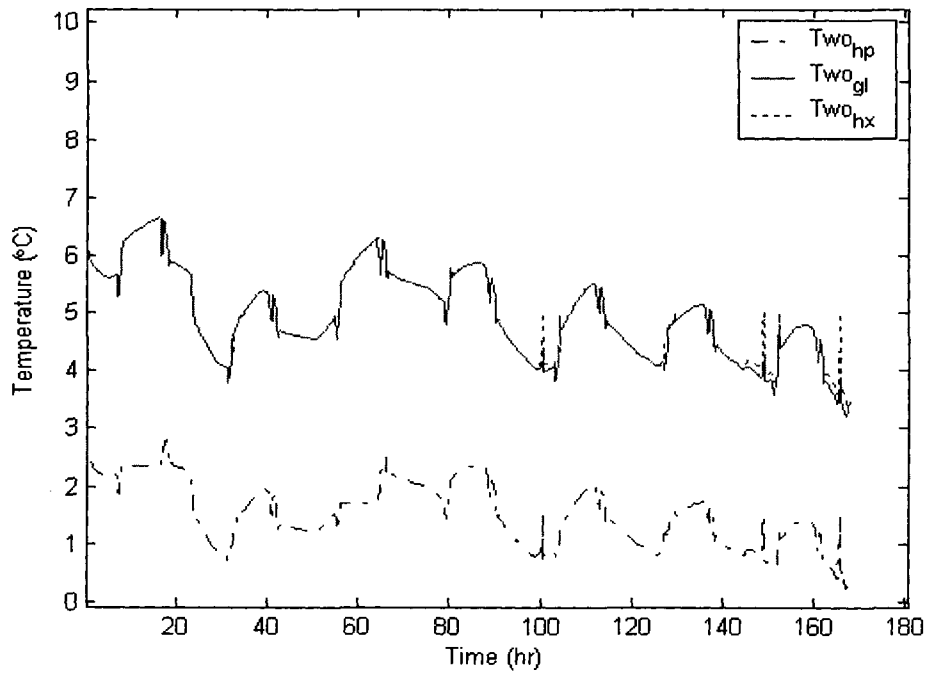


**Figure 5.94 Outlet water temperatures of HP, GL and HX**

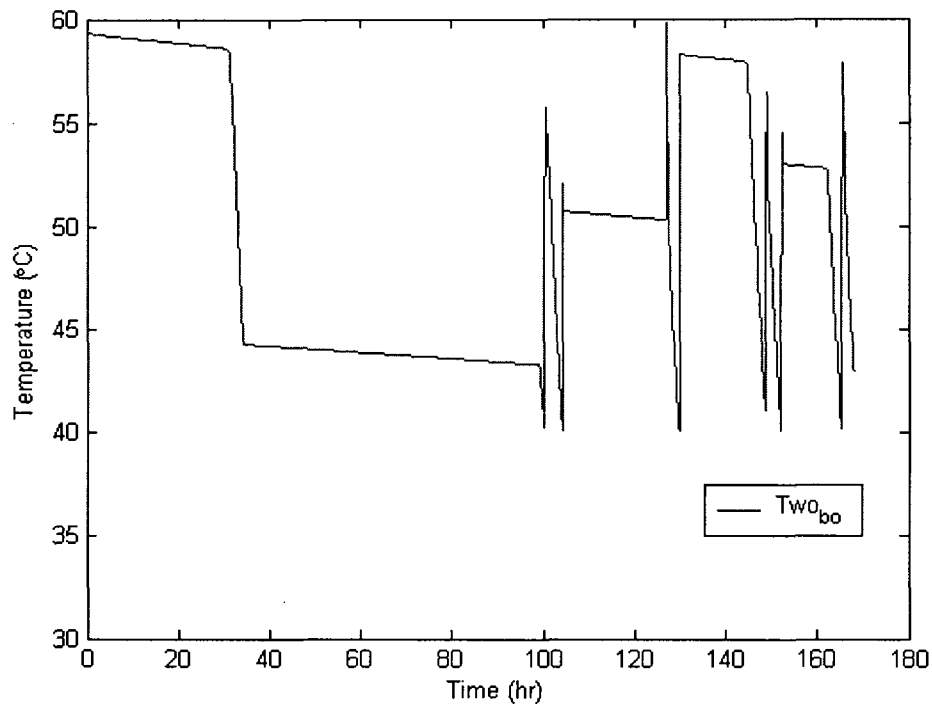


**Figure 5.95 Outlet water temperature of boiler**

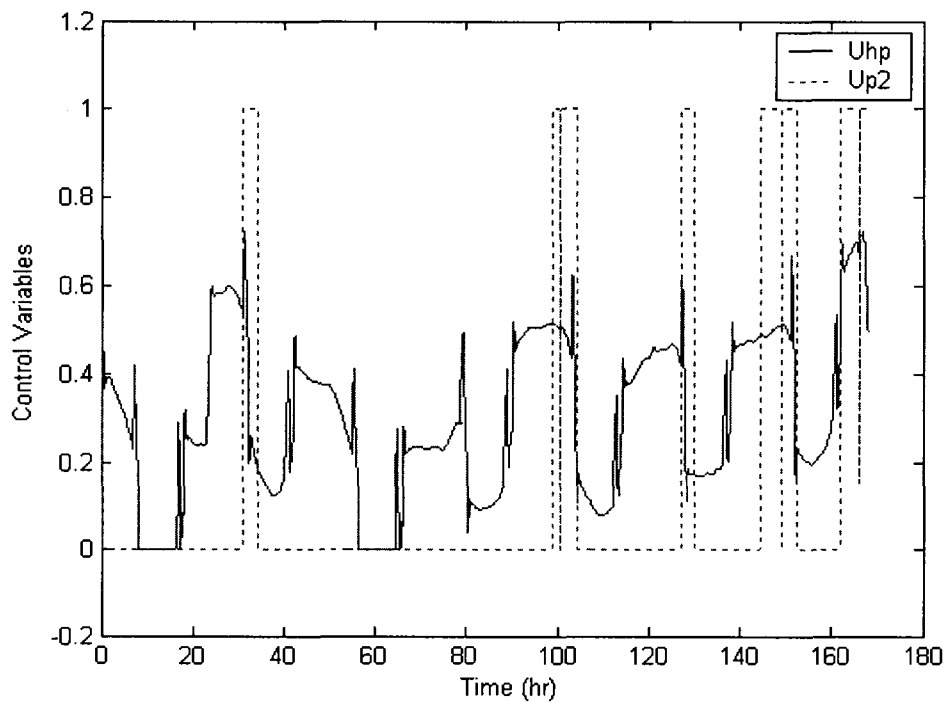


**Figure 5.96 Control variables of HP and pump 2**

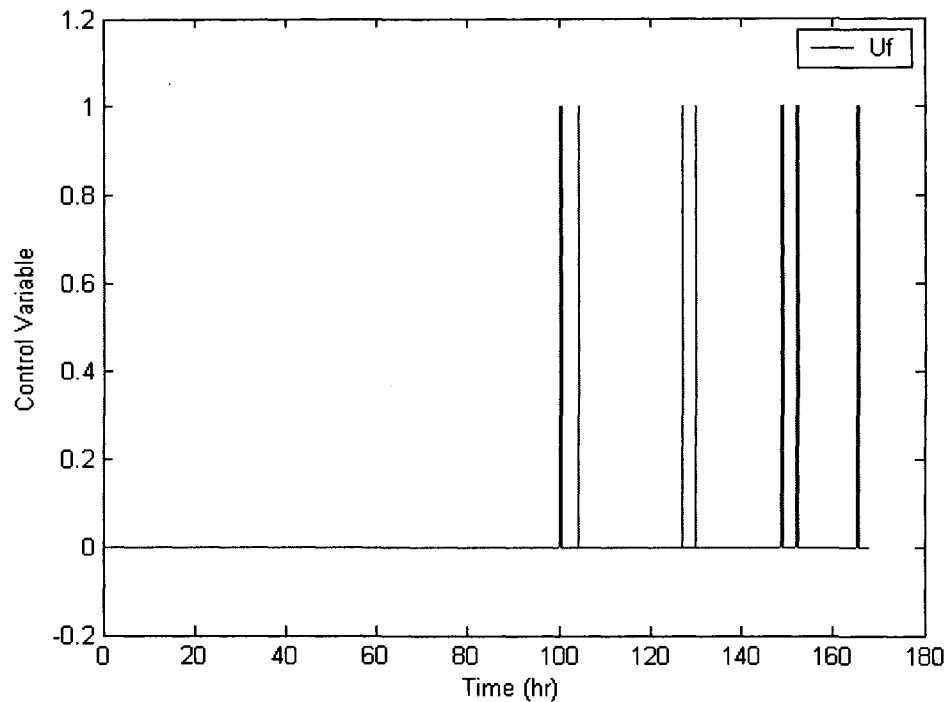


**Figure 5.97 Control variable of boiler**

The weekly total energy consumption was calculated as equal to 2,989.4kW-h. However, if the optimal supply water temperature is applied and controlled for the same week, the total energy consumption in the week was equal to 2,636.2kW-h. Thus, an energy saving of 353.2kW-h (13.4%) was achieved. Furthermore, if this case with optimal control strategy is compared to the same heat pump system with only boiler (without ground loop, which means the only heat source is the boiler) during the same period, a total energy of 5,126.3kW-h can be saved. Obviously, for whole heating season, much more energy can be saved.

## 5.5.2 Cooling Mode of Operation

Similarly, a realistic one-week outdoor condition in Montreal in design month of July is taken to study for the system in cooling mode of operation in this section. The hourly outdoor air temperatures of the week are listed in the following Table 5.10 and corresponding cooling loads are depicted in Table 5.11.

**Table 5.10 Hourly outdoor temperatures of a specific week in summer**

Hr	Day 1	Day 2	Day 3	Day 4	Day 5	Day 6	Day 7
0	17.5	20.0	15.7	15.8	12.9	16.9	14.8
1	17.5	19.4	14.6	14.8	12.1	16.6	14.5
2	17.5	19.2	13.3	13.8	12.1	16.6	13.2
3	17.5	19.2	13.5	13.8	12.0	16.2	13.1
4	16.4	18.9	12.8	12.9	10.5	16.1	11.7
5	16.3	18.7	12.2	13.5	11.4	16.6	12.3
6	16.6	19.5	13.6	13.7	12.8	17.4	13.4
7	18.6	21.1	16.0	15.5	14.7	17.3	14.8
8	18.9	23.8	16.8	16.9	16.0	17.8	15.9
9	19.9	25.1	18.6	18.6	18.8	19.4	19.9
10	20.0	27.0	18.9	15.0	20.6	21.2	21.9
11	20.5	28.0	21.9	14.5	21.4	22.2	22.9
12	21.5	28.0	21.6	17.0	22.0	20.9	23.9
13	22.5	28.9	21.2	19.8	22.9	22.9	23.2
14	23.9	28.6	22.6	20.1	21.0	23.6	24.4
15	23.9	24.7	23.9	20.3	20.8	23.4	24.5
16	23.7	22.8	23.2	19.8	21.9	22.6	24.1
17	25.1	21.0	22.9	20.7	19.9	23.0	22.3
18	24.3	20.8	22.0	19.6	18.9	22.3	22.9
19	23.7	20.9	20.7	18.3	18.6	20.4	21.3
20	22.5	20.1	19.6	15.8	17.8	18.1	18.3
21	22.1	18.3	17.8	13.6	17.6	16.3	18.9
22	20.8	17.1	17.0	13.5	17.4	15.6	17.3
23	20.3	16.0	15.0	13.3	16.7	15.4	16.1

The design indoor temperature for the office building is set 23°C from 8:00 to 17:00 and 26°C for the rest hours each day.

**Table 5.11 Hourly building cooling loads of a specific week in summer**

Hr	Day 1	Day 2	Day 3	Day 4	Day 5	Day 6	Day 7
0	0.0	11.8	0.0	0.0	0.0	0.0	0.0
1	0.0	0.0	0.0	0.0	0.0	0.0	0.0
2	0.0	0.0	0.0	0.0	0.0	0.0	0.0
3	0.0	0.0	0.0	0.0	0.0	0.0	0.0
4	0.0	0.0	0.0	0.0	0.0	0.0	0.0
5	0.0	0.0	0.0	0.0	0.0	0.0	0.0
6	0.0	5.2	0.0	0.0	0.0	0.0	0.0
7	4.7	31.5	0.0	0.0	0.0	0.0	0.0
8	235.8	288.4	213.3	214.4	204.7	224.0	203.6
9	288.1	343.9	274.2	274.2	276.3	282.8	288.1
10	305.5	380.6	293.8	251.9	312.0	318.4	325.9
11	333.8	414.2	348.8	269.5	343.5	352.0	359.5
12	368.1	437.8	369.2	319.9	373.5	361.7	393.9
13	390.4	459.0	376.5	361.4	394.7	394.7	397.9
14	407.8	458.2	393.8	367.1	376.7	404.5	413.1
15	408.8	417.4	408.8	370.2	375.6	403.5	415.3
16	386.2	376.5	380.8	344.4	366.9	374.4	390.5
17	173.2	129.2	149.6	126.0	117.4	150.7	143.2
18	127.7	90.2	103.0	77.3	69.8	106.3	112.7
19	94.2	64.2	62.0	36.3	39.5	58.8	68.5
20	65.1	39.3	33.9	0.0	14.7	17.9	20.0
21	52.7	11.9	6.6	0.0	4.4	0.0	18.3
22	31.4	0.0	0.0	0.0	0.0	0.0	0.0
23	21.5	0.0	0.0	0.0	0.0	0.0	0.0

The weekly simulation results – with control strategy of PI control for heat pump and On/off for cooling tower – are shown in Figures 5.98 to 5.102.

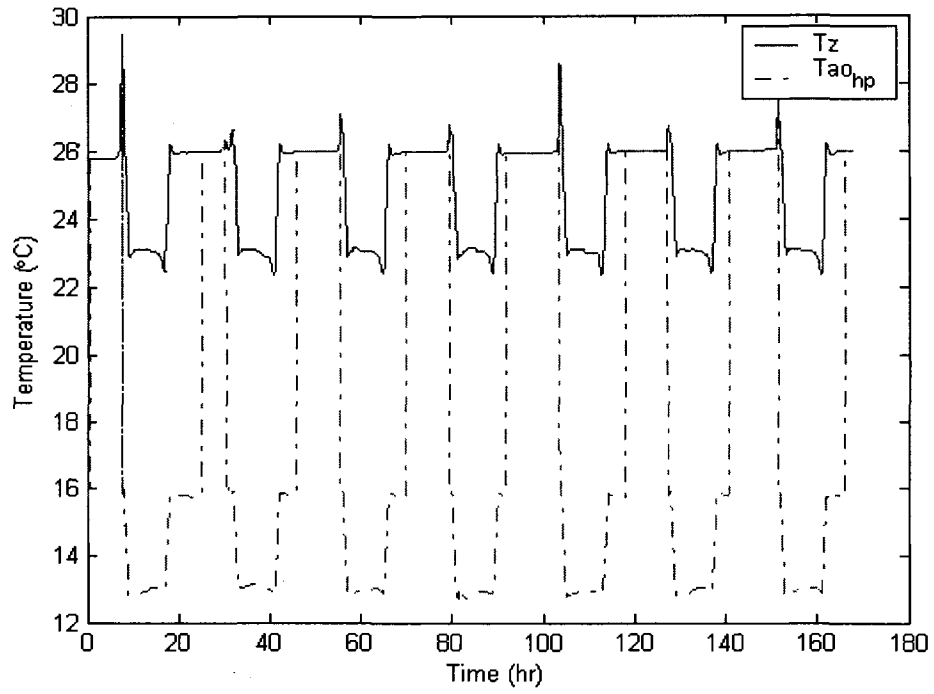


**Figure 5.98 Zone air and HP outlet air temperature responses**

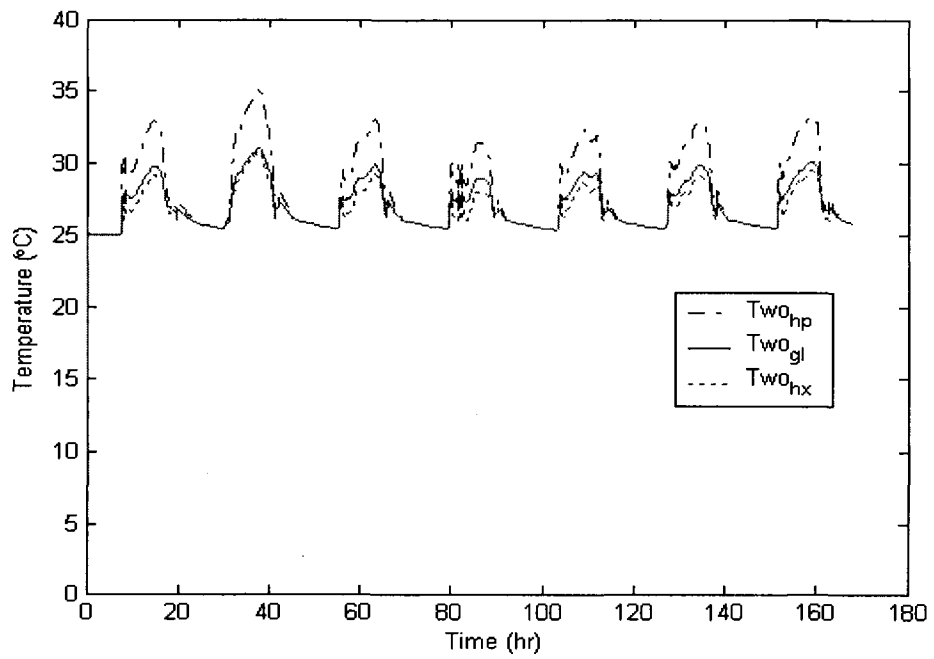


**Figure 5.99 Outlet water temperature responses of HP, GL and HX**

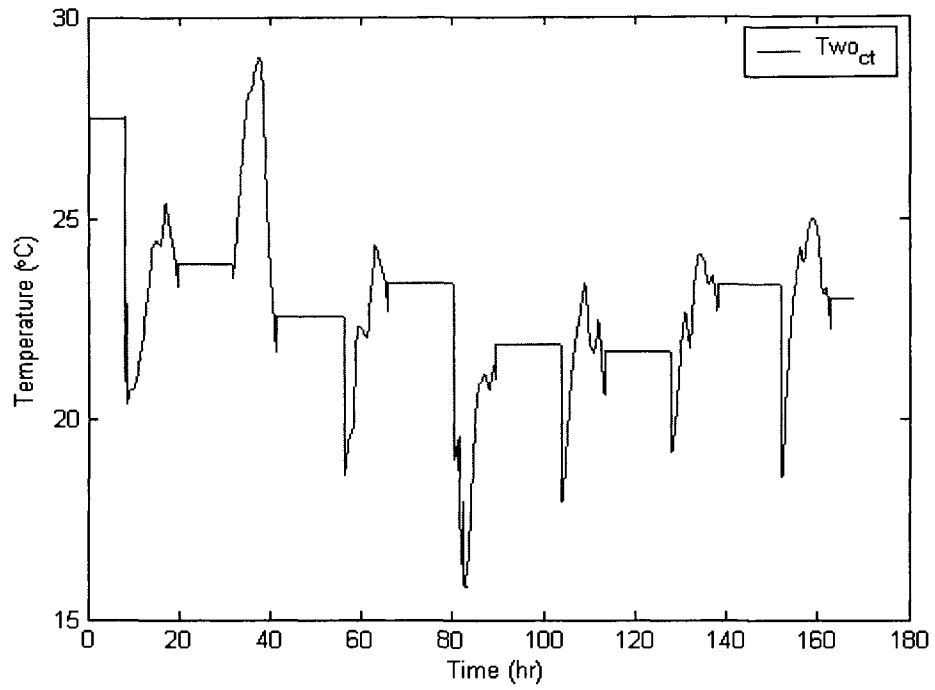


**Figure 5.100 Outlet water temperature response of cooling tower**

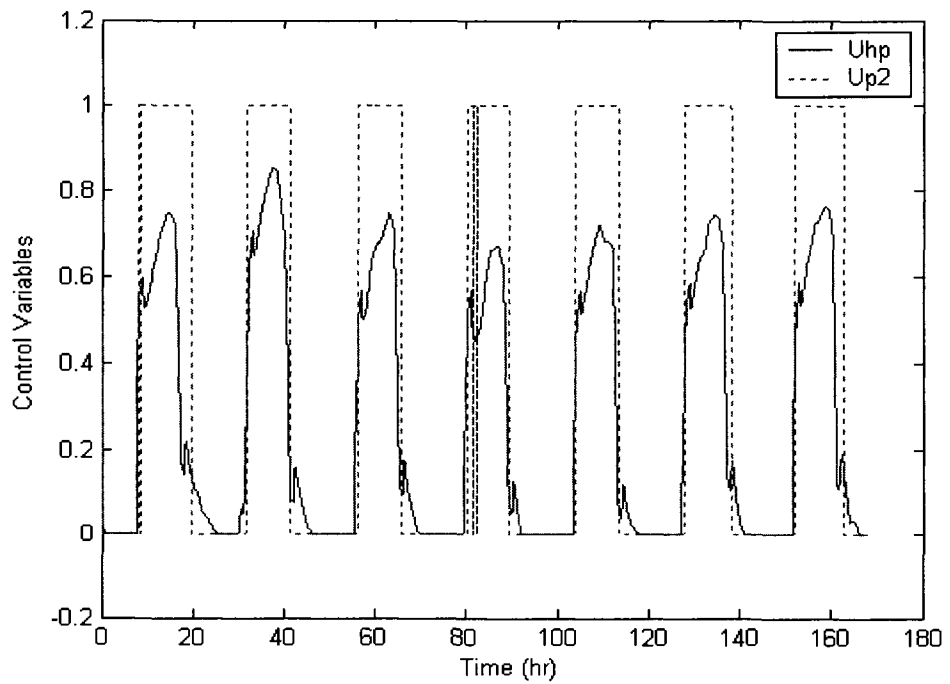


**Figure 5.101 Control variables of HP and pump 2**

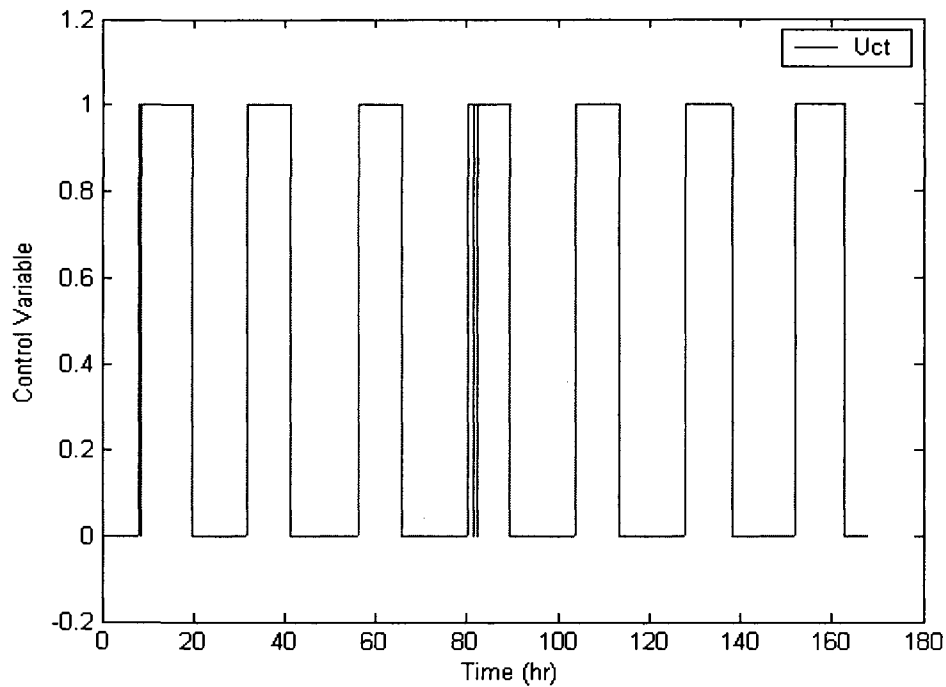


**Figure 5.102 Control variable of cooling tower**

After performing the simulations of whole HGSHp system with the control strategies in the specific week above, a total energy consumption of 2,406.1kW-h was obtained. However, if the optimal supply water temperature is used instead, the total energy consumption would be 2,287.1kW-h. This results in an energy saving of 119kW-h (5.2%). By comparing this case with the same heat pump system with only cooling tower (without ground loop, which means the only heat sink is the cooling tower), a total energy of 407.8kW-h can be saved. The above methodology for computing optimal setpoints can be easily extended to multiple heat pump systems as well.

# CHAPTER 6 CONTRIBUTIONS, CONCLUSIONS, AND RECOMMENDATIONS

## 6.1 Summary

Ground source heat pump (GSHP) systems are one of the fastest growing applications of renewable energy in the world, as they are potentially more efficient than conventional air-to-air heat pumps by using the relatively constant temperature of the geothermal energy to provide heating or cooling to conditioned rooms. Dynamic models of each component of a hybrid ground source heat pump (HGSHP) system have been developed for control strategy and analysis. PI feedback controllers for heat pump units and On/Off controllers for cooling tower and boiler are designed and utilized to match anticipated building loads, and to analyze transient response characteristics of such outputs as water flow rate of heat pump, outlet air temperature of heat pumps, outlet water temperatures of heat pump, boiler and cooling tower, and fuel flow rate of boiler. With the usage of On/Off controllers and well-tuned PI controllers, as well as optimal control strategies for HGSHP systems in heating or cooling modes, the systems are expected to give better operating performance and efficiency and accordingly achieve considerable energy savings in both heating and cooling modes of operation.

## 6.2 Contributions

The contributions of the research work in dynamic modeling and closed loop control of

hybrid ground source heat pump systems are briefly summarized as follows:

- ( i ) Component models of HGSHP systems, namely, heat pump model, cooling tower model, boiler model, and ground loop heat exchanger model, have been developed and a system model is developed.
- ( ii ) A detailed multiple-load aggregation algorithm has been presented so that it can be utilized to precisely account for and calculate the transient heat conduction in vertical ground heat exchanger model with different annual, monthly, and daily pulses of heat.
- ( iii ) Feedback PI controllers and On/Off controllers are introduced to sub-models of HGSHP system. Closed loop PI control simulations are carried out to study output responses of outlet air and water temperatures of heat pumps, while On/Off controllers were used to study responses of outlet water temperature of cooling tower, outlet water temperature of boiler, which are a function of time and certainly a function of varying building load.
- ( iv ) Control simulation results are used to show qualitatively the system performance improvement and energy savings.

### **6.3 Conclusions**

The conclusions of the research work are summarized below:

- ( i ) Aggregated modeling of multiple heat pump systems is shown to be useful approach for evaluating system performance.

- ( ii ) Results show that PI control for heat pumps and On-Off control for boiler and cooling tower give stable and good control performance.
- ( iii ) In spite of large time delays associated with ground loop, the feedback PI control is shown to be effective in maintaining zone temperature close to its setpoints without large overshoot or sluggish response.
- ( iv ) Among the several control strategies tested, the strategy using PI control for heat pumps and On-Off control for boiler or cooling tower was shown to be more energy efficient.
- ( v ) Results show that energy performance of HGSHP systems can be improved significantly by using optimal inlet water temperatures for the heat pumps.

#### **6.4 Recommendations for Future Research**

Research work presented in the study is clearly giving opportunities for future research developments of hybrid ground source heat pump systems in system component development, system model verification, control strategy study, and optimal system operation.

- ( i ) System component developments of HGSHP systems include development of each component model, development of improved grouting materials, development of borehole installation techniques, and short time-step modeling of ground loop heat exchangers (GLHX) and associated components.
- ( ii ) System models should be improved to be able to simulate not only in either heating

or cooling mode of operation in a day, but also in both modes in a single day, which will be more realistic for actual heat pump systems in office buildings.

- ( iii ) Comprehensive model-based computer programs of HGSHP are very convenient to simulate and analyze the impact of different operating conditions. As all models based on mathematical models are simulated with MATLAB program, they should be tested in realistic case to verify the model accuracy.
- ( iv ) With the usage of PI controllers and On/Off controllers, well tuned by inputting some user-defined optimal set-point values, the system has a better performance, but the optimal values can vary with time. It is advisable to take advantage of adaptive controllers to automatically track the variable set point to improve control system performance.
- ( v ) It is important to improve both control system and HGSHP system, especially the MLAA algorithm for the GLHX model, and to develop a multiple control loop strategy for optimal control of the whole HGSHP system. It will consequently have a higher efficiency and a better overall performance.

## REFERENCES

- [1] ASHRAE. 2000. *ASHRAE Systems and Equipment Handbook (SI)*. American Society of Heating, Refrigerating, and Air-Conditioning Engineers Inc.
- [2] ASHRAE. 2003. *ASHRAE Applications Handbook (SI)*. American Society of Heating, Refrigerating, and Air-Conditioning Engineers Inc.
- [3] ASHRAE. 2005. *ASHRAE Handbook – Fundamentals (SI)*. American Society of Heating, Refrigerating, and Air-Conditioning Engineers Inc.
- [4] Bendapudi, S. and J.E. Braun. 2002. *A Review of Literature on Dynamic Models of Vapor Compression Equipment*. ASHRAE Project Report.  
  
([http://www.nist.gov/tc75/1043-RP\\_Dynamic\\_Modeling\\_Literature\\_Review.pdf](http://www.nist.gov/tc75/1043-RP_Dynamic_Modeling_Literature_Review.pdf)).
- [5] Bernier, M.A. 2001. *Ground-Coupled Heat Pump System Simulation*. ASHRAE Transactions.
- [6] Bernier, M.A., P. Pinel, R. Labib, and R. Paillot. 2004. *A Multiple-load aggregation Algorithm for Annual Hourly Simulations of GCHP Systems*. HVAC&R Research.
- [7] Bose, J.E., M.D. Smith, and J.D. Spitler. 2002. *Advances in Ground Source Heat Pump Systems – An International Overview*. Proceedings of the Seventh International Energy Agency Heat Pump Conference. Beijing. May, 2002.
- [8] Browne, M. and P. Bansal. 2000. *Dynamic Modeling of in-situ Liquid Chillers*. Proc. 2000 International Refrigeration Conference at Purdue, pp. 425-431.
- [9] Carslaw, H.S. and J.C. Jaeger. 1947. *Conduction of Heat in Solids*. Oxford, U.K.,

Claremore Press.

[10] Cattan, Y. and L. Fabre. 1989. *Wind Effects on the Performance of Natural Draught Wet Cooling Towers Comparison of Constructors Proposals and Realization of Performance of Control Tests*. International Cooling-Tower Conference.

[11] Cecchini, C. and D. Marchal. 1991. *A Simulation Model of Refrigerating and Air-Conditioning Equipment Based on Experimental Data*. ASHRAE Transactions.

[12] Claus, G. 1985. *General Computer Simulation Model for Furnaces and Boilers*. ASHRAE Transactions. CH-85-02-1, 47.

[13] Deng O'neill, Zheng, J.D. Spitler, and S.J. Rees. 2006. *Performance Analysis of Standing Column Well Ground Heat Exchanger Systems*. ASHRAE Transactions.

[14] Du Preez, A.F. 1992. *The Influence of Cross-Winds on the Performance of Natural Draft Dry Cooling Towers*. Doctoral Thesis, University of Stellenbosch, South Africa.

[15] Eskilson, P. 1987. *Thermal Analysis of Heat Extraction Boreholes*. Doctoral Thesis. University of Lund, Sweden.

[16] Fischer, S.K. and C.K. Rice. 1983. *The Oak Ridge Heat Pump Models: I. A Steady-State Computer Design Model for Air-to-Air Heat Pumps*. Oak Ridge National Laboratory ORNL/CON-80.

[17] Fiveland, W.A. and R.A. Wessel. 1986. *Furmo: A Numerical Model for Predicting Performance of Three-Dimensional Pulverized-Fuel Fired Furnaces*. ASME. 1986. 14p.

[18] Hart, P. and R. Couvillion. 1986. *Earth-Coupled Heat Transfer*. Publication of the National Water Well Association.

- [19] Huang, B.J., R.H. Yen, and W.S. Shyu. 1988. *Steady-State Thermal Performance Model of Fire-Tube Shell Boilers*. Journal of Engineering for Gas Turbines and Power. ASME Transactions, v110, n2, p173.
- [20] Ingersoll, L.R. 1954. *Heat Conduction with Engineering, Geological, and Other applications*. University of Wisconsin Press.
- [21] Jin, H. and J.D. Spitler. 2002. *A Parameter Estimation Based Model of Water-to-Water Heat Pumps for Use in Energy Calculation Programs*. ASHRAE Transactions.
- [22] Kavanaugh, S.P. and K. Rafferty. 1997. *Ground-Source Heat Pumps: Design of Geothermal Systems for Commercial and Institutional Buildings*. American Society of Heating, Refrigerating, and Air-Conditioning Engineers Inc.
- [23] Kelvin. 1882. *Mathematical and Physical Papers. Vol. I*. Cambridge University Press.
- [24] Krakow, K.I. and S. Lin. 1983. *A Computer Model for the Simulation of Multiple Source Heat Pump Performance*. ASHRAE Transactions.
- [25] Krakow, K.I. and S. Lin. 1987. *A Numerical Model of Heat Pump Having Various Means of Refrigerant Flow Control and Capacity Control*. ASHRAE Transactions.
- [26] Liao, Z. and F. Parand. 2002. *Develop a Dynamic Model of Gas and Oil Burned Boilers for Optimisation of Boiler Control in Central Heating Systems*. (<http://www.esim.ca/2002/documents/Proceedings/Session%201-4.pdf>).
- [27] Lund, J., B. Sanner, L. Rybach, R. Curtis, and G. Hellstrom. 2004. *Geothermal (Ground-Source) Heat Pumps – A World Overview*. GHC BULLETIN, Sep. 2004. (<http://geoheat.oit.edu/bulletin/bull25-3/art1.pdf>).

- [28] MacArther, J.W. 1984. *Transient Heat Pump Behavior: A Theoretical Investigation*. International Journal of Refrigeration.
- [29] Murphy, W.E. and V.W. Goldschmidt. 1984. *Transient Response of Air Conditioners – A Qualitative Interpretation through a Sample Case*. ASHRAE Transactions, v90, n pt 1B, 1984, p997.
- [30] Patankar, S.V. 1980. 1991. *Numerical Heat Transfer and Fluid Flow*. New York, McGraw-Hill.
- [31] Rennie, E.J. and N. Hay. 1990. *Analysis of Full-Scale Natural-Draft Tower Measurements to Develop and Validate Tower Performance Computer Codes*. International Association for Hydraulic Research.
- [32] Rennie, E.J. 1992. *Thermal Performance of Power Station Cooling Towers*. University of Nottingham.
- [33] Richter, W., R. Payne and M.P. Heap. 1984. *Influence of Thermal Properties of Wall Deposits on Performance of P. F. Fired Boiler Combustion Chambers*. ACS, Division of Fuel Chemistry, v29, n4, p249.
- [34] Rossi, T.M. and J.E. Braun. 1999. *A Real-Time Transient Model for Air Conditioners*. Proc. of the IIR 28<sup>th</sup> Congress of Refrigeration on Refrigeration into the Third Millennium. Sydney, Australia.
- [35] Spitler, J.D., S.J. Rees, and C. Yavuzturk. 2000. *Recent Developments in Ground Source Heat Pump System Design, Modeling and Applications*. Proc. of CIBSE/ASHRAE joint conference “20 20 Vision”, Dublin, Sep. 2000.

- [36] Steward, F.R. 1974. *Heat Transfer in Flames*. Scripta Book Co.
- [37] Yavuzturk, C., J.D. Spitler, and S.J. Rees. 1999. *A Transient Two-Dimensional Finite Volume Model for the Simulation of Vertical U-Tube Ground Heat Exchangers*. ASHRAE Transactions. 105(2):465-474.
- [38] *Clean Energy Project Analysis: Ground-Source Heat Pump Project Analysis Chapter*. ([http://www.retscreen.net/download.php/ang/479/0/Textbook\\_GSHP.pdf](http://www.retscreen.net/download.php/ang/479/0/Textbook_GSHP.pdf))